Proceedings of the 23rd Annual Meeting

TUESDAY, JUNE 8, 1976

TUESDAY, 10:30-12:00 BALLROOM A

CARDIOVASCULAR 1

Chairman: William Ashburn
Co-Chairman: Ralph Gorten

DETECTION OF CORONARY ARTERY DISEASE BY REST AND EXERCISE Tl-201 MYOCARDIAL IMAGING. Glen W. Hamilton, Gene B. Trobaugh, James L. Ritchie, and W. Douglas Weaver. Veterans Administration Hospital, Seattle, Wa.

Tl-201 imaging was performed at rest and during maximal exercise in 34 patients with suspected coronary artery disease (CAD) who had cardiac catheterization. Camera images were obtained in 3 views (ANT, LAO, LLAT) using a FWHM window centered at 80 KeV and high resolution collimation. The delay from injection to imaging was 20 minutes at rest and 5 minutes for exercise. Maximal exertion was assured by injecting Tl-201 60 seconds prior to the termination of a repeat exercise test. The diagnostic quality of exercise images was routinely improved over rest images with increased myocardial/background ratio, diminished gastrointestinal activity, and visualization of the right ventricle. Image and arteriographic data were analyzed independently by 3 blinded observers; interobserver agreement for image interpretation was 82%.

Six patients without CAD (<50% diameter stenosis) had normal images at rest and exercise. None of the 6 without CAD had ECG Q waves; 1 had exertional ST depression. Of 28 patients with CAD (>75% stenosis), 11 (39%) had resting, 21 (75%) exercise induced, and 23 (82%) resting and/or exercise induced image defects; ECG Q waves were present in 5 (18%) and 17 (61%) had exertional ST depression. Tl-201 image defects occurred more often than ECG ST depression in all patients with either single, double, or triple vessel CAD.

Overall, Tl-201 imaging was more sensitive and specific for detection of CAD than resting and stress electrocardiography. The combined sensitivity of exercise ST depression and/or a Tl-201 image defect (25/28, 89%) was greater than that for either technique alone.

THALLIUM-201 MYOCARDIAL PERFUSION IMAGING AT REST AND STRESS: SENSITIVITY FOR DETECTION OF CORONARY ARTERY DISEASE. Ian Bailey, H. William Strauss and Bertram Pitt. The Johns Hopkins Medical Institutions, Baltimore, Md.

Myocardial imaging following injection of Thallium-201 at rest and stress offers a non-invasive means of detecting myocardial infarction and transient ischemia. In this study the relative sensitivity of thallium-201 myocardial perfusion imaging was compared to that of electrocardiography for the non-invasive detection of coronary disease in 63 patients with angiographically proven coronary artery narrowing (70% or greater). Forty-eight patients had a history of prior infarction: the resting scan was abnormal (transmural perfusion defect) in 31 (63%) while the ECG had significant Q waves in only 27 (56%) (P N.S.). All 63 patients performed maximum exercise ECG tests with injection of thallium at peak stress. New scan defects were found in 35 (56%) while ischemic ST segment depression occurred in 24 (38%)(p<.02). When both the rest and stress data were included coronary artery disease (infarction and ischemia) was detected by scanning in a total of 47 (75%) of patients while electrocardiography detected 41 (65%) (P NS). Eleven patients (17%) with coronary disease had both normal scans and ECG's. When the data were analyzed in terms of the number of diseased coronary vessels, scans detected 20/28 patients (71%) with single vessel involvement whereas ECG detected only 13/28 (46%) p<.05. In multiple vessel disease the scan detected 27/35 (77%) whereas the ECG detected 28/35 (80%) P NS.

We conclude that the scan is more sensitive than the ECG for the detection of stress induced ischemia and for the detection of single vessel coronary artery disease. However negative tests with both techniques do not exclude coronary artery disease in a significant number of patients.

COMPARISON OF Tl-201 STRESS MYOCARDIAL PERFUSION IMAGING TO STRESS ELECTROCARDIOGRAPHY. David Shames, Michael Taradash Elias Botvinick, and William Parmley. University of California, San Francisco, California.

To determine the clinical utility of stress Tl-201 myocardial perfusion imaging, 23 patients underwent treadmill electrocardiography, stress and rest myocardial imaging with Tl-201 and selective coronary arteriography. All imaging studies were performed to 300,000 counts in the anterior, left anterior oblique and left lateral views using the Searle Pho Gamma IV scintillation camera with LEAP collimator. Studies positive for significant ischemic coronary disease were defined as defects on the Tl-201 myocardial image present at stress and not at rest or present at stress to a greater degree than rest, stenoses by area $\geq$ 75% on the coronary arteriogram and flat or downsloping ST-segment depression of $\geq$ 1 mm on stress electrocardiogram. Treadmill stress was carried to at least 85% of maximal predicted heart rate or to angina.

19/23 patients had positive and 4/23 patients had negative coronary arteriograms. No false positive studies were found in either the stress electrocardiogram or Tl-201 image groups. However, 7/19 patients had false negative stress electrocardiograms and 1/19 patients had a false negative Tl-201 imaging study.

Although this study is formed by only a small number of patients in whom the incidence of significant coronary artery disease is high, some tentative conclusions may be drawn. Tl-201 stress imaging may be more sensitive for detecting significant coronary disease than stress electrocardiography although the specificity of the two tests may be about the same.

REPRODUCIBILITY OF THALLIUM-201 MYOCARDIAL IMAGING. S. Daspit, M. Goris, P. McLaughlin, R. Martin, W. Haskell, S. Lewis, P. Doherty, D. Harrison, and J. Kriss. Dept. of Nuclear Medicine, Stanford University School of Medicine, Stanford, California.

Fifty-seven Thallium-201 (Tl) myocardial perfusion studies were performed on 15 patients (pts) at rest and during light (L) exercise (Ex) and maximum (M) Ex to assess 1) reproducibility of Ex scintigraphy, 2) correlation with coronary arteriography (CAG) and Ex ECG, and 3) the effects of L Ex. Graded Ex was performed on two occasions to an end point of fatigue or angina (14 pts) and on one occasion to 33-50% of M workload (12 pts) for L Ex. Two mCi of Tl were

injected 2 min. before the end of Ex. Multiple views were taken with a gamma camera and were processed by interpolative background subtraction. Three observers without knowledge of the CAG or ECG findings analyzed 5 segments (sgs) on each study for the presence of perfusion defects (PD). Of the 70 sgs (14 pts) assessed on one M Ex test as having no PD, PD with both rest and M Ex, or PD with M Ex only, 64 (91%) were reproducible in the second M Ex study. Of the sgs correlated with sign CAD (≥ 50% narrowing), 17/17 ant. sgs (LAD), 11/11 inf. sgs (RCA), and 8/15 post. sgs (Circumflex) showed fixed or ischemic PD. Of the vessels without sign. CAD, 2/2 ant. sgs (LAD), 6/6 inf. sgs (RCA) and 6/6 post. sgs (Circumflex) showed no PD. L Ex produced PD in 7 pts (10 sgs) without associated ECG changes or angina. We conclude that Tl studies are 1) highly reproducible, 2) highly specific for exclusion of significant CAD and highly sensitive for detection of LAD and RCA lesions although less sensitive for circumflex lesions, and 3) sensitive in detecting PD in L Ex unaccompanied by angina or ECG changes.

VALUE AND LIMITATIONS OF THALLIUM-201 SCINTIGRAPHY IN ACUTE PHASE OF MYOCARDIAL INFARCTION STUDIED BY REPEATED MYOCARDIAL IMAGING. Frans Wackers, Jan v.d. Schoot, Ellinor Busemann Sokole, Gerard Samson, K.I.Lie, Koen Liem, Dirk Durrer and Hein J.J. Wellens. Depts. of Cardiology and Nuclear Medicine, Wilhelmina Gasthuis, Amsterdam, The Netherlands.

Scintiscans with Tl-201 were performed in 200 patients (pts) with acute myocardial infarction (AMI). Scintiscans were judged without knowledge of clinical data as positive (=defect), equivocal or negative. Scintiscans were made in 44 pts within 6 hr of AMI (group A), in 52 pts between 6 and 24 hr of AMI (group B), in 104 pts after 24 hr of AMI (group C). Group A: All 44 pts showed positive scintiscans. Group B: 51 pts showed abnormal scintiscans (46 positive, 5 equivocal), scintiscans were negative in 1 pt. Group C: 75 pts had positive, 21 equivocal and 8 negative scintiscans. When considering infarct size 19/26 equivocal and 7/9 negative results were in pts with small AMI (SGOT < 60 IU). Our results suggest a decrease in the ability of scintigraphy to detect AMI with increasing time interval, especially in small AMI. Therefore repeated scintigraphy was performed in 28 pts:once in 19 pts and twice in 9 pts. Repeated scintigraphy was performed in 3 groups: a) within 6 hr and at 24 hr (13 pts), b) within 6 hr and at 7th day (9 pts), c) at 24 hr and at 7th day (15 pts). Of 22 pts studied within 6 hr and at 24 hr or later, repeated scintigraphy showed decrease in size of defect in 16, increase in 4 and no change in 2 pts. Bij contrast, in 15 pts studied at 2nd day and at 7th day, repeated scintigraphy showed decrease in size of defect in 7 and no change in 8 pts.
Conclusions: Diagnosis by AMI with Tl-201 is highly reliable when made within 6 hr after onset of symptoms; 2) Sensitivity of scintigraphy to detect AMI decreases after 24 hr of AMI; 3) Repeated scintigraphy demonstrates a tendency for defects to decrease in size after 6 hr of onset of AMI.

IMPROVED DIAGNOSTIC ASSESSMENT OF ACUTE MYOCARDIAL INFARCTION: SENSITIVITY & SPECIFICITY OF Tc-99m PYROPHOSPHATE SCINTIGRAPHY. Daniel S. Berman, Ezra A. Amsterdam, Antone F. Salel, Gerald L. DeNardo, Gerald J. Bailey, Dean T. Mason. University of California, School of Medicine, Davis, California

In order to further define the diagnostic accuracy of Tc-99m pyrophosphate (PYP) imaging for acute myocardial infarction (MI), 140 patients (pts) admitted to the coronary care unit were evaluated by PYP scintigraphy, and the results were compared with the clinical diagnosis based on history, serial serum enzyme determinations, and serial electrocardiograms. Multiple scintigrams were obtained two hours after intravenous injection of PYP using a scintillation camera with a high resolution collimator. The use of a computer for rib and blood pool subtraction was also evaluated. Interpretation was performed independently by two observers who were unaware of the pt's clinical state. Of the 140 pts, 58 had definite clinical evidence of acute MI. Of 49 with transmural MI, all 49 had positive scintigrams. Of 9 with subendocardial MI, 5 were positive, 3 equivocal, and 1 falsely negative by scintigraphy. Five of the 140 had equivocal clinical evidence of infarction; of these, 3 had positive scintigrams, and 2 negative. The remaining 77 pts had no clinical evidence of infarction: 52 of these pts had definitely negative PYP images; in 22 the images were equivocal, and in 3 the scintigrams were definitely positive. Of 55 patients with definitely negative scintigrams, only 1 had clinical evidence of acute infarction. Consistent interpretation was demonstrated by agreement by the independent observers in 136 of the 140 pts. Computer processing strengthened certainty of visual impression, but only rarely contributed to change in the scintigraphic evaluation. It is concluded that if an equivocal category in the scintigraphic interpretation is employed, PYP myocardial imaging is both extremely sensitive and highly specific for acute MI.

TECHNETIUM-99m STANNOUS PYROPHOSPHATE MYOCARDIAL SCINTIGRAMS TO RECOGNIZE ACUTE SUBENDOCARDIAL MYOCARDIAL INFARCTS IN PATIENTS. Robert W. Parkey, Lawrence Poliner, Frederick J. Bonte, Ernest M. Stokely, L. Maximilian Buja, and James T. Willerson. University of Texas Health Science Center, Dallas, Tx.

Acute subendocardial myocardial infarction (SEMI) is difficult to recognize in pts from the ECG alone. The subendocardium, however, is the most vulnerable area of the heart to ischemic injury; thus the development of additional techniques that might help document the presence of SEMI would be of considerable usefulness. Accordingly, we have extended our previous observations to evaluate the ability of technetium-99m stannous pyrophosphate myocardial scintigrams (Tc-99m PYP) to recognize SEMI in 179 pts with chest pain but without ECG evidence of acute transmural myocardial infarction and without the syndrome of unstable angina pectoris. Fifty one, average age 61 yrs, had positive Tc-99m PYP scintigrams; in most the positive scintigram was characterized by having a "2+" and poorly localized pattern of uptake of Tc-99m PYP. Forty four of these pts had elevated serum enzymes that evolved for infarction and ECGs that demonstrated ST and T wave changes consistent with SEMI. Seven pts had positive Tc-99m PYP scintigrams and ST and T wave ECG changes consistent with SEMI, but their peak serum enzymes did not exceed normal values. One hundred twenty seven pts had negative Tc-99m PYP scintigrams and neither ECG nor enzyme evidence of SEMI. One pt had a negative Tc-99m PYP scintigram but ST and T wave changes and elevated serum enzymes suggestive of SEMI. The data suggest that Tc-99m PYP myocardial scintigrams recognize acute SEMI in pts; in addition acute SEMI seems to have a particular scintigraphic pattern that is itself suggestive of SEMI. The incidence of "false negative" Tc-99m PYP scintigrams with SEMI appears to be very small. This data also raise the question as to whether Tc-99m PYP scintigrams are more sensitive than enzymes and more specific than ECGs in recognizing acute SEMI.

TECHNETIUM-99m PYROPHOSPHATE MYOCARDIAL SCINTIGRAPHY IN PATIENTS WITH CHEST PAIN - LACK OF DIAGNOSTIC SPECIFICITY. H.B. Karunaratne, W.F. Walsh, H.R. Fill, L. Resnekov, and P.V. Harper. University of Chicago, Chicago, IL.

Tc-99m pyrophosphate (Tc-PYP) myocardial scintigraphy has been proposed as a diagnostic test of acute myocardial infarction (MI). The clinical specificity of the myocardial uptake of Tc-PYP was investigated in 75 unselected patients admitted to the Coronary Care Unit with chest pain. Bedside myocardial imaging was performed within 1-5 days of admission using a mobile gamma camera (Searle Pho/Gamma IV). 15 mC of Tc-PYP were injected intravenously and 800,000 count analog and digital images obtained in the AP and LAO views, 60-150 min (mean 90) later. The myocardial uptake of Tc-PYP was graded on a 0-3+ scale: 0, nil; 1+, faint; 2+, moderate; 3+, marked (equal to sternum). Grades 2+ and 3+ were regarded as positive. The 75 patients were divided into 5 groups on the basis of clinical, ECG and enzyme data: acute transmural myocardial infarction (TMI), acute nontransmural myocardial infarction (NTMI), unstable angina pectoris (UAP), cardiomyopathy (CM), and no cardiac disease (normal). The scintigraphic findings were correlated with the diagnosis of each patient.

		Tc-PYP Uptake Grade			
Diagnosis	No.	0	1+	2+	3+
TMI	10	-	-	4	6
NTMI	15	4	2	7	2
UAP	34	5	14	15	-
CM	7	2	3	2	-
Normal	9	6	3	-	-

It is concluded that (1) Tc-PYP scintigraphy may fail to detect acute nontransmural myocardial infarction. (2) Positive Tc-PYP scintigrams are not specific for acute myocardial infarction but occur in a significant proportion of patients without evidence of recent MI (17/41 UAP and CM).

DUAL MYOCARDIAL IMAGING WITH Tc-99m-PYROPHOSPHATE (PYP) AND THALLIUM 201 (TL) FOR DIAGNOSING AND SIZING ACUTE MYOCARDIAL INFARCTION (AMI). Hartmut Henning, Heinrich Schelbert, Robert A. O'Rourke, Alberto Righetti, Thordur Hardarson, William Ashburn. University of California, San Diego.

The diagnostic accuracy of PYP and TL in detecting and localizing AMI was compared in 22 patients (pts) with documented AMI. Infarct size (IS) was obtained in each pt using serial serum CPK values; the completed CPK curves were integrated and the fractional enzymatic decay rate measured for each curve. Imaging with PYP (15 mCi) was performed one to six days after AMI and with TL (2 mCi) within 24 hours after PYP. Anterior, 45° LAO and lateral projections (gamma camera) were obtained 2 to 3 hours after PYP and 1/2 to 2 hours after TL. All 22 TL scintigrams showed areas of decreased uptake and 21 corresponded to the ECG localization of MI; one pt with both AMI and a prior MI showed a separate defect in an area corresponding to new Q-waves. By contrast, PYP scans were positive in only 19 pts (86%) and the area of uptake corresponded to the ECG site in only 14 (74%) scans. Additional abnormal areas not suggested by ECG were seen by PYP in 6 and by TL in 11 pts. The average CPK-IS in the PYP negative group was smaller (3.3±0.6 (SE) IU/l·h) than that in the PYP positive group (27.2±4.3, $p < .04$). The 3 PYP negative scans included one subendocardial AMI. The largest area of PYP uptake in one of the 3 projections averaged 36.4 ± 4.5 (SE) cm^2 in the 11 pts with anterior or anterolateral MI and 18.1 ± 1.8 cm^2 ($p < .01$) in the 8 pts with inferior MI, while mean CPK-IS was not different in both groups. CPK-IS and PYP area correlated well ($r = 0.90$) in anterior MI but only fair ($r = 0.59$) in inferior MI. We conclude that TL is more accurate than PYP in detecting and localizing AMI in pts without prior MI and PYP may fail to identify small AMI. Infarct size can be estimated from areas of PYP uptake in anterior AMI but frequently underestimates the size of inferior AMI.

QUANTITATION OF SERIAL MYOCARDIAL SCINTIGRAM IN PATIENTS WITH ACUTE MYOCARDIAL INFARCTION. J.R. Logic, J.A. Mantle, W.J. Rogers, R.O. Russell, C.E. Rackley, University Hospital and Veterans Administration Hospital, Birmingham, Ala.

Serial radionuclide scintigrams were obtained in patients with acute myocardial infarction to identify, quantitate, and calibrate the ischemic area and to correlate these data with serial hemodynamic measurements and infarct size estimated by the MB-fraction CPK enzyme technique. Thirty-one randomized patients were studied in a Myocardial Infarction Research Unit; all were instrumented with a Swan-Ganz catheter and the pulmonary artery end-diastolic pressure (PAEDP) and cardiac index were monitored. Total CPK and MB isoenzyme were measured at 3-hour intervals for 96 hours. Scintigrams were obtained with a mobile gamma camera following the injection of 12-15 mCi of Tc-99m polyphosphates within the first 24 hours after onset of symptoms and repeated 48 hours later.

Maximal ischemic area on the scintigrams was calculated as the area of an elipse. Blood pool and transmission images were routinely recorded. A standardized solution of glucose-insulin-potassium was infused in 16 patients for 48 hours. Control patients received a standard intravenous solution. Positive scintigrams were obtained in 15 of 16 patients having enzyme evidence of infarction. One patient had serial negative scintigrams with an antero-lateral infarction; another remained positive from a previous infarction. Scintigraphic ischemic area size did not change in the majority of patients during the 48-hour intervention.

Scintigraphic ischemic area images did not correlate well with infarct size estimated from enzymes, suggesting that these techniques measure different parameters during infarction. Three patients experienced extension or reinfarction following the intervention and demonstrated an increase in scintigraphic areas. Scintigraphy appears valuable in quantitating myocardial infarction.

TECHNETIUM-99M PYROPHOSPHATE DETECTION OF PERIOPERATIVE MYOCARDIAL INFARCTION IN CARDIAC SURGERY PATIENTS. W. Robin Howe, Jack K. Goodrich, Fred P. Bruno, Robert H. Jones, Andrew S. Wechsler, and H. Newland Oldham, Jr.
Duke University Medical Center, Durham, N. C.

Establishing a diagnosis of myocardial infarction following cardiac surgery continues to be a difficult clinical problem. In an effort to define the usefulness of Technetium-99m Pyrophosphate myocardial imaging in this setting, seventy adult patients undergoing cardiac surgical procedures were studied. All patients survived the operation with one late death. Thirty-one patients (44%) were scanned preoperatively as part of their routine evaluation. Of these, 5 patients had abnormal scans; in 2 the abnormal uptake increased following surgery suggesting new myocardial injury. A total of 14 patients (20%) developed abnormal scans following surgery. Ten of these showed EKG changes diagnostic of new myocardial infarction; the remaining 4 showed nondiagnostic ischemic changes on EKG. Two additional patients developed EKG evidence of new infarct with normal scans and 4 patients showed equivocal uptake of radioisotope without EKG changes. Surgically related noncardiac uptake of isotope appeared in 4 patients without infarction and occasionally required special views for definition.

The results of this study demonstrate that postoperative myocardial scanning with Technetium-99m pyrophosphate is a sensitive and accurate method for detecting myocardial damage following cardiac surgical procedures. In addition, it has proved to be extremely helpful in the preoperative evaluation of patients. However, care must be taken to insure against misinterpretation of surgically induced artifacts.

TUESDAY, 10:30-12:00 BALLROOM B

RADIOPHARMACEUTICAL SCIENCE 1

Chairman: Katherine A. Lathrop
Co-Chairman: William C. Eckelman

SYNTHESIS AND STRUCTURAL EFFECTS OF SELECTIVE BILIARY EXCRETION OF HALOGENATED INDOTRICARBOCYANINES. S. Reiffers, R.M. Lambrecht, and A.P. Wolf, Chemistry Department and A. Ansari and H. Atkins, Medical Research Center, Brookhaven National Laboratory, Upton, N.Y.

Five indotricarbocyanines of structure I were synthesized and labeled with I-131 in the 5 position. The sub-

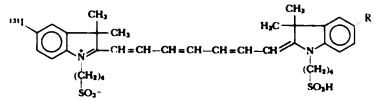

stituent was varied with R = H, F, Cl, Br and I. The dynamics of hepatic uptake and/or blood clearance of the labeled compounds were determined in mice. Kidney uptake in all cases was negligible. The hepatic excretion displayed 2 components. The initial hepatic disappearance rate of R = H and R = F were 7.3 and 4.5%/min respectively. The maximum liver activity in mice occurred at 2-5 min and the % remaining in the liver at 0.5 hr was 3.6%, 8.5%, 19%, 29% and 47% for R = H, F, Cl, Br and I substitution. It is surprising that a small change in the substituent at the 5' position in the molecule has such a pronounced effect. Whether electronic and/or steric effects are controling the mechanism of hepatobiliary clearance is not obvious. A correlation of the liver activity with the covalent radius of R was noted. The comparative studies were at an injected dose of 0.4-0.6 μmole/kg, and typically at a specific activity of 200 mCi/mmole. Loading dose effects were not appreciable under these conditions.

The compounds were synthesized in an attempt to find an analog of indocyanine green which can be more readily prepared than excitation labeled Iodine-123 ICG. The results suggest that I with R = H labeled with I-123 or R = F labeled with F-18 are potential radiopharmaceuticals for dynamic hepatobiliary function studies. This work was supported by ERDA and NIH Grant No. 5 P41 RR00657.

COMPARISON OF ONCOPHILIC RADIOPHARMACEUTICALS IN TUMOR BEARING RODENTS. Gerald DeNardo, Kenneth Krohn, Sally DeNardo, Jeanne Meyers. University of California, Davis,CA.

The ultimate tumor-localizing radiopharmaceutical has not been found. Several agents have proved useful, but there is diversity of opinion regarding which oncophilic radiopharmaceutical is most efficacious. To obtain information on this issue, the distributions of *I-fibrinogen, four bleomycins, Ga-67-Cit and *I-HSA have been determined serially over 48 hours in mice bearing three different tumors. Tumors were of mammary adenocarcinoma type: MMI was slow growing, MMII intermediate and KHJJ more rapid growing.

Greater amounts of all oncophilic radiopharmaceuticals localized in KHJJ tumors than in others. Tumor/blood and tumor/muscle were greatest in KHJJ. These results were not caused by differences in intravascular space (*I-HSA) and probably represent differences in tumor biology. The maximum absolute tumor concentrations of *I-Fib (11.8%) and Ga-67-Cit (10.5%) were greater than those of the other radiopharmaceuticals and were ten times greater than expected from intravascular space. The maximum tumor concentration of *I-Bleo was 100 times greater than expected from intravascular space and significantly greater than the maximum tumor concentrations achieved by other labeled bleomycins. Maximum concentrations of *I-Fib and the radiobleomycins were achieved within hours after IV administration, whereas the *I-HSA and Ga-67-Cit required 1-2 days. Maximum tumor/blood and tumor/muscle ratios for all radiopharmaceuticals were achieved at 1-2 days. *I-Bleo had the best tumor/blood ratio (30.7) followed by Ga-67-Cit (13.3).

In summary, the bleomycin with the best biologic characteristics was *I-Bleo. In view of the large amount of *I-Fib which concentrated in tumors, if fibrinogen can be modified to increase its blood clearance without impairing its localization in tumors, I-123-Fib could become a useful general oncophilic radiopharmaceutical. (Supported by American Cancer Society Grant DT-45.)

CARBON-11 LABELED N-METHYL 1,4 DIAMINOBUTANE: A PUTRESCINE ANALOG FOR PROSTATE AND TUMOR LOCALIZATION. Michael J. Welch, R. Edward Coleman, Maria G. Straatmann, Barbara E. Asberry, Joan L. Primeau, William R. Fair and Michel M. Ter-Pogossian. Washington University School of Medicine, St. Louis, Mo.

Putrescine (1,4 diaminobutane) was methylated by the addition of carbon-11 labeled formaldehyde to 1 mg of putrescine in 0.25 cc pH 7.9 buffer followed by 10 µmole of sodium borohydride. The C-11 formaldehyde was formed via C-11 methanol by adding lithium aluminum hydride to the C-11 carbon dioxide formed in the cyclotron target. After hydrolysis the methanol was catalytically converted into formaldehyde. Labeling yields in excess of 70% were obtained and the methylated putrescine was purified by neutralization and boiling of the solution. The boiling decomposes excess sodium borohydride and removes C-11 labeled formaldehyde and methanol by evaporation. The overall reaction from C-11 carbon dioxide takes 15 minutes and the final radiochemical purity determined by high pressure liquid chromatography is >90%. Ten mCi of methylated putrescine has been formed from 50 mCi of carbon dioxide.

The organ distribution in male rats was very similar to that previously obtained using tritiated putrescine with ventral and dorsal prostate to abdominal wall muscle ratios of 8.8 and 10.1 respectively being obtained 40 minutes after injection. In tumor bearing (B-16 melanoma) mice the tumor to blood ratios were 9.6 and 8.0 thirty and fifty minutes after injection, and the tumor to muscle ratios were 4.1 and 6.6 thirty and fifty minutes after injection. This animal data shows that methylated putrescine has potential for prostate and tumor localization, especially if used in conjunction with a positron device such as the PETT scanner.

(This work was supported by USPHS Grant No. 5 PO1 HL13851.)

SYNTHESIS OF RADIOLABELED ENZYME INHIBITORS OF THE ADRENAL CORTEX. D.M. Wieland, R.D. Ice, and W.H. Beierwaltes, College of Pharmacy and Division of Nuclear Medicine, The University of Michigan, Ann Arbor, Mich.

Many enzyme inhibitors possessing aniline or pyridine residues are known to reversibly bind with enzymes of the adrenal cortex. A series of H-3 and I-125 labeled analogs of these compounds was synthesized to determine if a reversible enzyme inhibitor can achieve diagnostic localization in the adrenal cortex. The 20α-hydroxylase inhibitor 4-aminoglutethimide, 11β-hydroxylase inhibitors metyrapone and SKF-12185, 17α-hydroxylase inhibitor SU-1063 were H-3 labeled by catalytic exchange of the parent compounds with HTO/Pt/acetic acid. Specific activities were 1-2 mCi/mg for the aniline compounds and 10-16 mCi/mg for the pyridine derivatives. Both 4-aminoglutethimide and SKF-12185 were radio-iodinated with nascent Iodine-125 in refluxing ethanol to give monoiodination ortho to the aromatic amine function. Radiochemical yields of 20-35% and specific activities of 85-400 µCi/mg were obtained. The adrenal uptake of 4-aminoglutethimide I-125 was specific activity dependent. A positional isomer of 4-aminogluthethimide, 3-aminoglutethimide H-3, showed a ten-fold lower adrenal uptake than 4-aminoglutethimide H-3.

Metyrapol, the major metabolite of metyrapone, was H-3 labeled by NaBH4-reduction of metyrapone H-3. Phenylmetyrapol H-3 and methylmetyrapol H-3 were synthesized by reaction of metyrapone H-3 with phenyllithium and methyllithium respectively.

Metyrapol H-3 showed the highest uptake (8.9 %Kg dose/gm at one hour) in the dog adrenal. SKF-12185 I-125 gave the highest uptake (4.5 %Kg dose/gm at one hour) of the radioiodinated compounds.

The present study shows that diagnostic concentrations can be achieved with labeled reversible inhibitors of organ specific enzymes.

TUESDAY, 10:30-12:00 BALLROOM C

BONE/JOINT 1

Chairman: G. T. Krishnamurthy
Co-Chairman: Hirsch Handmaker

SCINTIGRAPHIC ASSESSMENT OF FACIAL-MANDIBULAR ABNORMALITIES. Gary F. Gates, and Michael L. Goris. Stanford University, Stanford, Ca.

Facial-mandibular abnormalities are detected by bone scanning but anatomic localization of lesions may be imprecise and misleading unless multiple, properly positioned views are obtained. Eighty-eight patients with such abnormalities were studied with Technetium-99m labeled phosphate compounds. Three anterior views (one straight view with the canthomeatal line perpendicular to the plane of the scintillation crystal, a second with the canthomeatal line shifted to form a 60 degree angle with the crystal surface, and a third similar to a Waters projection with the canthomeatal line further shifted to 45 degrees), 25 degree oblique orbital, and lateral scintigraphic projections of the facial area were obtained as indicated and correlated with transmission scintigrams of a dried skull placed in these same positions. Thallium-201 was used for transmission scintigraphy as its 69 - 80 Kev emission was suitable for photoelectric absorption by bone and detection by a scintillation camera. Abnormalities were discovered in 125 separate anatomic regions: 46 in alveolar ridge, 22 maxilla, 20 temporomandibular joint (TMJ) region, 19 supraorbital, 10 mandible, 6 zygoma, and 2 in the sphenoid (involving orbit and pterygopalatine fossa). Pathologic processes included: 45 inflammatory reactions, 33 neoplasms, 11 surgical effects, and 8 radiation effects. Interpretation of frontal views alone may be limited by superimposition of zygoma on TMJ, medial maxilla on upper alveolar ridges, pterygopalatine fossa on maxilla, and lesions in a single alveolar ridge upon each other. Lateral and oblique views separate these areas but in turn superimpose other structures. Multiple, carefully positioned views allow for accurate localization of abnormalities which is crucial if radiation therapy, biopsy, or corroborative radiographic studies are planned.

RADIONUCLIDE ARTHRITIS INDEX WITH Tc-99m EHDP FOR EVALUATION OF RHEUMATOID ARTHRITIS. H. M. Park, S. A. Terman, A.S. Ridolfo, Nuclear Medicine, Radiology Department, Indiana University and Lilly Clinic, Indianapolis, Ind.

Because of frequent involvement of the periarticular and subchondral bones in arthritis, Tc-99m EHDP was evaluated as a quantitative scanning agent. 10 adult rheumatoid arthritis patients and 15 control patients were studied.

Following an IV administration of 20 mCi of Tc-99m EHDP, activity countings over specific joints and adjacent non-articular bones were obtained using a thyroid uptake probe and a gamma camera with a specially designed lead template with paired windows.

The hourly counting of the joints up to 5 hours demonstrated double exponential uptake pattern reaching a plateau at 4-5 hours. The mean net joint uptake at 5th hour in rheumatoid knees was 1,000 cps/mCi compared to a normal knee of 400 cps/mCi. The joint to background bone ratio increased with time up to 5 hours. The ratio at 4th hour (Radionuclide Arthritis Index-RAI) of frequently involved joints of rheumatoid patients and of control patients are shown in the table below. At the RAI of 1.8, an involved or a normal joint could be distinguished with a 95% accuracy (132 of 136 joints studied). In a limited new drug trial, changes in RAI correlated well with the clinical response to the therapy.

Radionuclide Arthritis Index using Tc-99m EHDP may be a useful quantitative parameter in the evaluation and follow-up of rheumatoid arthritis.

Mean Value of Radionuclide Arthritis Index

	MCP	Elbow	Knee	Ankle
Normal	1.29 ± 0.28	1.38 ± 0.12	1.38 ± 0.22	1.22 ± 0.22
R.A.	3.24 ± 1.00	3.29 ± 1.94	2.62 ± 0.52	3.00 ± 0.78
p.	<0.001	<0.01	<0.001	<0.001

DETECTION OF TOTAL HIP ARTHROPLASTY COMPLICATIONS WITH Tc-99m PYROPHOSPHATE. R. J. Campeau, M. F. Hall, and A. Miale, Jr. University of Miami, School of Medicine, Miami, Fl.

Total hip arthroplasty (THA) is associated with certain complications which result in a painful hip. Many of these, e.g. prosthetic dislocation, fracture, trochanteric avulsion, and heterotopic calcification are easily diagnosed by conventional radiography. However, radiographic evaluation for infection and/or loosening of the prosthesis often contributes little to the resolution of the diagnostic problem. Unfortunately, one or both of these two complications are the most frequent causes of hip pain after a THA.

Tc-99m PYP scintigraphy was studied as a potential method for identification of THA complications. PYP hip scintigraphy was performed in 36 patients pre and post-operatively and at various time intervals up to 54 months. In the uncomplicated THA, increased PYP activity occurred in all patients for the first 3 months. By the third to sixth month, the acetabular and femoral shaft areas returned to normal activity levels. A trace of activity persisted in the greater trochanter when osteotomy was performed. All symptom free patients had normal activity in the femur after six months; only one patient had persistent acetabular activity as long as six months post-op. Increased activity in the acetabulum and/or femur six months or more post-op was observed in 16 symptomatic patients who had loosening and/or infection of the prosthesis. In 7 of these patients no radiographic abnormality was evident. In 3 proven infected THA's, radioactivity was markedly increased while radiographs including arthrograms showed no evidence of infection or loosening. No patient with a proven complication had a normal scan. PYP hip scintigraphy deserves wider clinical application in patients who develop hip pain after a THA.

NUCLEAR MEDICINE TECHNIQUES IN THE EVALUATION OF POSTMENOPAUSAL OSTEOPOROSIS. Charles H. Chesnut III, Wil B. Nelp and Tom K. Lewellen. University of Washington Hospitals, Seattle, Washington.

Diagnostic procedures in postmenopausal osteoporosis should ideally identify the presence of osteoporosis, quantitate its severity, and assess its response to therapy. The techniques of total body calcium determination by neutron activation analysis (TBC-NAA), regional bone mass by ^{125}I photon densitometry (RBM-PD), and radionuclide bone imaging may provide such data by accurately and precisely quantitating total or regional bone mass, and by establishing relative skeletal metabolic activity.

The TBC-NAA procedure provides precise (± 2%) and accurate (± 5%) assessment of total bone mass. Current data suggests the technique does discriminate diagnostically between compression fracture osteoporotic females and age/sex-matched normals, and also assesses severity. The technique's value in assessing response to therapy is well proven by serial total bone mass change following I.V. calcium infusion (negative effect) and the anabolic steroid methandrostenolone (Dianabol) (positive-effect).

Data obtained by the RBM-PD technique from the SI site of distal radius (cortical and trabecular bone) provides regional bone mass with however an 8% error (SEE ± 60 grams) in predicting TBC from RBM. While the technique may precisely quantitate regional bone mass, whether the technique may discriminate compression fracture osteoporotics from normals, and assess response to therapy, remains to be proven.

Radionuclide bone imaging with ^{99m}technetium-polyphosphate provides assessment of current skeletal metabolic activity and correlates well with clinically active or quiescent disease, as opposed to the radiograph which establishes only the presence of compression fractures of indeterminate age and may have little correlation to the clinical state of the disease.

PATTERN OF DISTRIBUTION OF METASTATIC BONE DISEASE IN MAN. G. T. Krishnamurthy, J. M. Hiss, Jr., Manuel Tubis, and W. H. Blahd. Veterans Administration Wadsworth Hospital Center, and UCLA School of Medicine, Los Angeles; and Santa Monica Medical Center, Santa Monica, CA.

A clinical study was undertaken to find out whether or not there was any need to image the small and medium size bones of the rib cage and distal extremities in 62 patients with known soft-tissue cancer. Total body bone images were obtained with a scintillation camera fitted with a divcon collimator, 3-4 hr after 15 mCi of Tc-99m pyrophosphate. Individual bone lesions were counted for each anatomic site and the number of bone lesions were correlated with serum alkaline phosphatase.

The overall distribution of 403 bone lesions in 62 patients was 26% in ribs, 22% thoracic, 10% lumbar, 4.9% cervical, and 2.5% in sacral vertebrae, 9% skull, 10% in small bones of the extremities which include hands, forearms, feet, legs, and ankles. Forty-three percent of the lesions were in ribs in patients with lung cancer as against only 13% in patients with breast cancer. Serum levels of alkaline phosphatase when elevated, correlated with the number of bone lesions (r=0.78), but in 9 patients with definite bone lesions (total 21), the alkaline phosphatase was within normal limits.

Even though the breast cancer lies in very close proximity to the ribs anatomically, cancer of the lung shows relatively more predilection for rib metastases. The results of this study indicate that it is essential to include small bones of the distal parts of the extremities during imaging in the pursuit of metastatic bone disease, and that the serum levels of alkaline phosphatase are poor indicators of early bone lesions even though the levels, when elevated show good correlation with the total number of bone lesions. Of interest to note that several of the bone lesions detected in the camera studies were not visualized in the images obtained with the scanner.

DYNAMICS OF F-18 AND Tc-99m-HEDP UPTAKE IN NORMAL AND ABNORMAL BONE. A.Creutzig, K.-G.Gerdts, and H.Creutzig, Institut für Nuklearmedizin, Med. Hochschule, Hannover, West Germany

There is a difference in the bone uptake of different bone seeking radionuclides (BSR) in the same animal and a difference in the uptake of the same BSR in different species of animals. Again there is a difference of uptake in normal and abnormal bone. Measurement of bone uptake in one species of laboratory animal is inadaequate to determine the clinical usefulness of a BSR for special indications of bone scanning.

Therefore we compared the uptake and its dynamics in the experimental fracture of rabbits and beagles during healing or developing hypertrophic pseudarthrosis. The following data of F-18 and Tc-99m-HEDP studies were compared with intra-vitam staining and microautoradiographs: total activity in the fracture region and in

normal bone 5 and 120 min p.i., their relationship ("perfusion-corrected activity PCA"), the accumulation curve integrals - all data corrected for background activity - and k_1 and k_2 using a open two-compartment model.

Best correlation was found between intravitam staining as part of bone metabolism and compartimental analysis of fluorine uptake. Next in correlation was the F-18-PCA.

Bone scanning for measurement of bone metabolism in non-malignant disease should be done with Fluorine-18 as sequential scintigraphy to determine the PCA as a good fit for bone metabolism.

Supported by a grant of Deutsche Forschungsgemeinschaft, Bonn-Bad Godesberg (Cr 52/1)

QUANTITATIVE BONE IMAGING AS A SCREENING METHOD FOLLOWING RADIATION THERAPY. David A. Weber, George A. Wilson, Robert E. O'Mara, Philip Rubin, Henry Keys, and Margaret Jaconski. University of Rochester Medical Center, Rochester, N.Y.

The need for screening methods to assess irradiated sites for residual tumor involvement or possible reactivation of disease has been a major problem in the clinical management of patients undergoing radiation treatment for metastatic bone disease. As a possible solution to this problem, an investigation has been initiated to evaluate the potential use of quantitative bone imaging with Tc-99m pyrophosphate to assess bone repair or tumor extension at sites of osseous metastases treated with radiation therapy.

Serial quantitative bone images obtained in patients pre- and post-radiation treatment are correlated with periodic radiographs of the irradiated field, the dose fractionation schedule, pertinent blood chemistries, the clinical symptomatology, the time post-treatment and the type of primary tumor. The initial group of patients included in the study have shown markedly different uptake patterns in serial studies following radiation therapy. Variations in uptake at treatment sites are observed to change by as much as a factor of two, within a four week period. Although no single pattern of uptake change can be specified as an indicator of tumor response to treatment at this time, the observed findings provide significant information for the interpretation of uptake changes at sites of treated metastases. The quantitative bone imaging procedure appears to be a sensitive measure of both changes in bone metabolism and of blood perfusion at treatment sites.

TUESDAY, 2:00-3:30 BALLROOM A

NEUROLOGY 1

Chairman: Frederick S. Mishkin
Co-Chairman: C. Douglas Maynard

ANATOMY OF VENOUS STRUCTURES IN NORMAL BRAIN SCANS. Dennis D. Patton, and Richard E. Moore. University of Arizona Medical Center, Tucson, Az., and Vanderbilt University Hospital, Nashville, Tn.

Activity in normal brain scans done with the usual Tc-99m preparations resides mainly in vascular structures and extracellular fluid. The compartment having the greatest activity is the venous pool. To identify the venous structures seen on brain scans a cadaver study was designed. The cerebral vessels of 3 cadavers were cleared of blood and clots; the neck vessels were clamped and cannulated. A suspension of Tc-99m pertechnetate and barium sulfate in warm gelatin was injected into the jugular veins so as to fill the venous side of the circulation. The viscous gelation prevented filling of the capillary or arterial vessels. Radiographs and scans of the cadaver head were taken in the same projections and were correlated.

Venous structures identified include the large dural sinuses as well as cortical veins and superficial anastomotic veins (Labbé, Trolard, Sylvian). Deep veins (Galen, straight sinus) were dimly seen on scans. The study provided good correlation of venous structures seen on scans with their size and depth.

A mound of activity frequently seen at the base on anterior and posterior views of brain scans was found to represent the cavernous sinus, which may appear as a mound or as an inverted V. It can interfere with interpretation of the suprasellar area on anterior views, and of the posterior fossa on posterior views.

The temporalis muscle was found not to contain enough activity to account for the "temporalis activity" seen on lateral views. The Sylvian plexus of veins is a more likely explanation.

CEREBRAL RADIOISOTOPE ANGIOGRAM: THE SIGNIFICANCE OF INCREASED EXTERNAL CAROTID CIRCULATION. Gary Watts, Ismael Mena, Stanton H. Joe. Division of Nuclear Medicine, UCLA-Harbor General Hospital Campus, Torrance, Ca.

Cerebral radioisotope angiography (CRAG) is primarily used in diagnosing intracranial disease. The rapid accumulation of activity in the nasopharyngeal area during the arterial or capillary phase ("hot nose" phenomenon) has been noted to occur with internal carotid arterial occlusion or increased intracranial pressure.

In 387 consecutive Tc-99m pertechnetate CRAG's we established objective criteria for identifying the presence of a "hot nose" in the anterior and lateral positions and to define the entities associated with this phenomenon. Fifteen patients were found to have increased nasopharyngeal activity on anterior CRAG, 12 of whom were subsequently studied with lateral CRAG.

Time/activity curves were generated from lateral CRAG in the nasopharyngeal and suprasellar regions-of-interest (ROI). The build-up time (initial rise to peak activity) and peak activity/plateau ratio were obtained in the 12 "hot nose" and 12 control patients.

	Build-up Time, sec. (mean ± S.D.)		
ROI	Hot Nose	Control	
Nasopharyngeal	7.0 ± 1.6	9.3 ± 1.7	$p < 0.01$
Suprasellar	6.4 ± 1.4	6.6 ± 1.4	
	Peak/Plateau Ratio		
Nasopharyngeal	1.8 ± 0.25	1.0 ± 0	$p < 0.001$
Suprasellar	2.73 ± 0.64	2.55 ± 1.54	

Of the 15 patients who had a "hot nose" on CRAG only 4 have internal carotid occlusion and none had increased intracranial pressure. Of the other 11 patients 8 were on large doses of psychotropic drugs and 3 were anemic. The mechanism of action of psychotropic drugs in patients with a "hot nose" is through increasing blood flow in the external carotid circulation.

PROGNOSTIC VALUE OF RADIONUCLIDE ANGIOGRAPHY IN CEREBRAL VASCULAR DISEASE. Ivan R. Barrett, Fred D. Powell, and Fred S. Mishkin. Martin Luther King, Jr. General Hospital, Los Angeles, Calif.

In order to ascertain the prognostic value of the radionuclide angiogram in ischemic cerebral vascular disease, we reviewed, of over 2200 who underwent this procedure, 175 cases in which the arterial phase showed decreased activity. Thirteen of 175 probably represented increased perfusion to one hemisphere related to seizures rather than ischemia as initially thought. Three of 175 had decreased activity due to subdural hematomata.

Of the 120 cases with ischemic disease and neurologic signs, three patterns appeared during the venous phase: diminished, equal, or increased perfusion. Following the initial incident, the clinical prognosis varied from no change to marked clinical improvement.

Of the 49 patients with diminished venous perfusion, 90% showed no change from the initial incident. In the 12 with equal hemispheric venous perfusion, the results were similar. Of the 59 with increased venous perfusion 54% showed no clinical improvement.

In the first two groups with either diminished or equal venous perfusion, the chances against improvement are greater than 6:1. A majority of the patients that died were in these two groups. In the last group with increased venous activity, the chances for improvement or deterioration are equal.

The data suggests that the increased activity during the venous phase represents collateral blood flow and a better clinical prognosis.

SIX YEARS OF EXPERIENCE WITH DYNAMIC-STATIC BRAIN SCANNING IN THE DIAGNOSIS OF CHRONIC SUBDURAL SPACE LESIONS. Severiano Valenzuela, Anton N. Hasso and Carl Jansen, Loma Linda University Medical Center, Loma Linda, Calif.

The authors will present their investigation of the accuracy and the role of the static and dynamic brain scan in screening for chronic subdural space lesions (CSDL) and a new classification of the different dynamic and static scan patterns found in pathologically proven cases of chronic subdural hematoma (CSDH).

All brain scans and neurosurgical procedures done between January, 1969 and June, 1975 were reviewed for the diagnosis of CSDH. Only those patients who had either a brain scan with a diagnosis (classical or suggestive) of CSDH or surgically proven CSDH with a presurgical brain scan were selected. Our technique for the dynamic-static brain scan has been reported elsewhere.

Of 113 patients studied, 111 had a retrospective scan diagnosis of CSDH. Of these 57 had proven CSDL, 48 of which were surgically proven CSDH. Of 43 cases with a scan classical of CSDH, 39 (91%) were proven CSDH. Of 69 patients with interpretable dynamic studies, 39 were of the CSDL group with 29 of these being positive (74%). In patients with non-subdural lesions, the dynamic study was negative in 19 of 30 cases (63%). In the 48 surgically proven CSDH, the static scan was positive in 96% while the dynamic study was positive in 74% of the cases (28 of 38). Four different patterns were found in the dynamic and static scans in surgically proven cases of CSDH.

The static brain scan continues to be accurate in the diagnosis of CSDH. The dynamic study proved helpful only when it was positive as an adjunct to the static scan. A negative dynamic study did not help in the diagnosis. By itself, the dynamic study is not sufficiently accurate in the diagnosis of CSDH. A classification of the dynamic and static scan patterns found in CSDH may be useful.

THE EFFECT OF DEXAMETHASONE UPON THE ACCUMULATION OF MEGLUMINE IOTHALAMATE AND TECHNETIUM PERTECHNETATE IN CEREBRAL TUMORS AS DETERMINED BY COMPUTED TOMOGRAPHY. Ernest F. Crocker, Robert A. Zimmerman, Michael E. Phelps, and David E. Kuhl. Hospital of the University of Pennsylvania, Philadelphia, Pennsylvania.

Dexamethasone therapy is known to suppress the accumulation of technetium pertechnetate in cerebral tumors. It has been suggested that meglumine iothalamate (Conray) accumulates in cerebral tumors by a similar mechanism to technetium pertechnetate. Our purpose was to determine whether dexamethasone also suppressed the accumulation of meglumine iothalamate in cerebral tumors reducing their enhancement on computed tomography.

Four primary brain tumors and four cerebral metastases were investigated over the 7 month period ending January 1976. The lesions were examined by x-ray computed tomography (EMI scanning) with and without contrast enhancement and by radionuclide computed tomography (Mark IV scanner) using technetium pertechnetate. These studies were performed both prior to and during dexamethasone therapy.

Steroids significantly reduced the level of accumulation of both technetium pertechnetate and iothalamate in each of the cases investigated. The effect was apparent within 24-hours of the commencement of dexamethasone therapy.

Results confirmed that the avidity of a tumor for technetium pertechnetate and its degree of contrast enhancement on EMI scanning are significantly reduced by dexamethasone therapy. This effect may lead to problems in the interpretation of progress EMI scans of patients with cerebral tumors who have been commenced on steroid therapy.

THE EFFICACY OF INTRAVENOUS SODIUM PERCHLORATE IN CHOROID PLEXUS BLOCKING. John D. Scheu, Marc R. Tetalman, Otaviano Araujo, Richard A. Sheriff. Ohio State University, Columbus, Ohio.

Intravenous administration of sodium perchlorate eliminates many of the problems associated with oral administration of perchlorate prior to brain imaging: poor G.I. tract absorption, comatose patient, and nursing errors. A study was conducted to determine the optimum intravenous dose of sodium perchlorate which would have maximal blocking effect with the least amount of injection side effects.

A sterile, pyrogen free solution of sodium perchlorate was added to a syringe containing 15 mCi of Tc99m-pertechnetate and both were injected simultaneously. Post injection side effects were recorded, such as arm pain, nausea, headache. Brain imaging was performed with a scintillation camera 60 minutes following injection. The choroid plexus uptake of Tc99m-pertechnetate was rated independently by 2 observers into 3 categories: distinct visibility, trace visibility, and no visibility.

Previous experience has shown that doses of less than 300 mg of sodium perchlorate were not ideal. Doses of 300 mg, 400 mg, 450 mg, and 600 mg were evaluated and compared. At 300 mg, 19% of 141 patients had positive uptake of pertechnetate in the choroid plexus; at 400 mg, 12% of 202 patients had uptake; and at 450 mg, 7.7% of 207 patients showed uptake. Doses of 600 mg were evaluated briefly, but the study was terminated because of severe transient local pain upon injection. Localized transient pain, the major side effect, was observed in 2% of the cases with 300 mg, 5% with 400 mg, and 4.8% with 450 mg.

Intravenous sodium perchlorate, circumventing the problems of oral administration, was found to be a safe, easily administered, and economical method of blocking choroid plexus uptake of Tc99m-pertechnetate. An adult dose of 450 mg was found to be optimum.

TUESDAY, 2:00-3:30 BALLROOM B

INSTRUMENTATION 1

Chairman: William R. Hendee
Co-Chairman: Bryan Westerman

A MOSAIC INTRINSIC GERMANIUM RADIOISOTOPE SCANNING DEVICE. J.A. Patton, R.R. Price, A.B. Brill, and R. Pehl, Vanderbilt University, Nashville, Tn. 37232* and Lawrence Berkeley Radiation Laboratory, Berkeley, Ca.

Clinical evaluations of semiconductor detectors with energy resolutions vastly superior to that of NaI(Tl) have been limited due to the relatively small size of currently available detectors. We have designed and fabricated a 9 element array of intrinsic germanium detectors for a high resolution scanning device to be used in conjunction with radioisotopes in diagnostic studies in nuclear medicine. The detectors are 35mm in diameter by 10mm thick and are positioned in a 3x3 array with 50mm between centers. All detectors are housed in a common cooling system. The energy resolution of the detectors range from 1.06 to 1.18 Kev at 140 Kev. The crystals and associated electronics are very closely matched with a maximum deviation in sensitivity of 15% from the average for the uncollimated detectors. Each detector is connected to a separate preamplifier, linear amplifier, and two SCAs and is interfaced to our PDP-9 and PDP-11 computers by CAMAC data acquisition systems.

For routine frontal plane scanning 19 hole focussed collimators with a FWHM resolution of 0.23 in. and a focal length of 3.25 in. have been designed and constructed. A mounting system has been designed and is currently being fabricated to support the detectors, collimators, and electronics. The system will be suspended over a computer-driven scanning bed and will remain stationary while the patient is moved in an x-y raster beneath the system.

Comparing the relative surface areas and sensitivities, we expect the system to be about 40% as sensitive as a 5 in. NaI(Tl) crystal at 140 Kev and thus should permit an adequate study of the capabilities of a semiconductor scanning system in a routine clinical environment.

*Supported in part by ERDA contract #AT-(40-1)-2401 and NIH grant #1 R01 GM 21722-01.

NOISE ANALYSIS OF ANNULAR APERTURE IMAGERY. R. G. Simpson, H. H. Barrett. Optical Sciences Center and Dept. of Radiology, University of Arizona, Tucson, AZ.

The increased collection efficiency of coded apertures compared to conventional collimators does not necessarily mean improved signal-to-noise source. The larger the object, the greater the additional noise. This paper reports

a detailed analysis of this effect in the case of an annular coded aperture.

A single annular aperture has an inherent field-of-view limitation (1) that can be overcome by using two or three annuli, but the analysis here was restricted to the case of a single annulus. Objects larger than 10 cm in diameter were therefore not considered. The signal-to-noise ratio and exposure time relative to a pinhole were calculated as a function of number of counts, object size, overall system resolution and processing algorithm for uniform disc objects.

The results show that, even for the worst case considered, the annular coded aperture image enjoys a factor of 3 advantage in exposure time over a pinhole camera operating at the same magnification and resolution. To test the theory, noisy processed images were in good agreement with predicted values. Fair agreement was also found for real images obtained with a scintillation camera.

In conclusion, for all cases considered, the annulus used with an Anger camera offers a distinct exposure advantage over the pinhole collimator. This advantage, combined with the tomographic capability, make the annulus attractive for imaging organs such as the heart, kidney and thyroid.

(1) R. G. Simpson, H. H. Barrett, J. A. Subach and H. D. Fisher, Opt. Eng., Sept.-Oct. 1975.

MEASUREMENT OF TOTAL BODY CALCIUM BY ARGON-37 EXCRETION. Tom K. Lewellen, Wil B. Nelp, Robert Murano, Gervas M. Hinn and Charles H. Chesnut. University of Washington Hospitals, Seattle, Washington

A technique to quantitate body calcium in humans by total body neutron irradiation utilizing the $^{40}Ca(n,\alpha)^{37}Ar$ reaction has now been developed.

The facility uses a 14 MeV neutron generator and an irradiation enclosure which surrounds the patient with water from the neck down. Activation uniformity for the $^{40}Ca(n,\alpha)^{37}Ar$ reaction within the area occupied by the patient is $\pm$ 2.7%.

When the ^{37}Ar is formed it is exhaled in the patient's breath and is collected by means of a closed circuit breathing system. Samples can be drawn from the system at any time and stored in gas cylinders. The gas is then purified by selective absorption and the argon is placed in a low-background proportional detector and counted for several hours.

Our studies of the ^{37}Ar excretion rate in humans (J. Nucl. Med. 16:672, 1975) indicate that breath collection may be required for 1 to 5 hours post irradiation. Quantitative studies have been undertaken comparing the total ^{37}Ar activity exhaled after 1, 3 and 5 hours to total body calcium as determined by an independent ^{49}Ca activation technique. The mean values for the yield of ^{37}Ar expressed as picocuries per Kg of body calcium (20 mrad dose) are 5.3, 7.7 and 8.6 for 1, 3 and 5 hours respectively.

From this we conclude that the uniformity of activation and the consistent ^{37}Ar yield obtained are adequate for TBC measurements in humans at very low levels of irradiation (20 mrad). Studies are continuing to tabulate the accuracy and precision of the method in a large population of subjects.

ESTIMATION OF THYROID GLAND DEPTH AND CORRECTION FOR I-123 UPTAKE MEASUREMENTS. Peter M. Martin, F. David Rollo. V.A. Hospital, San Francisco, CA 94121

One major source of inaccuracy in the conventional method (ORINS) of estimating thyroid uptake of radioiodine lies in the presumption that the depth of the standard source approximates the actual thyroid depth. While the assumption was acceptable for high energy I-131, the variability from different tissue thicknesses for the lower energy I-123 can cause a significant error in uptake measurements. It was the purpose of this study to examine the effect of tissue attenuation on I-123 uptake and to evaluate various methods of correcting the estimated iodine uptake determined in the standard fashion.

Estimations were made of the depth of the thyroid gland, and correction factors were established, for I-123 uptake measurements, using a scintillation crystal detector and a neck and gland phantom. An index for the gland depth was generated by three methods, each based on count ratios for different conditions: 1)gamma photopeak/K shell X ray, 2) gamma photopeak/Compton scatter region, 3) gamma photopeak at two detector distances. The results indicate that a ratio of gamma peak/X ray peak was the most sensitive index of gland depth. The physical principle employed is the tissue absorption on photons of different energies. A calibration curve for the depth correction factor was determined. The curve is sensitive to depth changes, is not significantly dependent on detector distance ($p>.05$), for distances $\geq$18 cm, nor is it dependent on gland size ($p>.25$), within the range of 20 ml to 40 ml. The method has applications for corrections of I-123 uptake measurements as well as corrections of endogenous iodine content, from fluorescent excitation measurements. Clinical measurements on over forty patients indicate that the depth correction by this method can change the uptake by as much as 50%. In several cases this affected the diagnosis.

TUESDAY, 2:00-3:30 BALLROOM C

ONCOLOGY 1

Chairman: Richard C. Reba
Co-Chairman: Samuel E. Halpern

THE ROLE OF COBALT-57 BLEOMYCIN SCANNING IN CLINICAL TUMOR IMAGING. Paul C. Kahn, Cyril Milunsky, Mrinal K. Dewanjee and Richard A. Rudders. Tufts-New England Medical Center, Boston, Mass.

This study evaluated Co-57 bleomycin scanning in a clinical setting in which other nuclear, radiographic and ultrasonic imaging methods were already widely utilized. 83 scans were performed in 80 patients with known malignant disease. Dual probe total body rectilinear scans 4 hours after injection of 1mCi of Co-57 bleomycin and detail camera views were employed. The scans were interpreted blindly as well as together with other pertinent studies, such as gallium, bone, liver, and brain scans.

Positive studies were obtained in 17/27 head and neck tumors. However, remote uptake was seen in only 5 cases, one of which was a false positive. Metastases were missed in 3 cases with uptake in the primary lesion. 11/11 lung tumors gave positive studies with clinically important sites of disease demonstrated in 3 cases. Colon tumors gave positive results in 6/8 instances, with documentation in liver metastases in 2 cases. There were positive scans in 5/7 uterine cancers, but only 1 useful demonstration of remote disease. Only 1/6 lymphoma patients had a positive bleomycin study, although 3 had positive gallium scans. The bleomycin scan failed in 4/4 breast cancer patients, all with widespread disease. There were positive scans in 10/17 miscellaneous tumors, including an adrenal carcinoma, melanoma, medulloblastoma, bladder carcinoma and an osteosarcoma.

We conclude that Co-57 bleomycin scanning may be useful as an initial screening technique in lung cancer, and possibly other anaplastic carcinomas, and in evaluating hepatic metastases in patients with equivocal liver scans. We consider Co-57 inferior to gallium in lymphomas, and are pessimistic about its value in breast tumors. The role of this technique in head and neck and pelvic tumors requires further study.

EFFICACY OF MULTIORGAN SCANNING IN THE STAGING OF EPIDERMOID AND ADENOCARCINOMA OF THE LUNG. Andrew Taylor, Jr., Joseph W. Ramsdell, Naomi P. Alazraki, Sheldon R. Hurwitz, Richard M. Peters, and Gennaro Tisi. VA Hospital and University of California, San Diego, CA.

A prospective study of preoperative patients with suspected lung carcinoma was undertaken to evaluate the effectiveness of routine liver, bone, brain, and gallium scanning in the detection of clinically unsuspected metastases. Scans were compared with the patients' clinical evaluations. Patients with known metastatic disease or oat cell carcinoma were excluded. Of 22 patients subsequently shown to have epidermoid carcinoma, four patients had abnormal brain scans, two had abnormal liver scans, and five had

abnormal bone scans, all suggesting metastatic disease; two gallium scans showed abnormal uptake outside of the thorax. With one exception, all patients had either localized pain, an abnormal physical exam, abnormal liver function test, or elevated alkaline phosphatase to suggest metastatic disease. The exception, one liver scan, was felt to be falsely positive on the basis of laparotomy, open biopsy and one year followup. Of the 21 patients subsequently shown to have adenocarcinoma, one liver scan and one bone scan suggested metastatic disease. All brain scans were normal and there was no abnormal gallium uptake outside the thorax. The patients with the abnormal brain and liver scan had clinically suspected metastases.

In these 43 patients with primary lung cancer, multiorgan scanning failed to reveal unsuspected metastatic disease in the asymptomatic patient with a normal physical exam and normal laboratory parameters. Based on these data, we suggest that liver, bone, and brain scans be obtained only when the clinical and laboratory data suggest the possibility of metastatic disease. Gallium scanning, though not of value in detecting clinically unsuspected extra thoracic metastases, may prove useful in evaluating the resectability of the primary tumor.

EFFICACY OF RADIONUCLIDE PROCEDURES IN STAGING OF BRONCHOGENIC CARCINOMA. Judith A. Operchal, Robert D. Bowen, and R. Barry Grove. VA Hospital Nuclear Medicine Service, Vanderbilt University, Nashville, Tenn.

This study was undertaken to determine the utility of brain, bone, and liver imaging in the detection of occult metastatic disease in patients with bronchogenic carcinoma. The case histories of 178 patients with primary carcinoma of the lung have been reviewed. Staging procedures included radiographic studies, spirometry, bronchoscopy, and brain, bone, and liver imaging with Tc-99m labeled compounds. Most patients had mediastinoscopy performed immediately prior to thoracotomy. There were 79 patients who had no radiographic, bronchoscopic, or other evidence, exclusive of radionuclide studies to suggest the presence of metastatic involvement or unresectable tumors. Radionuclide procedures indicated the presence of occult metastatic lesions in 24 patients (30.4%), who were directed to radiation and/or chemotherapy. There were 4 additional patients (5.1%) with scan evidence of metastatic disease, who were subjected to thoracotomy. Staging procedures were negative in 14 patients (17.7%) who had unresectable lesions at thoracotomy. Analysis of the radionuclide procedures showed that positive studies were obtained in 9 of 61 brain scans (14.8%), 4 of 70 liver scans (5.7%), and 19 of 65 bone scans (29.2%). Patients with oat cell and anaplastic tumors had the highest frequency of scan detected metastatic involvement. Brain scans were positive in 4 of 9 patients (44%) without neurological symptoms. This study demonstrates that radionuclide staging procedures are of considerable importance in the detection of clinically occult metastatic disease in patients with bronchogenic carcinoma. However, in those patients with negative staging procedures, a significant number will be found to have unresectable lesions at thoracotomy. Bone and brain studies are shown to be the radionuclide procedures with the highest yield.

UPTAKE OF 67-GALLIUM IN PAROTID GLANDS OF PATIENTS WITH SJOGREN'S SYNDROME. J.R. Logic, G.V. Ball and W.N. Tauxe. University Hospital and Veterans Administration Hospital, Birmingham, Ala.

We report the observation that gallium-67 (Ga) is intensely retained in the parotid glands of patients with Sjogren's Syndrome (SS) and that the degree of retention is inversely related to the loss of pertechnetate (Tc) transport function. Although benign infiltration of salivary and other tissues by lymphocytes and plasma cells is fundamental to SS, malignant lymphoproliferative involvement may occur. Interest in the development of "pseudolymphoma" or lymphoma in SS led to studies to determine the utility of Ga surveys in such patients.

Seventy-two hour Ga whole body scans were performed in conjunction with Tc flow studies of the parotid glands. Both studies were performed in 14 patients, with parotid enlargement, clinical symptoms suggestive of the sicca complex or other strong evidence of SS. No significant Ga accumulation in the parotid glands was found in 10 patients including 2 in whom parotid enlargement was most likely related to alcohol abuse. Two of the 10 had decreased Tc transport, including 1 patient with modest parotid enlargement, hypergamma globulinemia, reactive rheumatoid factor without arthritis and a normal labial biopsy.

Four patients showed intense Ga retention in the parotid glands and evidence of absent Tc transport. These patients all had SS documented by labial biopsy. One patient reverted to normality following cytoxan therapy. Pheripheral blood lymphocytes from 2 of these 4 patients showed no increased Ga incorporation, in comparison with normals.

Abnormal Ga retention may parallel the loss of Tc transport in SS. Ga retention may occur in those lymphocytes which are secreting B-2 microglobulin in SS.

TUESDAY, 4:00-5:30 BALLROOM A

PULMONARY 1

Chairman: Roger Secker-Walker
Co-Chairman: Robert J. Lull

ESTIMATION OF REGIONAL LUNGVENTILATION USING Kr-81m. M.L. Goris, J.F. Lamb, L.P. Walter, S.G. Daspit, and J. McRae. Dept. of Nuclear Medicine, Stanford University Medical Center, Stanford, California.

The diagnosis of pulmonary embolism is made by the demonstration of a segmental perfusion defect in a region with normal ventilation. But, while the regional perfusion can easily be estimated from the distribution of labeled macroaggregates injected intravenously, the present methods for the estimation of regional ventilation are cumbersome. British investigators (Br. Med. J. 3:673-675, Sept.20,1975) showed that the equilibrium activity of an inert gas administered at a constant rate is proportional to $V(F/V)/(F/V+\lambda)$, where V is the considered lung volume, F/V fractional ventilation rate and λ the decay rate of the tracer. We have investigated the use of on-line Rb81+Kr81m generator, to estimate regional ventilation using this principle. Since λ is of the same order of magnitude (0.693/13 sec) as F/V in a normal lung, poorly ventilated regions never accumulate significant activity levels. The generator is placed on an oxygen line, leading to a nose-mouth mask with adequate openings to room air. The patient is positioned in front of the camera, and breaths at his own pace. When oxygen flow (2L./min) is started equilibrium activity in the lungs is reached within a minute, and using a 2mCi generator 100,000 counts can be collected in 160 seconds. Interruption of the oxygen flow is promptly followed by the disappearance of all activity, so that repositioning can be performed at leisure, and multiple views collected without unduly increasing the radiation burden. Since the energy of Kr-81m is higher (190 keV) than that of Tc-99m, used to label the macroaggregates, the ventilation study can be performed immediately following an abnormal perfusion study. The method is easy and convenient for sick and well patients.

COMPARISON OF Kr-81m VENTILATION Tc-99m MICROSPHERE PERFUSION SCANS AND STANDARD CHEST RADIOGRAPH IN ASSESSMENT OF REGIONAL LUNG FUNCTION. Ferruccio Fazio, Peter Lavender, R.E. Steiner Hammersmith Hospital, London, U.K.

The purpose of the present paper is to examine the ability of chest radiographs to assess regional lung function in comparison with ventilation perfusion scintigraphy. Four groups each of 20 patients were studied; emphysema, airways obstruction (chronic bronchitis and asthma), pulmonary embolism, left heart disease. Each patient had a standard chest x-ray (CXR) anterior and lateral view, and ventilation/perfusion scans in 4 views. Perfusion (Q) scans were obtained after I.V. injection of Tc-99m microspheres; ventilation scans (V) following continuous inhalation of Kr-81m. This technique produces high quality functional images of regional ventilation during tidal breathing. (Fazio & Jones, Brit.Med.J.3,673,1975). CXR and scans were independently scored to assess required V/Q and correlated. In emphysema CXR correlate poorly with these scans, showing a trend to underestimate the functional

impairment. In both airways obstruction and pulmonary embolism gross defects are commonly observed on lung Q scans and corresponding V defects are present as well in airways obstruction. All these abnormalities are almost undetectable from CXR which usually show normal V and Q pattern. In left heart failure CXR are inaccurate in detecting alteration of the normal base to apex Q gradient. A redistribution of regional ventilation in these patients frequently seen on Kr-81m scans is not apparent on the radiographs.

In conclusion, V/Q scans provide unique information in: diagnosis and followup of pulmonary embolism; functioning evaluation of chronic bronchitis, asthma or emphysema; early detection of pulmonary changes in left heart disease. (This work is supported by the British Heart Foundation.)

IMAGING SMALL PULMONARY ISCHEMIC LESIONS AFTER RADIOACTIVE CARBON MONOXIDE INHALATION. George V. Taplin, Sawtantra Chopra, Norman S. MacDonald and Dennis Elam. University of California, Los Angeles, California.

This report describes a new method for imaging small ischemic regions in the lung as areas of high radioactivity in a low radioactive field immediately after a single breath of radioactive carbon monoxide labeled either with carbon-11 or oxygen-15. A tungsten-collimated gamma scintillation camera is used to visualize the 0.51 MeV annihilation photons emitted from the CO. In normal dogs the entire lung field is cleared of CO within 10 seconds, because the CO traverses the airway and alveolar membrane in milliseconds and combines instantly with the hemoglobin of the circulating red blood cells as stable carboxy hemoglobin. However, in dogs with completely occluded 2.0 mm caliber segmental arteries produced by placement and inflation of a balloon catheter, under fluoroscopic control and in conjunction with arteriography, the ischemic but well ventilated segment appears as a region of relatively high radioactivity, ten times that of normal surrounding lung, due most likely to temporary entrapment of the CO labeled red blood cells in the ischemic region.

This method not only opens a new dimension in the assessment of regional lung function with radionuclides, i.e. ventilation-perfusion and diffusion lung imaging procedures. It provides a simple inhalation method for instantly labeling the systemic circulation without left heart catheterization. Some of its potential applications in obstructive disorders of the arterial and venous components of the systemic circulation are listed.

EFFECT ON INTERPRETATION OF LUNG PERFUSION IMAGES WITH THE ADDITION OF LUNG VENTILATION IMAGES. Robert W. Burt and Gordon McLaughlin. Indiana University Medical Center and Veterans Administration Hospital, Indianapolis, Ind.

An experiment was designed to determine if the addition of ventilation images produced differences in the interpretation of lung perfusion images.

Examinations were presented in a random fashion to 3 observers. During phase I they were provided a perfusion lung scan, brief clinical history, and a chest radiograph. Interpretations were limited to the following choices: (1) normal (2) pulmonary embolism (3) indeterminate or (4) other lung disease. During phase II a ventilation study was added. Over 500 blind interpretations per observer were performed over a 4½ month period. For study purposes all examinations not specifically performed for detection of pulmonary embolism were eliminated from the final evaluation.

Forty-seven percent of the perfusion studies alone were interpreted as being consistent with pulmonary embolism (range 43% to 49%); however, when the ventilation images were added this changed to 29% (range 24% to 38%) ($p<.005$). This was associated with a 75% decrease in the observer response "indeterminate".

This group of observers reduction of the interpretation "pulmonary embolism" with the combination examination was 40% compared to interpretation of perfusion scintiphotography alone. If these results are typical, it appears that 4 of 10 patients diagnosed as probable pulmonary embolism on the basis of perfusion imaging would not have this interpretation made with the addition of a ventilation examination. Survey data indicated only 7% of perfusion lung scans are accompanied by ventilation studies. All laboratories performing lung scanning procedures should be strongly encouraged to offer a ventilation study as part of the examination.

TUESDAY, 4:00-5:30 BALLROOM B

DATA ANALYSIS 1

Chairman: Patrick T. Cahill
Co-Chairman: Barbara Y. Howard

THALLIUM-201 MYOCARDIAL SCANNING: ENHANCED QUANTIFICATION WITH REGIONAL MAPPING TECHNIQUES. J.Fletcher, P.Chaowaratana, J.Daly, F.Herbig, R.Donati, K.Walter, St. Louis VA Hospital, St. Louis University, St. Louis, Mo.

Regional myocardial distribution of Thallium-201 (Tl-201) was evaluated in 46 studies in 32 patients. Determination of heterogeneity of regional myocardial blood flow was made in normal subjects and patients with single and multi-vessel disease utilizing a mini-computer/plotter system. Distribution of regional myocardial Tl-201 activity was related to capillary beds distal to major coronary vessels at rest and with injection of Tl-201 after treadmill exercise in 20 studies. The myocardial distribution of Tl-201 was expressed as a percentile of maximal cardiac activity or as a selected standard deviation from the mean value. Patients without disease demonstrated a uniform distribution of Tl-201 activity at rest and post exercise, with the majority of the myocardial activity distributed closely about the maximum value. Progressive abnormalities in flow homogeneity were observed following exercise in patients with single and multi-vessel disease, with the majority of myocardial activity in diseased areas distributed 50%-60% below the maximum value. Comparison of results in normal subjects and patients with coronary artery disease (CAD) suggests that frequency distributions of myocardial activity can be constructed which characterize flow heterogeneity and reflect the severity and extent of CAD. Improved quantification of flow heterogeneity was obtained utilizing the computer mapping technique and the results of the study indicate a close relationship between distribution and degree of flow heterogeneity and number and site of diseased vessels.

ADVANCES IN IMAGING AND ANALYSIS OF THE CEREBRAL "FLOW" STUDY. James G. Bonifield, J. Michael Uszler, and Ismael Mena. Division of Nuclear Medicine, UCLA-Harbor General Hospital, Torrance, Ca.

We report clinically useful advances in imaging and analysis of the brain "flow" study using: a) non-interpolated and interpolated 128 x 128 and 256 x 256 computer matrix color images and b) development of an objective standard to judge the asynchrony of cerebral perfusion.

A minicomputer system with software-controlled levels of color scale and a 19 inch (diagonal) color video monitor was employed to simultaneously display either one image, 4, or 16 sequential images of the dynamic study. Images based on time/activity (T/A) curves were also composed from selected phases of a study to illustrate any perfusion asynchrony present in a particular phase. In one case asynchrony not readily visible in the sequential analog images was demonstrated.

Region of interest (ROI) placement and subsequent T/A curve generation is efficiently achieved by user-defined linkage of appropriate computer sub-routines to produce a macro-program in which the only operator intervention required is that of ROI placement. The ROIs, their placement and their associated T/A curves are simultaneously displayed on the video monitor, and are coordinated by the use of individual color for each ROI.

Mean transit time (MTT) of each T/A curve is calculated by a separate computer routine. MTT difference for the two middle cerebral arteries was calculated for both normal and CVA patients. The difference was significant ($p < .001$) between the two groups, suggesting that asynchrony of perfusion can be detected in the range of a second or less.

In the case with asynchrony not visible on the analog images, the MTT difference was one second. In another case with analog images showing initial decrease and subsequent "flip-flop", the curves showed this due to both delayed onset of perfusion and a 1 second MTT difference.

A FAST ACCURATE ALGORITHM FOR AUTOMATED CEREBRAL FLOW ANALYSIS. Dennis L. Kirch, Peter M. Ronai and Michael T.Lefree The Denver VA Hospital and the Univ. of Colo. Med. Center

An algorithm has been developed which enables an online minicomputer to define automatically areas-of-interest and analyze time-activity curves for cerebral flow abnormalities with greater accuracy and reproducibility then techniques dependent on manual interaction and subjective judgement. The technique is applicable to anterior or posterior Anger camera studies recorded in 0.5 second frames. The analysis is implemented in three computational modules (running time is 2 minutes). First, the time segments providing best visualization of arterial and venous structures are used to define anatomical reference coordinates. An adaptive algorithm then outlines the carotid arteries and tracks the sagittal sinus (while avoiding the transverse sinuses) resulting in definition of 5 areas-of-interest (both carotids, both middle cerebral, and midline anterior cerebral). Finally, output for clinical interpretation is prepared in the form of corrected time-activity curves and printout of flow symmetry and bolus spread parameters. The algorithm is flexible enough to produce correct results (as verified by visual interpretation of the dynamic images) even in the presence of significant positioning error (head tilt or rotation). Erroneous results were always associated with poor bolus arrival or extreme jugular reflux. This occurred in less than 1% of 500 studies analyzed. In no case did a vascular lesion distort the areas-of-interest. This program represents a refinement to the point that daily, fluid-filled flood corrections and constant spectrum settings are important for error minimization. The automated methods reported here provide significant labor savings while eliminating as many sources of human and instrument error as possible. This work brings us to the limits of instrument stability, uniformity, and resolution for detecting unilateral flow abnormalities where normalization of hemispheric flow is the key to improved detection of bilateral disease.

COMPUTER GENERATED FUNCTIONAL IMAGES OF REGIONAL HEPATIC PERFUSION. Robert E. Henry, Erica A. George and Robert M. Donati. St. Louis VA Hospital and St. Louis University, St. Louis, Missouri.

Normal hepatic tissue receives 1/3 of its blood supply from hepatic artery and 2/3 from the portal vein. Hepatic tumors have arterial (A) but not portal perfusion (PV) whereas cysts, hematomas and abscess have neither. Determination of regional perfusion with radiotracers in focal hepatic lesions should provide information about the nature of the lesion. Visual assessment of serial images of hepatic perfusion is suboptimal due to the low count rate during the first transit. A computer assisted technique utilizing the first transit hepatic A/PV ratio to generate a functional (parametric) map of regional perfusion has been developed for assessment of vascularity of hepatic mass lesions. Patients were administered 3-8 mCi of Tc-99m sulfur colloid and the first transit through the liver was detected by a gamma camera and recorded on disc (2 sec/frame). Curves of first transit were generated and A and PV phases were identified. Frames corresponding to A or PV phases were integrated and the A/PV ratio was determined for each matrix element. The functional image was displayed on the CRT with darkest areas representing normal hepatic perfusion and brightest areas representing disproportionate A/PV ratio. Eleven patients with anatomic confirmation of disease process have been studied. In 4/5 with intrahepatic tumor the functional image showed bright (abnormal) areas corresponding to mass lesions seen on scans. In 2 with hepatic cysts no vascular abnormality was detected. In 3 whose scans had suspicious areas a normal functional image was obtained correlating with subsequent anatomic findings. One with a hepatic defect due to subhepatic abscess had a normal functional image. Thus, computer generated functional images appear to augment and increase the specificity of the routine hepatic imaging procedure.

TUESDAY, 4:00-5:30 BALLROOM C

ENDOCRINE/METABOLISM

Chairman: Steven M. Pinsky
Co-Chairman: James Thrall

FERTILITY AND BIRTH HISTORIES OF PERSONS TREATED WITH I-131 FOR THYROID CANCER BEFORE 1960 AT THE AGE OF 20 YEARS OR LESS. S. D. Sarkar, W. H. Beierwaltes, S. P. Gill, and B. J. Cowley. University of Michigan Hospital, Nuclear Medicine Section, Ann Arbor, Mich.

One method of studying possible genetic effects of I-131 therapy has been to evaluate the reproductive histories of persons treated in childhood with I-131 for hyperthyroidism. We have seen no similar study of persons < 21 yrs treated for thyroid cancer with much higher doses of I-131.

Forty patients, treated with I-131 following surgery for papillary and follicular thyroid carcinoma between 1947 and 1960, were contacted by telephone. 2 were not married; 5 were deceased before marriage. A standard fertility and birth history was taken directly on the remaining 33 pts.

The mean total dose of I-131 was 196 mCi (80-691 mCi). The mean age at the time of the first I-131 therapy was 14.6 yrs (6-20 yrs) with an average followup interval from the first dose to this study, of 18.7 yrs (14-25 yrs).

Of 13 males, 2 are childless. 11 patients' spouses have had 28 live births. 6 children were premature; 2 of these were twins. Of the 4 others, one died in the neonatal period. Of 20 females, one is childless. Another was infertile for 3 years before a fruitful pregnancy. This patient also had a miscarriage. One woman is pregnant. 18 women have had 43 live births. There was one infant with congenital cardiac anomaly that died soon after birth.

Males and females together, 33 patients (or their spouses) had 71 live births. There were four (12%) with infertility (Normal incidence N=12%), six (8%) cases of prematurity (N=7-14%), one (1.4%) miscarriage (N=15%) and one (1.4%) birth with a significant congenital anomaly (N=1-2%).

Thus, the reproductive history of persons < 21 years receiving I-131 therapy for thyroid cancer and the health status of the first generation offspring appear to be within the accepted published standards for the general population.

EFFECTS OF MEDICAL AND SURGICAL THERAPY ON MORBIDITY IN PAPILLARY AND/OR MIXED PAPILLARY-FOLLICULAR THYROID CARCINOMA. R. L. Young, E. Mazzaferri, W. Kemmerer, C. Page and J. Ortell, Wilford Hall USAF Medical Center, Lackland AFB, San Antonio, Texas

The problem of morbidity has not been addressed in any previous large series of patients with papillary and/or mixed papillary-follicular thyroid carcinoma (PF). In a review of patients entered into the Armed Forces tumor registry, 576 patients with PF were identified. All available material in the registry was reviewed by one of the authors. Pathological material was reviewed at the Armed Forces Institute of Pathology. Prognosis was not influenced by the duration of disease, extent of intra thyroid involvement, extent of lymphatic involvement or extent of lymphatic surgery. Recurrence rate was highest in those receiving thyroid surgery and no post operative medical therapy (32%); less in those given thyroid hormone post operation (11%); and least in those receiving I-131 therapy followed by thyroid hormone therapy post operation (2.7%) ($P < .001$) for all three). In those patients treated with surgery and thyroid hormone only, recurrence rate was 15% if only lobe or isthmus removed; 9% with more extensive subtotal or total ($P < .05$). Multifactoral analysis confirmed the benefit from thyroid hormone and I-131 therapy. The role played by amount of thyroid surgery could not be stated with certainty and must be balanced by the increased complication rate with more extensive surgery.

DISPARATE IMAGING OF THE AUTONOMOUS FUNCTIONING THYROID NODULE WITH 99m PERTECHNETATE AND RADIOIODINE. J. Martin Miller, Albert G. Kasenter & Daniel S. Marks, Henry Ford Hospital, Detroit, Michigan.

Four nodules imaged as "hot" with ^{99m}Tc pertechnetate at 20-60 minutes were not visualized with 123 or ^{131}I at 4-24 hours. Each nodule was demonstrated to have autonomy of function in excess of surrounding normal tissue when imaged

with radioiodine after suppression of TSH. Comparison studies in one nodule were obtained by administering 5 mCi of 99m pertechnetate and 5 mCi of sodium 123_I intravenously on separate days. A Picker Dyna Camera 2C interfaced to a Medical Data Systems computer was used to collect the data. Uptake of pertechnetate in normal thyroid paralleled that of iodine for five minutes, but plateaued at 10 minutes while iodine was still increasing at 30 minutes. In the nodule, the rate of iodine uptake exceeded that of pertechnetate at all times from one to 30 minutes, but the avidity for both radionuclides was greater than in adjacent normal thyroid. Pertechnetate uptake plateaued in the nodule at 30 minutes when iodine uptake was rising rapidly. 20 minute scintiphotos and one hour scintiscans were identical with both radionuclides, and the nodule was visualized as "hot". At 24 hours it was not delineated with 123_I. Following 5 day T3 administration the nodule was visualized as "hot" with 123_I at 4 hours and 131_I at 24 hours.

A rapid turnover of an as yet unidentified iodine moiety would seem to explain the disparate imaging in these lesions rather than the "trapping only" function previously ascribed to nodules which visualized with pertechnetate and not with iodine radionuclides.

IN VITRO TESTS OF THYROID FUNCTION IN PREGNANCY, Stephen Plymate, Jerry L. Prather, Martin L. Nusynowitz. William Beaumont Army Medical Center, El Paso, Tx.

The action of estrogens on hepatic production of thyroid hormone binding proteins results in alterations in serum concentrations of the thyroidal hormones during pregnancy. To clarify discordant results of prior studies, we have studied a number of in vitro tests of thyroid function during various stages of pregnancy to (1) define their range of normal, (2) relate results to known mechanisms controlling thyroid physiology, and (3) indicate the utility of calculating free thyroxine (FTI) and free triiodothyronine (FT3I) indices in order to normalize alterations caused by changes in binding protein capacity. Throughout pregnancy FTI and FT3I values are identical to those of nonpregnant normals, whereas alterations of triiodothyronine uptake, total thyroxine, and total triiodothyronine are attributable to changes in thyroxine binding protein capacity, which achieves near maximal values by the early second trimester and stabilizes throughout pregnancy. An apparent slight elevation of thyroid stimulating hormone concentrations (TSH), noted in the early second trimester, represents an assay artifact due to cross reactivity of TSH antibody with human chorionic gonadotropin; thereafter, TSH concentrations are normal. Thus, the serum concentrations of the free hormones which determine the metabolic state remain normal during pregnancy, as does the concentration of TSH. The maintenance of normal free hormonal concentrations result from the redistribution of nonmetabolically (reversibly) linked stores of thyroxine and triiodothyronine, without necessitating an increase in TSH. By six weeks after delivery, values which deviated from normal as a result of alterations in thyroxine binding protein capacity return towards, but do not quite achieve, normal, indicating persistence of slight estrogen effect.

EFFECT OF THYROID HORMONE ON PLASMA IMMUNOREACTIVE INSULIN (IRI). Stanley J. Goldsmith, Mt. Sinai School of Medicine, N.Y., N.Y. and Avir Kagan, Coney Island Hospital, Brooklyn, N.Y.

With an increasing use of insulin radioimmunoassay to evaluate patients with diabetes mellitus and insulinoma, it becomes necessary to be aware of the influence of other clinical and pharmacologic states on plasma insulin levels. Thyroid deficiency is of interest since hypometabolism may influence secretory response to stimuli and/or degradation of secreted insulin.

Oral and/or intravenous (IV) glucose tolerance (GT) tests were performed in 16 patients (pts) with hypothyroidism, none known to have abnormal GT. Increased plasma insulin levels were observed in all pts. 6/13 pts had normal GT; Peak mean plasma insulin 220 μU/ml at 1 hr. 6/13 had "diabetic" GT; Peak mean plasma insulin 212 μU/ml at 4 hrs. Sephadex fractionation of a plasma sample with 425 μU insulin/ml demonstrated 6% IRI in the proinsulin range. 3/7 IVGT tests had impaired glucose utilization with normal plasma insulin.

7 patients were studied after thyroid hormone replacement. Reduction of mean plasma insulin levels was observed with no worsening in GT.

It is concluded that elevated plasma IRI is found in thyroid deficient patients regardless of glucose tolerance. Thyroid status should be noted in evaluating plasma insulin response to glucose.

RADIOIMMUNOASSAY OF CALCITONIN IN VARIOUS THYROID DISEASES. Rikushi MORITA, Junji KONISHI, MASAO FUKUNAGA, Itsuo YAMAMOTO, Shigeharu DOKOH and Kanji TORIZUKA. Dept. Radiology and Nuclear Medicine, University Hospital, Kyoto University.

Plasma calcitonin levels were measured by a radioimmunoassay before and after an infusion of calcium in 12 patients with simple goiter, 13 with Graves' disease, 19 with chronic thyroiditis, 1 with subacute thyroiditis, 8 with thyroid adenoma, 13 with thyroid cancer involving 11 cases with medullary thyroid cancer and 2 with adenocarcinoma, and 6 with hypothyroidism.

Reactivity of calcitonin secreting cell was expressed by the index of CT/ Ca in which CT and Ca represented the increments of plasma calcitonin and calcium levels after the calcium infusion. Basal plasma calcitonin levels were strikingly high in medullary thyroid cancer, while within normal limits in a majority cases with other thyroid diseases. CT/ Ca values were significantly higher in patients with Graves' disease than in those with other thyroid diseases except medullary thyroid cancer having the highest values of all. A significant correlation was seen between CT/ Ca values (r=0.86) in patients with thyroid diseases except those with medullary thyroid cancer and those placed on thyroxine medication. All hypothyroid patients showed low CT/ Ca values regardless of the causes of hypothyroidism whether due to ^{131}I treatment, surgery or chronic thyroiditis. It was suggested that hyperactivity of C-cell prevailed in hyperthyroidism, while C-cell function was decreased or extinct in hypothyroidism.

AN EVALUATION OF THREE DIAGNOSTIC PROCEDURES FOR THE DETECTION OF BONE INVOLVEMENT IN PRIMARY HYPERPARATHYROIDISM. G. T. Krishnamurthy, Arnold S. Brickman, and W. H. Blahd. Veterans Administration Wadsworth Hospital Center; and UCLA School of Medicine, Los Angeles, CA.

A clinical study was undertaken to evaluate the relative merit of bone imaging, bone x-ray, and bone calcium estimation by Norland-Cameron photon-absorptiometry technique in 26 patients with primary hyperparathyroidism (PHP). Total body bone images were obtained with a scintillation camera 3 to 4 hr after 15 mCi of Tc-99m pyrophosphate (Tc-pyro) injection, with special attention given to small and medium size bones to the distal part of the extremities, rib cage, and skull bones. Clearance of Tc-pyro was calculated in 9 patients with PHP by using the formula UV/P, and compared with 6 control patients. Bone calcium was measured at the distal radius of the dominant arm.

Eighteen of 20 patients who had all three tests showed bone changes in at least one test, and only 2 showed changes in all three tests. Of 24 patients, the bone lesions were demonstrated in 15 patients in the image study, 14 patients in the x-ray study, and 10 patients by both studies. Of 20 patients who had both the bone image study and bone calcium determinations, 13 showed bone lesions in the image study, 10 had low calcium, and 5 had abnormalities in both tests. Plasma clearance of Tc-pyro during the first hour was 54.7 ml/min in patient PHP and 36.8 ml/min in control patients. It is concluded that bone changes are almost universal in PHP and are detected by a combination of three diagnostic procedures of which bone imaging is the most sensitive. The location of the bone lesions is distinct in PHP; as being more common in small bones to the extremities.

WEDNESDAY, JUNE 9, 1976

WEDNESDAY, 8:30-10:00 BALLROOM A

CARDIOVASCULAR 2

Chairman: Glen W. Hamilton
Co-Chairman: David M. Shames

INFARCT SIZING IN AWAKE, UNSEDATED DOGS WITH ACUTE ANTERIOR MYOCARDIAL INFARCTS. James T. Willerson, L. Maximilian Buja, Ernest M. Stokely, Lawrence Poliner, Marvin J. Stone, Frederick J. Bonte, and Robert W. Parkey. University of Texas Health Science Center, Dallas, Tx.

There has been controversy regarding whether one can accurately measure infarct size (IS) with any of the currently available techniques. In an attempt to obtain a definitive evaluation of IS techniques we have performed a study to test the ability of the technetium-99m stannous pyrophosphate (Tc-99m PYP) myocardial scintigram, precordial ECG mapping, creatine phosphokinase (CPK) release and myoglobin radioimmunoassay measurements to predict histological IS. Eight awake, unsedated dogs had acute anterior myocardial infarcts (MI) produced by proximal left anterior descending coronary artery occlusion. Precordial maps ("Maroko Blanket") and blood samples for CPK and myoglobin were obtained prior to and at frequent intervals after LAD occlusion. Tc-99m PYP myocardial scintigrams were obtained approximately 30 hrs after LAD occlusion. At necropsy 2 of the 8 dogs had anterior subendocardial and 6 had transmural MI varying from 2.1 to 26.5 gms in histological IS. The results between each of the different in vivo measurements were compared with the histological measurement of IS. Strong correlations were obtained between histological IS and IS determined by Tc-99m PYP scintigraphy ($r=0.779$, $p=0.02$), CPK release ($r=0.747$, $p=0.05$), the number of precordial sites with at least 50% R wave loss ($r=0.656$), the sum of ST elevation ($r=0.759$), the number of precordial sites with $\geq$ 2mm elevation ($r=0.784$), peak serum myoglobin ($r=0.83$) and peak serum CPK ($r=0.88$). The data suggest that Tc-99m PYP scintigrams, CPK release measurements, peak serum CPK and myoglobin, the sum of precordial ST segment elevation and the number of precordial sites with $\geq$ 2mm elevation or 50% R wave loss all serve as accurate predictors of histological IS in this canine model of acute anterior MI.

COMPARISON OF POSITIVE AND NEGATIVE LOCALIZATION OF MI IN DOGS. H. Nishiyama, V. Sodd, J. Van der Bel Kahn, M. Gabel, E. Saenger, J. Blue and D. Romhilt. Nuclear Medicine Laboratory, BRH, FDA, and Cincinnati General Hospital, Cincinnati, Ohio.

Clear demarcation of myocardial infarction was attempted using both negative (^{201}Tl) and positive (^{99m}Tc-EHDP) agents. It was our observation that the lesion was not well demonstrated by both; but most frequently one or the other was superior in image quality. From this observation it was hypothesized that image quality correlates with extent and degree of cell damage. Infarction was made by ligating left anterior descending artery for 2 hr then releasing. Images with ^{201}Tl followed by ^{99m}Tc-EHDP at 48 hr post-infarction were made and the dog was sacrificed at 72 hr. A mixture of Monastral red, Barosperse and gelatin was injected through the catheter inserted in the left main coronary artery for visual, radiographic and histologic studies. The degree of image quality of both agents was rated without correlating either dogs or two corresponding images. Radiographic images were rated for either decreased microcirculation or distorted branching of the vasculature. Histologic examination of the lesion was correlated with radiographic and scintigraphic imaging. The more severe the degree of obstruction of the vessel lumen and degenerative changes the clearer the images obtained by ^{201}Tl. Mild to moderate histological changes or decreased blood supply was demonstrated better by the ^{99m}Tc-EHDP image. These were well correlated with the degree of patent and/or distorted microcirculation seen by radiograms. Findings suggest complementary role of negative and positive myocardial imaging agents.

SCINTIGRAPHY OF CANINE MYOCARDIAL INFARCTS: ROLE OF CALCIUM AND Tc-99m DIPHOSPHONATE/PYROPHOSPHATE BONE AGENTS. A. J. Tofe, L. M. Buja, R. W. Parkey, F. J. Bonte and J. T. Willerson. Miami Valley Laboratories, The Procter & Gamble Company, Cincinnati, Oh. and Depts. of Pathology, Radiology and Medicine, Univ. Tx. Health Science Center, Dallas, Tx.

Localization of calcium within damaged myocardial cells has been postulated as the reason for uptake of the Tc-99m phosphorus (Tc-P) bone imaging agents following acute myocardial infarctions (AMI). In an attempt to better elucidate the uptake mechanism, AMIs were induced in eight dogs by permanent ligation of the left anterior descending coronary artery.

One to 3 days after ligation, Tc-99m diphosphonate or pyrophosphate was administered followed by a second intravenous administration of tritiated diphosphonate (H-3 EHDP) as a radiotracer for the non Tc-99m component of the bone imaging agent. Positive scintiphotos of AMIs were obtained from all dogs. Normal and infarcted myocardial muscle and bone were taken at necropsy and quantitated for Tc-99m, calcium and/or tritium uptake. Average mean values for Tc-P (% dose/gram x 1000) and calcium (ppm/gm) were 3.3 ± 1.3 and 17 ± 1.7 respectively, in normal myocardium. Abnormal to normal ratios for Tc-P uptake ranged from a ratio of 17.4 ± 1.87 in peripheral zones of AMI with extensive to confluent necrosis to 6.5 ± 1.48 in central zones of AMI with confluent necrosis. Corresponding abnormal to normal calcium ratios are 16.7 ± 6.36 and 6.2 ± 0.98 respectively. Radioassay of the dual labeled (Tc-99m and H-3) bone agent components within infarcted muscle sections from epicardium to endocardium, as well as osseous tissue, yielded equivalent uptake.

It is concluded that the positive scintiphotos are a function of elevated calcium levels in necrotic muscle cells and that the complete Tc-P complex is chemisorbed to the AMI tissue.

UPTAKE OF Tc-99m PYROPHOSPHATE (PYP) AND CALCIUM (Ca) IN IRREVERSIBLY DAMAGED MYOCARDIUM. Heinrich Schelbert, Joanne Ingwall, Harley Sybers, William Ashburn, University of California, San Diego, Calif.

PYP is thought to bind to intramitochondrial hydroxyapatite-like Ca phosphate deposits in acutely infarcted myocardium (IM). However, deposition of calcium and PYP in IM apparently is related to regional blood flow. In order to examine the relationship between ultrastructural changes, Ca and PYP uptake independent of flow, fetal mouse hearts (FMH) in organ culture were insulted by oxygen and glucose deprivation for 4 hours at 37° (I37) or at 42° (I42) and studied upon reperfusion with oxygen and glucose (t_0) or after a 24 hour recovery (t_{24}). Electron microscopic findings in FMH after I37 were consistent with primarily reversible injury; after I42, signs of irreversible injury were present: condensation of nuclear chromatin, swelling and disruption of mitrochondria and occurence of mitochrondrial dense bodies. Compared to control FMH, PYP uptake after I37 was increased by 35 ± 8% (SEM) ($p < .05$) at t_0 and by 33 ± 7% ($p < .005$) at t_{24}. After I42, PYP uptake was increased by 117 ± 18% ($p < .05$) at t_0 and by 180 ± 11% ($p < .001$) at t_{24}. Ca-45 uptake was elevated similarly: by 52 ± 11% ($p < .005$) after I42 at t_0 and 227 ± 44% ($p < .002$) at t_{24}. However, uptake of PYP and Ca-45 in matched litter mates FMH after I42 at t_0 and t_{24} correlated only loosely ($r = 0.49$). Moreover, deprivation of Ca from culture media during I42 and the 24 hour recovery did not reduce PYP uptake in FMH after I42. We conclude, that (1) FMH is a useful model for studying myocardial infarct imaging agents; (2) PYP localizes primarily in irreversibly injured myocardium; (3) PYP uptake apparently is independent of cellular calcium uptake.

UPTAKE OF SIX TECHNETIUM-99m RADIOPHARMACEUTICALS AND STRONTIUM-85 IN VASOPRESSIN-INDUCED RABBIT MYOCARDIAL INFARCTION. Zachary D. Grossman, Alan B. Foster, Robert Richardson, John G. McAfee, Gopal Subramanian, Bedros Markarian, Daniel Bassano and George Gagne, The Upstate Medical Center, Syracuse, New York

The induction of ischemic myocardial necrosis in dogs requires time-consuming surgical ligation or catheterization of the coronary arteries. A less expensive, rapid method of producing infarcts in rabbits was therefore developed, suitable for screening myocardial agents in larger groups of animals.

A special needle was inserted percutaneously into the myocardium of sedated animals and 0.4 cc vasopressin in peanut oil were injected. This vasoconstricting agent induced grossly visible localized infarcts in 97 of 195 animals (50%). Microscopically, the cellular necrosis, leukocytic infiltration and mild hemorrhagic areas were similar to those of human lesions. When the infarcts were 24 hours old, the Tc-99m agents and Sr-85 were simultaneously injected IV, and the animals were sacrificed at 1, 6 and 24 hours for tissue radioassay.

Surprisingly, Sr-85 failed to accumulate appreciably in the infarcts. Three bone-seeking Tc-99m complexes [pyrophosphate, methylene diphosphonate (MDP) and imidodiphosphonate (IDP)] produced infarct to myocardial ratios at 1 hour of 5, 5 and 14, and at 6 hours of 20, 30 and 33 respectively. In contrast, the ratios for Tc-99m glucoheptonate were only 2:1 at 1 hour and 4:1 at 6 hours. The ratios for other renal agents, Tc-99m acetylcysteine and citrate were even lower. Moreover, the absolute infarct concentrations of the Tc-99m skeletal complexes were much higher than the Tc-99m renal complexes. These results suggest that Tc-99m-MDP and IDP localize in myocardial infarcts at least as well as pyrophosphate and that clinical trial of these agents is warranted.

EFFECT OF PROPRANOLOL AND DIGITALIS UPON RADIOACTIVE THALLIUM AND POTASSIUM UPTAKE IN MYOCARDIAL AND SKELETAL MUSCLE. Jim C. Costin and Barry L. Zaret, Yale University School of Medicine, New Haven, CT.

The effects of the commonly employed cardiac drugs propranolol and digitalis upon myocardial uptake of thallium-201 and potassium-42 were investigated in 16 dogs. These data were compared to the effects of these same drugs upon uptake of Tl-201 and K-42 in both resting and post-contraction skeletal muscle. The uptake of Tl-201 and K-42 following intravenous administration was assessed from tissue activity in myocardial and skeletal muscle samples as well as arterial-venous differences (AVD) across the coronary and skeletal muscle vascular beds. The vascularly isolated, innervated gracilis muscle was used as the representative skeletal muscle.

In the myocardium, digitalis IV (intravenously), and propranolol IV both significantly ($p<.05$) decreased Tl-201 uptake by 22 percent and 32 percent respectively as well as significantly narrowed Tl-201 AVD across the coronary vascular bed. Myocardial K-42 uptake was similarly decreased by 27 percent and 48 percent with correlative changes noted in K-42 coronary AVD. In post-contraction skeletal muscle, digitalis IV decreased Tl-201 uptake by 16 percent; propranolol IV, 30 percent; propranolol intra-arterially (ia), 55 percent; and digitalis IV + propranolol ia, 73 percent (all $p<.05$). In resting skeletal muscle, digitalis IV had no effect; whereas propranolol IV decreased Tl-201 uptake by 26 percent; propranolol ia, 54 percent, and digitalis IV + propranolol ia 68 percent (all $p<.05$). Similar results were obtained with potassium in skeletal muscle.

Thus, the kinetics and uptake of radioactive thallium and potassium by myocardial and skeletal muscle are significantly decreased by intravenous propranolol and digitalis. These findings may have significance in quantitative myocardial imaging with potassium analogues.

THALLIUM-201 REDISTRIBUTION FOLLOWING TRANSIENT MYOCARDIAL ISCHEMIA. G.M. Pohost, G.A. Beller, K.A. McKusick, R.H. Moore, L.M. Zir and M.S. Potsaid. Massachusetts General Hospital, Boston, MA.

Serial imaging after administration of Thallium-201 (Tl) to patients during exercise-induced ischemia has shown disappearance of perfusion defects over a 4-hour period. In order to further investigate this phenomenon, 10 dogs were given 1mCi of Tl 10 minutes after acute ischemia produced by snaring of confluent branches of the left coronary system to obtain a discrete region of apical ischemia. In 8 dogs reperfusion (RP) was instituted by snare release after 20 minutes. Serial images were obtained during occlusion and every 30 minutes during the RP period. Serial images obtained during RP demonstrated redistribution of Tl activity into a discrete apical defect. Tl images returned to normal in all dogs by 4 hours of RP. In 2 control dogs occlusion was continued for 4 hours and serial images showed no change. The mechanism for Tl redistribution was studied after transient ischemia in 14 additional dogs receiving 1mCi of Tl 10 minutes after occlusion. Ten of these underwent RP after 20 minutes and were sacrificed after 100 minutes. Regional myocardial bloodflow was determined during occlusion and prior to sacrifice by the microsphere technique. Microsphere (Sr-85, Ce-141) and Tl activities were measured in multiple specimens of ischemic (I) and nonischemic (NI) myocardium. Flow in the center of the I zone was reduced to 18±5% of NI flow during occlusion and returned to normal after RP. Tl activity in the I zone after RP was 60±5% of NI activity, substantially higher than flow at the time of Tl administration.

In conclusion, redistribution of Tl into previously ischemic myocardium was demonstrated during transient coronary occlusion in dogs and after exercise-induced ischemia in man. Reversibility of ischemia may be detected by serial imaging after a single dose of Tl.

QUANTITATIVE MYOCARDIAL IMAGING WITH I-123 HEXADECENOIC ACID. Norman D. Poe, Gerald D. Robinson, Jr., and Florian W. Zielinski. Department of Radiology and Laboratory of Nuclear Medicine, University of California, Los Angeles, Calif.

Quantitative myocardial imaging would be most useful in sequential studies where small changes in regional perfusion need to be detected and measured. Radiopharmaceuticals capable of providing high photon fluxes are required to produce statistically valid, high count images in short time spans. Iodine-123 gives low patient radiation doses and is efficiently detected with available scintillation cameras. In preliminary human studies 5 mCi of I-123 hexadecenoic acid (HA) provide myocardial images containing 300K counts net in less than 10 minutes. As HA is rapidly cleared from the myocardium, a repeat image following injection of a second tracer dose can be acquired within 30 minutes using computerized background subtraction.

To determine the sensitivity of the test, repeat studies in canine models were obtained at 20 minute intervals (1) before and after occlusion of the anterior descending coronary artery, (2) following arterial occlusion but before and after stress induced by atrial pacing, (3) before and after the release of an arterial ligature, and (4) in normals before and after atrial pacing. In the first three groups measurable changes in the magnitude of the ischemic defect were seen in all animals. In the atrial paced normal group demonstrable changes in relative flow were seen in half the studies. This observation indicates that changes in total myocardial blood flow, stress and/or cardiac geometry can affect the regional perfusion pattern.

Although multiview qualitative imaging studies can be obtained rapidly with HA, this radiopharmaceutical can be used most effectively in repeated high count, single projection studies of patients with acute myocardial infarcts to determine the influence of therapy on regional perfusion.

CONTINUOUS MEASUREMENT AND IMAGING OF REGIONAL MYOCARDIAL PERFUSION USING KRYPTON-81m. J. Harvey Turner, Andrew P. Selwyn John C. Clark Terry Jones Maurice J. Raphael Robert E. Steiner, and J. Peter Lavender. MRC Cyclotron Unit. Department of Radiodiagnosis and Cardiovascular Research Unit Royal Postgraduate Medical School Hammersmith. London. UK.

The 13 sec. half-life of freely-diffusible Kr-81m allowed the development of a technique for continuous observation of regional myocardial blood flow in dogs and man.

40mCi Kr-81m generators produced in the MRC Cyclotron Unit after a 20 min. α-particle bombardment of sodium bromide yield the Rb-81 parent. Continuous elution of the generator allows constant infusion of Kr-81m into the aortic root at 10 ml/min. through a modified ring catheter.

Experimental studies in 40 dogs demonstrated regional changes in myocardial perfusion related to varying periods of coronary artery occlusion. These changes in blood flow were recorded as serial high resolution gamma camera images. In addition a strip chart recording allowed continuous assessment of myocardial perfusion in selected areas of interest. Within 30 sec. of snare occlusion of the left anterior descending coronary artery Kr-81m count rate in the affected area fell 30-50%. Release of the snare after

1 min. was followed by a rapid rise in this regional count rate to attain peak levels of up to 140% which gradually returned to baseline over the next 5 min. Count rates over an area of myocardium remote from that affected by coronary occlusion showed reciprocal changes. Longer occlusion times produced progressive diminution in the post-release hyperaemia. At occlusion periods over 20 min. blood flow in the ischaemic region generally failed to regain control levels after snare release. Preliminary studies using Kr-81m to assess cardioactive drug effects showed that nitroglycerin improved perfusion in acutely ischaemic myocardium.

Kr-81m infusion in 10 patients at coronary arteriography gave images comparable to those obtained by infusion of Tc-99m microspheres and correlated with angiogram lesions.

WEDNESDAY, 8:30-10:00 BALLROOM B

RADIOPHARMACEUTICAL SCIENCE 2

Chairman: Roy Tilbury
Co-Chairman: Buck Rhodes

DEVELOPMENT OF RHODIUM-101m FOR USE IN NUCLEAR MEDICINE. Kenneth L. Scholz, Vincent J. Sodd, Nuclear Medicine Laboratory, Bureau of Radiological Health, FDA, Cincinnati General Hospital, Cincinnati, OH and James W. Blue, Lewis Research Center, NASA, Cleveland, OH.

The purpose of this work was to determine the feasibility of producing high-purity Rh-101m for nuclear medicine use. Rhodium-101m has desirable decay characteristics for use in imaging studies. It decays by electron capture (93%) and isomeric transition (7%); has a 4.3-day half-life; and emits 307-keV photons with an 88% abundance. Recent studies with platinum metals such as rhodium have shown that they can be complexed with organic compounds to form stable products useful for cancer chemotherapy. We produced carrier-free Rh-101m by isolating its natural palladium precursor, 8.4-hr Pd-101, free from all directly produced rhodium activities, and, after suitable decay time, isolating high-purity Rh-101m. Yields from reactions studied show that up to 4 mCi/μA-hr can be produced by irradiating thick rhodium powder targets with 37-MeV protons using the Rh-103(p,3n)Pd-101 → Rh-101m reaction. Rhodium-101m can also be produced by irradiating palladium targets with protons; the yield using 42-MeV protons in a procedure similar to that used in the rhodium target irradiation was 40 μCi/μA-hr. Chemical procedures were developed to isolate high-purity Rh-101m from a cyclotron target, and to then incorporate the rhodium into rhodiumII butyrate with an 80% yield; this is one of a series of carboxylates useful in chemotherapy. We conclude that substantial amounts of high-purity Rh-101m can be produced and that it can be incorporated into biologically significant organometallic radiopharmaceuticals.

EVALUATION OF RUBIDIUM-82 GENERATORS FOR IMAGING STUDIES. Y. Yano, T.F. Budinger, P. Chu, P.M. Grant, A.E. Ogard, H.A. O'Brien, Jr., and B. Hoop, Jr. Donner Laboratory, University of California, Berkeley, Calif.; Los Alamos Scientific Laboratory, Los Alamos, New Mex.; and Massachusetts General Hospital, Boston, Mass.

Rubidium-82 is a positron emitter with application to brain-blood-flow analysis and myocardial imaging. This has a 75 sec half-life and is obtained in multi-millicurie amounts from a Sr-82 (25d half-life) generator which is portable. Methods of eluting the Rb-82 from either Bio-Rex 70 or Chelex-100 resins were evaluated under column conditions designed to maximize Rb-82 yield per volume of eluant and minimize Sr-82 breakthrough. These factors were determined for newly prepared columns and for columns monitored over a period of a few days to a month for changes in elution characteristics. Sterility and apyrogenicity of the Rb-82 eluates were determined in generators prepared for human studies.

Two Bio-Rex 70 columns gave Rb-82 elution yields of 60-80% with 20 ml of 2% saline eluant at pH 8.0 and the breakthrough of radioactive Sr was about 0.001 μCi (5×10^{-8}) for freshly prepared columns. In one of the columns monitored for over one month, the breakthrough of Sr increased to 0.05 μCi (1.3×10^{-6}) after 55 elutions (1.1 liter of 2% saline) and to 0.3 μCi (7.3×10^{-6}) after 70 elutions (1.4 liters). A freshly prepared Chelex-100 resin column gave Rb-82 elution yields of about 60% with 0.1 M NH_4Cl - 0.1 M NH_4OH eluant at pH 9.2 and the breakthrough of Sr was 0.6 μCi (9.5×10^{-6}).

The results of this study indicate that the Bio-Rex 70/saline system gave superior elution characteristics compared to the Chelex-100/NH_4Cl - NH_4OH system. Multi-millicurie amounts of Rb-82 in sterile and pyrogen free solutions of 2% saline were obtained for imaging studies in phantoms, dogs and humans.

QUANTITATIVE UPTAKE DETERMINATION OF TECHNETIUM LABELED AGENTS IN HUMAN SUBJECTS. Bruce H. Mock, Katherine A. Lathrop, and Paul V. Harper. University of Chicago, Chicago, IL.

The reliability of radiation absorbed dose estimates for the commonly used Tc-99m radiopharmaceuticals would be markedly improved by the availability of quantitative in vivo uptake measurements in humans. By utilizing the depth independence of positron coincidence detection, quantitative serial uptake measurements in various organs can be obtained from the positron emitting Tc-94m (52m, 66% β+). The abundant 871 keV gamma radiation (91%) contributes to the singles counts but does not interfere significantly with the coincidence quantitation. An efficient production method has been developed for this nuclide by bombarding enriched Mo-94 oxide with 15 MeV protons. The target is easily dissolved in NH4OH and the Tc-94m is extracted as pertechnetate with methylethylketone. The enriched Mo-94 is reconverted to the oxide by evaporation and heating to constant weight. Mouse studies with Tc-94m prepared in this way, using simultaneous double label technique, showed identical tissue distribution at 30 and 60 min after injection to that of commercially available Tc-99m, verifying the chemical form of Tc-94m as pertechnetate, the starting material for all radiopharmaceutical preparations. Accurate measurement of the RE uptake of the various available technetium labeled colloids is needed both for dosimetry and for liver-spleen ratio measurements. In addition, because the cyclotron-produced Tc-94m decays directly to Mo-94, specific activity is constant, so that the study of the "carrier effect" on technetium labeling or biological distribution becomes feasible using this isotope since Tc-99m always contains a varying amount of Tc-99. Thus Tc-94m allows quantitative uptake measurements, and the investigation of Tc carrier effect in labeling radiopharmaceuticals. (Supported in part by E(11-1)-69 and 18940-03.)

CELLULAR LOCALIZATION OF ^{99m}Tc RADIOPHARMACEUTICALS BY RADIOAUTOGRAPHY. S. Treves, D.A. Martinez, M.A. Davis, and E.T. Hedley-Whyte. Harvard Medical School, Boston, Mass.

The objective of this work was to study the cellular localization of ^{99m}Tc-labeled radiopharmaceuticals used for scintigraphic imaging of the kidney.

Cellular localization of ^{99m}Tc-glucoheptonate (GH) and ^{99m}Tc-2,3-dimercaptosuccinic acid (DMSA), was ascertained in the rat kidney by frozen section microradioautography utilizing the low energy electrons of ^{99m}Tc. Rats injected (IV) with high specific activity GH or DMSA were sacrificed at one hour. The kidneys were removed, sectioned and frozen in isopentane, cooled in liquid nitrogen. One and 2 micron sections were cut at -40°C and placed on glass slides with Ilford G-5 nuclear track emulsion. After four hours of exposure at -40°C, the sections were fixed with acetone at -40°C and then stained with hematoxylin and eosin.

Intense radioautographic labeling of tubular cells on the inner aspect of the renal cortex (site of proximal and distal tubules) was noted with both GH and DMSA. No significant radioactivity was noted in the renal medulla. Radioautographic labeling appears to be predominantly over the tubular cytoplasm with only background levels seen over nuclei, glomeruli, collecting tubules and blood vessels.

This study demonstrates the feasibility and utility of frozen section high-resolution radioautography in defining microcellular localization of ^{99m}Tc-labeled diffusible radiopharmaceuticals.

The sensitivity and resolution of the technique was investigated to allow determination of the amount and the subcellular localization of the ^{99m}Tc. This technique offers a rapid and accurate means for elucidating the cellular distribution of ^{99m}Tc-labeled radiopharmaceuticals.

WEDNESDAY, 8:30-10:00 BALLROOM C

RENAL/ELECTROLYTES

Chairman: Robert J. Cowan
Co-Chairman: David Lilien

IS THERE A "GOOD" Tc-99m-ALBUMIN? G. Meinken, S. C. Srivastava, T. D. Smith, and P. Richards. Brookhaven National Laboratory, Upton, N.Y.

It has generally been presumed that Tc-99m is a poor label for HSA owing to its slow breakdown in vivo. Present work attempts to show that Tc-99m-HSA with biological behavior similar to the commercially available RIHSA can be prepared using a stannous tagging procedure followed by a purification step. Evaluation of paper chromatography, electrophoresis (cellulose acetate and gel) and gel filtration demonstrated the inability of most existing Tc-HSA quality control methods to differentiate between bound and unbound reduced technetium. Reliable separations of unbound activity can be carried out by either gel electrophoresis, or filtration using long columns of G-100 Sephadex or Agarose A 0.5 M gels. Tc-99m-HSA (total~70-85%) separates as dimeric and monomeric fractions, while denatured albumin, if any, is either eluted at the void volume or is retained by the column as is unbound reduced technetium.

Tagging procedure involved reducing pertechnetate with $SnCl_2$ in presence of DTPA and HSA at pH 2 for 30 min, and adjusting to pH 6.5. Blood clearance data in goats and dogs showed 67-78% unpurified Tc-99m-HSA in the blood up to 2 hr, after an initial rapid clearance. Comparable data for purified fractions and other preparations were as follows: Monomer, 85-88%; Dimer, 70-76%; Electrolytic preparation, 64-71%; I-131-HSA, 79-81%. An initial fast clearance of activity was observed in all cases. Large species like goats or dogs appear to provide better data for comparison with the human system, unlike mice studies. It is concluded that a "good" Tc-99m-HSA preparation comparable to RIHSA is achievable and that the label per se is good. The rapidly clearing technetium activity encountered in most preparations is not associated with albumin itself but is present as unbound reduced technetium.

RADIOCHEMISTRY OF TC-N-[N'-(2,6-DIMETHYLPHENYL CARBAMOYLMETHYL)] IMINODIACETIC ACID (TC-HIDA) M. Loberg, A. Fields, E. Harvey, M. Cooper. University of Maryland Hospital, Baltimore, Maryland 21201

Tc-HIDA is an N-substituted iminodiacetic acid found to exhibit rapid hepato-biliary clearance. Its radiochemical structure and stability were studied in order to better appreciate the mechanism of clearance. This work helps explain the radically different in-vivo distributions of Tc-HIDA and HIDA and substantiates the inertness of the bond between reduced technetium and N-substituted iminodiacetic acid.

The stability of Tc-HIDA and its associated overall formation constant were studied by following the exchange reaction between Tc-HIDA and EDTA as a function of time and pH. The reaction was followed quantitatively using paper electrophoresis and confirmed by tissue distribution studies in mice. Tc-HIDA exhibited an overall K_f of 10^{12} and undergoes acid catalyzed unimolecular dissociation with rate constants of 0.3/hr and .002/hr at pH's of 3.5 and 6.0, respectively. Paper electrophoresis revealed Tc-HIDA to be anionic existing in two discrete radiochemical forms at a pH around 3.0 with only one of these structures in evidence at pH's greater than 4.5. The radiochemical structure of Tc-HIDA was examined further by synthesizing Tc-99-C-14-HIDA using Tc-99 and C-14 HIDA of known specific activity. Similarity of Tc-HIDA with and without carrier was confirmed by tissue distribution studies in mice and by paper electrophoresis. The dual labeled HIDA was separated from both HIDA and Sn-HIDA using descending paper chromatography in 95% acetonitrile. The molar ratio of HIDA to technetium was determined by this technique to be 1.8 ± 0.3. This work suggests that Tc-HIDA exists as an anionic dimer and that the bond between technetium and N-substituted iminodiacetic acids should remain intact for relatively long periods of time at physiologic pH.

A COMPARISON OF Tc-99m DTPA AND I-131 OIH IN THE EVALUATION OF RENAL TRANSPLANT FUNCTION. E. V. Staab, T. M. Jones, C. L. Partain, S. R. Mandel, W. P. Webster, and R. L. Clark. University of North Carolina, Chapel Hill, North Carolina.

Tc-99m DTPA has been proposed as an alternative radiopharmaceutical for renal transplant studies; with the apparent advantages of decreased study time, shorter biological half-life, and improved anatomical detail of the collecting system, peri-renal area and vasculature.

The relative accuracy of Tc-99m DTPA versus I-131 OIH in describing renal function and in predicting early rejection was compared in canine and human renal transplants. One hundred paired studies in 25 dogs, surgically modified as Webster-Mandel transplant models, and 80 paired studies in 20 different transplant patients were evaluated. Data was digitized, displayed, and stored using an on-line Gamma 11 mini-computer.

Abnormal renograms were quantitatively graded and correlated with the clinical picture of each patient and the pathological findings in dogs. Parameters were defined and evaluated for each study; including, time after injection to peak activity and fraction of maximum activity cleared.

I-131 OIH had slightly greater sensitivity in the early diagnosis of transplant rejection. Generally, both agents correlated well with the clinical and pathological findings. Therefore, it is desirable to balance the advantages of Tc-99m DTPA with the greater sensitivity of I-131 OIH in selecting a radiopharmaceutical for renal transplant evaluation.

CLINICAL OBSERVATION OF IMPULSE RESPONSE CURVE OF KIDNEY WITH RADIO-HIPPURAN AND RADIO-CHELATE ADMINISTRATION. Yasushi Ishii, Juichi Kawamura, Masaharu Takahashi, Tsutomu Sakamoto, Takao Mukai, Yoshiharu Yonekura, Shinichi Hosokawa and Kanji Torizuka. Kyoto University School of Medicine, Kyoto, Japan.

A bolus of 131-I Hippuran and 99m-Tc(Sn)DTPA were introduced into a renal artery and subsequent transit process of these tracers through the kidney was observed using a scintillation camera and analyzed by a computer. On inspecting a battery of time-activity curves selected from various parts of the kidney such as outer part of cortex and inner part of pelvis, any differences in the temporal events between these tracers were not evident, indicating that such were tagged tubular fluid which ran preferentially down and up again along the course of nephrons. Impulse response of this tubular transit process of the parenchymal part of the kidney revealed a bimodal distribution function. On loading osmotic diuresis, the distribution function became unimodal with shortened spread, which corresponded with increased rapid flow component and reciprocal decrease of slow component, the decentralization of intrarenal blood flow, according to the radioxenon washout study simultaneously carried out. In patients with essential hypertension, definite centralization of the intrarenal blood flow distribution was accompanied by significant shortening of the spread of the renal tubular transit times. Present results indicated that intrarenal urine and blood flows were invariably related and utilization of the present investigative process made feasible a regional delineation of intrarenal physiology.

CLINICAL APPLICATION OF KIDNEY TO AORTIC BLOOD FLOW INDEX. Richard F. Kiepfer, Peter T. Kirchner, and Frederic H. Gerber. National Naval Medical Center, Bethesda, Maryland

The kidney to aortic blood flow index (K/A ratio) is the quotient of the slopes, determined by linear regression analysis, of the upstrokes of renal and aortic histograms, derived from region of interest flags, applied to sequential gamma camera images, framed at one per second by a digital computer. We have reported studies in dogs showing linear correlation (r=.92) with electromagnetic flow measurements.

226 clinical radio isotope renal studies were performed during an 11 month period. 34 patients were classified as normal by excluding all patients with known renal disease or chronic hypertension, as well as studies found abnormal by other criteria or technically unsatisfactory. These 34 studies (68 K/A ratios) established our normal mean of 1.07 and normal range as above 0.80.

The K/A ratio has been found to be low in hydronephrosis (2 cases), urinary tract infection (12 cases), hypertension (36 cases including patients in whom both urinalysis and serum creatinine were normal) and patients with mass lesions (16 cases).

In transplants (105 studies in 16 patients) application of the K/A ratio has been of significant aid in the differential diagnosis of early anuria. Ratios have been low in rejection, acute tubular necroses (ATN) and obstruction (both vascular and ureteral) and have risen with recovery. During anuria, ATN can be differentiated from rejection since only the latter presents progressively falling K/A ratios.

In our hands, the K/A ratio has been a valuable addition to the routine renal scan.

VALIDATION OF A SIMPLE TECHNIQUE OF MEASURING RELATIVE RENAL BLOOD FLOW. David Shames, Melvyn Korobkin and Sybil Swann. University of California, San Francisco, CA.

To test the hypothesis that the externally monitored early renal uptake of I-131 hippurate (I-HIPP) is proportional to renal blood flow (RBF), the 1 to 2 minute post-injection renal uptake of I-HIPP was compared with the renal accumulation of radioactive carbonized microspheres in dogs. Catheters were placed in the jugular vein, left ventricle and in one of the renal arteries of anesthetized dogs. The renal artery catheter was equipped with a balloon to experimentally lower the blood flow of that kidney. One minute following the intravenous injection of 100 uCi of I-HIPP, about 1 uCi of Sr-85 labeled carbon microspheres were injected into the left ventricle. Radioacitivity measurements over both kidneys were recorded with a scintillation camera interfaced to a digital computer. The dog was sacrificed, and both kidneys were excised and counted for the appropriate energy of the radioactive microspheres. The scintillation camera data were first flood field corrected for non-uniform crystal response and a region of interest cursor was drawn around each kidney and a background region below the kidneys. The amount of radioactivity within each kidney was corrected for background radioactivity and integrated over the 1 to 2 minute interval following injection. Fourteen separate measurements of relative RBF were performed on 7 dogs. There was a good linear correlation between the 1 to 2 minute relative renal uptake of I-HIPP and relative microsphere uptake (r=.94, p<.005).

This study suggests that relative RBF can be measured by monitoring the renal uptake of I-HIPP using the scintillation camera interfaced to a small digital computer. This measurement may be valuable in screening hypertensive patients for renovascular disease, in monitoring renal hemodynamics following renovascular surgery and in following patients with known asymmetric renal disease.

DETERMINATION OF EXTRACTION EFFICIENCY BY DUAL TRACER METHOD. Helmut Weich, H. William Strauss, and Bertram Pitt. The Johns Hopkins Medical Institutions, Baltimore, Md.

The measurement of extraction efficiency requires either administration of the total dose of test substance (X) into the arterial inflow of the organ and collecting the total venous effluent, or maintaining a level concentration of (X) in the arterial blood while collecting a sample of venous effluent from the organ. Determination of extraction efficiency could be simplified by simultaneous bolus injection of two tracers one of which is vascular marker (VM) (not absorbed or extracted) and the other is (X). Sampling of a representative fraction of the venous effluent would permit determination of extraction efficiency of the initial passage of bolus through the organ by calculating the ratio of tracer concentrations in the observed venous effluent to that in the injectate subtracted from one.

$$1 - \left[\frac{\text{observed X/VM}}{\text{injected X/VM}}\right]$$

Experiments were carried out in 13 anesthetized dogs: I-131 albumin was the vascular marker in all, Hg-203 chlormeridrin was the test substance in 5, while Tl-201 was the test substance in 8. The renal vein was cannulated, injections were made into the renal artery and the kidney removed within 40 seconds of tracer injection. Extraction efficiency calculated both by the dual tracer method and by direct measurement of renal activity/injected dose. Dual tracer method had a mean of .41±.13 for chlormeridrin and .81±.05 for thallium, whereas the direct method had a mean of .38±.07 for chlormeridrin and .81±.06 for thallium.

These data suggest that the dual tracer method can be used to measure extraction efficiency. The dual tracer method offers the advantage of simplicity since only a bolus injection is required rather than infusion and only a representative venous sample is required from the organ rather than collection of the entire venous effluent.

WEDNESDAY, 10:30-12:00 BALLROOM A

IN VITRO 1

Chairman: Steven M. Larson
Co-Chairman: Stanley J. Goldsmith

GALLIUM-67 BINDING ASSAY: A POSSIBLE INDEX OF BIOLOGIC RESPONSE TO IONIZING RADIATION. J.W. Fletcher, F.K. Herbig, D.J. Klos, R.M. Donati. Section of Nuclear Medicine, St. Louis VA Hospital, St. Louis University, School of Medicine, St. Louis, Missouri.

A dose response relationship was established for decreases in serum binding of Ga-67 citrate and radiation exposure (Cs-137 source, 150R/min) at doses between 45R and 720R. Pooled sera obtained from irradiated or sham irradiated rats 24 hrs after a single whole-body exposure to 45R, 105R, 195R, 400R, or 720R was incubated with 0.1uCi of Ga-67 citrate for 2 hrs at 37°C. Stable non-radioactive Ga-69 citrate was then added to all samples to a final concentration of 10^{-5}M. 3ml aliquots of the pooled labeled sera were dialyzed against 6.0ml of 0.9% NaCl solution for 180 min utilizing cellulose membrane with a 20,000 M.W. exclusion. 0.5ml aliquots of dialysate were obtained and analyzed for Ga-67 radioactivity from 15 to 180 min after initiation of dialysis. Radioactivity of the aliquot was compared to the total Ga-67 activity initially added to the system, and results were expressed as the percent dialyzed fraction of Ga-67 per unit time. The rate of dialysis of Ga-67 was significantly greater in irradiated rat sera compared to control sera and the magnitude of change correlated with the exposure level:

DIALYZED FRACTION OF GALLIUM-67 AT 15 MIN AFTER DIALYSIS (MEAN % ± S.E.M.)					
CONTROL	45R	105R	195R	400R	720R
2.36±.08	5.4±.70	6.25±.50	9.1±.30	15.7±.50	20.4±.10

These results suggest that serum binding of Ga-67 significantly decreases following radiation exposure, and that the degree of change, as assessed by a simple in vitro assay, is directly related to the level of radiation exposure.

A MICROBIOLOGICAL RADIOMETRIC METHOD FOR VITAMIN B_{12} ASSAY. Marianne F. Chen, Patricia A. McIntyre and Henry N. Wagner, Jr. The Johns Hopkins Medical Institutions, Baltimore, Maryland.

The diagnosis of vitamin B_{12} deficiency continues to be of clinical importance. A radiometric method has been developed for assaying vitamin B_{12} in serum. Lactobacillus leichmannii utilizes arginine for pyrimidine synthesis releasing CO_2 as a by-product. The $^{14}CO_2$ produced from ^{14}C-arginine is quantitated in an ionization chamber. In the presence of ^{14}C-arginine

and cyanocobalamin this organism produces significant amounts of $^{14}CO_2$ within 17-20 hours. The amount of $^{14}CO_2$ evolved is optimized with the use of guanido-labelled arginine and is proportional to the amount of cyanocobalamin added. The amount of $^{14}CO_2$ produced increases from 0.0018 uCi to 0.175 uCi for 10 pg to 100 pg of cyanocobalamin with 2 uCi (U)^{14}C arginine, and from 0.002 uCi to 0.289 uCi for 10 pg to 100 pg with 1 uCi of (guanido)-^{14}C-arginine.

Preliminary studies of sera extracts show that the new radiometric method gives values comparable to the standard microbiological (turbidimetric) method using this organism. Cyanide is not required for the extraction of vitamin B_{12} from whole serum. Extraction may be accomplished by autoclaving with the assay medium at 15 lbs p.s.i. for 3 to 5 min. The precipitated serum proteins do not need to be separated and do not interfere with this assay.

This new semi-automated microbiological radiometric method may prove to be a more sensitive and simple assay for determining the level of vitamin B_{12} in sera of patients.

A NEW RADIOASSAY FOR FIBRINOLYTIC ACTIVITY Sally DeNardo, Gerald DeNardo, Show-Mei Huang, Lynda Parziale, Jeffrey Wortman, Kenneth Krohn. University of California, Davis, CA

Activation of the coagulation system with production and subsequent lysis of fibrin is a feature of many physiological and pathological situations. Standard methods for measurement of fibrinolytic activity are not quantitative and lack objectivity and reproducibility. Our investigations have led to the development of a radioassay for fibrinolytic activity in blood and tissue specimens from various animals and man. The assay is capable of discriminating levels of fibrinolytic activity by virtue of the rate of clot lysis as demonstrated by the time dependent release of radiolabeled fibrin(ogen) degradation products from a clot formed with the sample to be tested, radiolabeled fibrinogen and a control euglobulin. (The coefficient of variation for intra assay reproducibility for blood was 4.3%, and for inter assay was 9.5%. Similar values for tissue intra and inter assay were 6.3% and 14.7% respectively).

The assay has been utilized to distinguish different fibrinolytic activities in tissue and blood samples. For example, brain and lung fibrinolytic activities were greater than blood, liver or muscle from the same animal. Also, different tumor types demonstrated different degrees of fibrinolytic activity. Fibrinolytic activity of blood from patients with diseases associated with fibrinolysis was greater than for normal subjects. Estrogen induced increases in human blood fibrinolytic activity were detected.

This radioassay technique allows reproducible, objective and quantitative measurement of fibrinolytic activity of blood or tissue and is potentially applicable to detection of coagulation disorders, including those associated with thrombophlebitis and cancer. (Supported by American Cancer Society Grant #DT-45.)

PLASMA ANTITHYROGLOBULIN RADIOIMMUNOASSAY: EVIDENCE FOR A SINGLE IMMUNOLOGIC THYROID DISEASE. Michael D. Okerlund, Gary Carpenter, Mary Beth Caro and Evelyn Lam. University of California Medical Center. San Francisco, California.

To determine if human thyroglobulin antibodies could be determined by a direct antigen binding technique, we evaluated the binding of highly purified radioiodinated human thyroglobulin to patient serum with precipitation of complexes with goat antiserum. Our tabulated data:

Group	n	%bound	Elevated* No.	%
Normal	155	4.0±2.9	4	2.6
Hashimoto's thyroidits				
Pathologically diagnosed	26	48.0±12.1	26	100.0
Clinically suspected	96	41.2±11.2	89	92.7
Primary hypothyroidism	26	48.1±10.4	23	88.5
Graves' disease, untreated	72	42.1±9.9	66	91.6

*Greater than 3 standard deviations above mean normal

Sera were also tested by an agglutination method for microsomal antibodies in serial quadrupling dilutions from an initial 1:100 dilution. 85% of sera from patients with thyroiditis, primary hypothyroidism or Graves' disease showed positive tests, with median levels of 1:6400 in all 3 disorders. Five years or more after initial diagnosis of any of the 3, and regardless of the form of therapy, 80% of patients had no thyroglobulin antibodies detectable by this technique although microsomal agglutination antibodies remained in 80% with median levels of 1:1600. Radioimmunoassay for thyroglobulin antibodies is the most sensitive test for immunologic thyroid diseases, and the similarity in both titers and temporal sequences of two different antibodies suggests that Hashimoto's thyroiditis, primary hypothyroidism and Graves' disease may represent variant forms of a single immunologic thyroid disorder, differing in clinical manifestations.

WEDNESDAY, 10:30-12:00 BALLROOM B

DOSIMETRY

Chairman: Edward Smith
Co-Chairman: Robert Rohrer

GENETIC IMPLICATIONS OF GONADAL RADIATION DOSE IN IODINE-131 TREATMENT OF HYPERTHYROIDISM. James S. Robertson and Colum Gorman. Mayo Clinic, Rochester, MN.

A literature survey shows a range of 0.05 rad/mCi to 5.37 rad/mCi in the published estimates of the ovarian radiation dose from iodine-131. Some of this disparity is due to assumptions that do not apply to the hyperthyroid patient. To establish a more definite basis for evaluating the genetic risks in I-131 therapy of hyperthyroidism, a model of iodine metabolism using a range of variables for renal iodide excretion, thyroid iodine uptake and thyroid hormone release rates was developed, and the gonadal radiation doses were recalculated by the absorbed fraction method. The results show that a typical hyperthyroid patient treated with 10 mCi I-131 will receive a radiation dose to the ovaries or testes of less than 3 rad. This is 0.1 to 0.01 of the estimated human mutation rate doubling dose. Also, it is in the radiation dose range reached by some diagnostic roentgenographic procedures. The significance of chromosomal anomalies which may be seen at this radiation dose level has not been established. Considering the hazards of alternative treatment modes, it does not appear logical to withhold I-131 treatment on the grounds of genetic hazard alone.

RADIATION DOSE ESTIMATES TO THE EMBRYO. Edward M. Smith and Gordon G. Warner. Oak Ridge National Laboratory, Oak Ridge, Tn.

These studies provide a direct means of estimating the radiation dose to the embryo when a radiopharmaceutical has been intentionally or unknowingly administered to a female who is at the beginning of her pregnancy. They were performed on a computer using Monte Carlo techniques and mathematical models of the organs of interest. The embryo was assumed to be a sphere with a radius of 0.13 cm located in the center of the uterus weighing 65 gms. It was assumed that the embryonic period was from 10 to 41 days post-conception and that, during this period of time, there was minimal enlargement of the uterus. In addition, it was assumed that the presence of the placenta could be neglected for the purpose of estimating dose. Specific fractions of energy absorbed in the embryo from sources in 19 other organs were computed for 12 monoenergetic photon energies. Tables of absorbed dose per unit cumulated activity, S, for the embryo as a target organ have been assembled for Tc-99m, In-111, In-113m, I-123, I-131, and Xe-133. In addition to our previous studies, the effect of the implantation site of the embryo, the relative location of the uterus to other organs in the abdominal cavity and the variable size of the bladder and its contents on the dose to the embryo have been evaluated. The dose to the embryo was cal-

culated for several of the radiopharmaceuticals for which the MIRD Committee has published dose estimate reports. (Research sponsored by the U.S. Energy Research and Development Administration under contract with Union Carbide Corporation).

RADIATION DOSIMETRY OF I-131-6-IODOMETHYLNORCHOLESTEROL. Rodney D. Ice, Louis T. Kircos, Jack L. Coffey*, Evelyn Watson*, Salil D. Sarkar, and William H. Beierwaltes. College of Pharmacy and Nuclear Medicine Division, The University of Michigan, Ann Arbor, Michigan, and Radiopharmaceutical Internal Dose Information Center*, Oak Ridge Associated Universities, Oak Ridge, Tenn.

The tissue distribution of I-131-6-Iodomethylnorcholesterol (NP-59), Sp. Act. ≅ 1-5 mCi/mg, was determined in rats at 2 hrs., 1, 5, 10 and 15 days, and in dogs at 2 hrs, 1, 2, 3, 5, 7, 10, 15 and 20 days. Total body retention of radioactivity in eight patients over 26 days and urine and feces radioactivity from five patients over nine days were measured.

Cumulated activity, $\tilde{A}$, in all source organs was obtained by integrating the extrapolated dose per total organ of reference man from time of dose administration to infinity. Cumulated activity, $\tilde{A}$, times the rad/μCi-hr (S) was used to calculate absorbed dose in rads.

Percent total body retention (R) of NP-59 was described by

$$R = 39.5\%e^{-0.49t} + 35.5\%e^{-0.154t} + 25\%e^{-0.001t}$$

where (t) is time in days. The absorbed dose to the adrenals was 150 rads/mCi. Thyroid uptake in the animals indicated product deiodination and the need for adjunct thyroid blocking agents when NP-59 is administered to humans. All other organ doses were about the same as I-131-19-Iodocholesterol (NM-145).

Although the adrenal gland absorbed dose per millicurie of NP-59 is about five times the dose per millicurie of NM-145, the dose in other organs is no greater than that of NM-145, and better adrenal images are obtained at earlier time intervals.

EFFECT OF $NaClO_4$ ON BLOOD LEVELS AND EXCRETION OF ^{99m}Tc AFTER I.V. ADMINISTRATION AS $Na^{99m}TcO_4$ IN THE HUMAN. Katherine A. Lathrop, Ignacio V. Gloria, and P.V. Harper. University of Chicago, Chicago, IL.

The clinically well known inhibition by perchlorate of ^{99m}Tc uptake in the choroid plexus, stomach, and thyroid and salivary glands is accompanied by less well recognized alterations in blood levels, excretory rates, and partition between excretory pathways which may affect radiation absorbed doses and image quality. Seven subjects (3 males, 4 females) fasted overnight received 1 mCi $Na^{99m}TcO_4$; blood concentration was measured at 2.5,5,10,20,...320 min; and urinary and fecal excretion were followed for a 72h period. The procedure was repeated 3 to 4 days later 15min after the oral administration of 1g of $NaClO_4$. When the data from these two situations were looked at as average values, $NaClO_4$ appears to increase ^{99m}Tc in the blood. Inspection of the data for each individual, however, shows that perchlorate increases the blood level in 4 cases, and decreases it in 3. Perchlorate may increase the plasma concentration to approximately 150% or decrease it to 60%. These differences are not accounted for by gender or physical activity. The consistent effect of perchlorate is approximately to double the half-times for each of the three components of the blood disappearance curve. The magnitude of these components, however, may be either increased or decreased. These changes of ^{99m}Tc in the blood are accompanied by changes in total urinary excretion, but the slopes of the urinary excretion rate curves are essentially unchanged. These observations suggest that upper and lower radiation absorbed dose estimates should be calculated for $Na^{99m}TcO_4$, and that body background on images obtained with this agent may be increased for some individuals.
(Supported in part by GM-18940-03 and E(11-1)-69.)

WEDNESDAY, 10:30-12:00 BALLROOM C

PULMONARY 2

Chairman: Gerald DeNardo
Co-Chairman: August Miale

MICROBIOLOGIC AND GALLIUM SCAN CORRELATION IN LUNG INFECTIONS. Haragopal Thadepalli, Fred S. Mishkin, Kamalakar Rambhatla, Man M. Khurana, and Albert H. Niden. Martin Luther King, Jr. General Hospital, Los Angeles, Calif.

The role of Ga-67 imaging in patients with suspected lung infections was retrospectively analyzed in 70 consecutive patients who underwent gallium 67 imaging and had a proved bacteriologic diagnosis. Diagnosis was established by culture of transtracheal aspirates in 23, thoracentesis in 13, blood cultures for aerobic and anaerobic bacteria in 25 and sputa for TB and fungi in 13. Included were 12 patients with endocarditis and embolism, 9 with TB, 8 with aspiration pneumonitis, 7 with anaerobic infections, 7 with aseptic pulmonary embolism, 6 with pneumococcal pneumonia, 5 with malignancies, 4 with fungal infections, 3 with intra-abdominal sepsis, 2 with mycoplasma pneumonia and 7 with other infections. The image, interpreted without culture results, was abnormal in 47/70. Increased uptake was noted in all with anaerobic lung infections, pneumococcal pneumonia and malignancies. None with aseptic pulmonary embolism, mycoplasma pneumonia or bacteremia due to skin infections showed Ga-67 uptake. In endocarditis 9/12 had lung uptake, the 3 negative patients presumably having aseptic embolism since their transtracheal aspirates showed no pathogens. Seven of eight images in aspiration pneumonia were abnormal, the one normal being in a patient receiving antibiotic therapy. Four of nine with culture proved TB had normal Ga-67 images. Lupus, sarcoidosis and superinfection in COPD each showed abnormal uptake. Culture and Ga-67 image results correlated well in 65/70 cases. Ga-67 images failed to detect infection in 4 patients with TB and 1 with treated pneumonia. These results suggest that most non-tuberculous bacterial lung infections show increased Ga-67 uptake. When increased uptake is found in a patient with suspected lung infection, there should be vigorous pursuit of a microbiologic diagnosis when routine techniques do not yield the answer.

THE GALLIUM LUNG INDEX: A METHOD TO EVALUATE Ga-67 PULMONARY LOCALIZATION. Bruce R. Line, Stanley M. Levenson, A. Eric Jones, Jack D. Fulmer, Ronald G. Crystal, and Gerald S. Johnston. National Institutes of Health, Bethesda, Md.

Gallium lung localization has been reported in infectious, toxic and fibrotic lung disorders. Because of the subjectivity in assessing varying degrees of Ga-67 pulmonary localization, a semi-quantitative method, the Gallium Lung Index (GaLI), was created to standardize interpretation for clinical use. The GaLI is defined as a summation of terms, each representing a local percentage of lung area (0-100%), weighted by relative tracer intensity (0-4) and type of tracer pattern (patchy=0.5, diffuse=1.0, focal=1.5). Regional lung determinations were normalized relative to tracer accumulations in liver, bone, and background regions beneath the renal bed.

To validate this technique, 48 hr. post-injection rectilinear gallium scans were performed in 24 patients with documented idiopathic pulmonary fibrosis (IPF) and in 21 controls. Each study was evaluated independently by four observers without knowledge of the patient's history. The GaLI in the IPF group (mean 77, range 2-230) was significantly higher ($p<.001$) than in the control group (mean 23, range 0-115, 20/21 controls < 50). GaLI in untreated IPF (n=8, mean 93, range 2-193) was higher ($p<.2$) than in the prednisone treated group (n=19, mean 70, range 7-155). In the IPF group, the GaLI was also compared with biopsy histopathology (n=12) and bronchioalveolar lavage (n=13). GaLI correlated (p values) with the degree of fibrosis (<.05) and amount of alveolar cellularity (<.05) noted on lung biopsy, as well as the percent lymphocytes (<.02) and neutrophils (<.03) in the lavage fluid. The significant correlation of the GaLI with biopsy and lavage data suggests the efficacy of this method in the quantitation of Ga-67 lung accumulations.

DYNAMIC IMAGING OF THE DUAL CIRCULATION OF THE LUNG IN LUNG CANCER. J. Michael Uszler and Marcel Krauthammer. Divisions of Nuclear Medicine and Pulmonary Disease. UCLA-Harbor General Hospital, Torrance, Ca.

Pulmonary arterial perfusion (PAP) scanning is a standard static technique. No technique has been described for dynamic imaging of the systemic circulation of the lungs or of the PAP. We report a technique, dynamic lung circulation scintigraphy, to image both parts of this dual circulation in carcinoma of the lung.

Each patient was positioned to best view the lesion along with normal lung area and cardiac structures. Both Tc-99m pertechnetate transmission and Tc-MAA perfusion scans were performed. Immediately thereafter Tc-99m pertechnetate was injected IV with bolus technique. Passage of the radioactivity through both circulations was recorded on analog images and in digital mode for minicomputer processing. The digital images were formed in both 64 x 64 and non-interpolated 128 x 128 matrices, and displayed with software-controlled levels of color on a 19-inch diagonal color video monitor.

So far seven cases (biopsy proven) have been studied. All 7 cases showed diminution of PAP in the tumor region on both static perfusion scan and the dynamic lung circulation scintigram (LCS). Three cases showed markedly increased activity in the tumor region during the systemic arterial phase; these were easily visualized on both sequential analog and sequential digital images of the LCS. Time/activity curves from these areas showed that their ratio of systemic/pulmonary (s/p) arterial peak counts were 5.5, 9.8 and 12.1 times those of the normal lung regions.

The 4 other cases showed systemic phases with lesser increases or with activity visually equal to the surrounding lung. Their tumor area (s/p) ratios were 1.3 to 3.9 times those of the normal lung regions.

DYNAMIC IMAGING OF THE PULMONARY AND SYSTEMIC ARTERIAL CIRCULATIONS OF THE LUNG IN NON-NEOPLASTIC DISEASE. Marcel Krauthammer and J. Michael Uszler. Divisions of Pulmonary Disease and Nuclear Medicine, UCLA-Harbor General Hospital, Torrance, Ca.

Pulmonary arterial perfusion (PAP) scanning is a static technique. We report a dynamic method, lung circulation scintigraphy (LCS), to image both pulmonary and systemic arterial circulations of the lung in non-neoplastic disease.

Each patient was positioned to view the lesion along with normal lung area. Both Tc-99m transmission and Tc-99m MAA perfusion scans were performed. Immediately thereafter a bolus of Tc-99m pertechnetate was injected IV. Passage of radioactivity through both circulations was recorded on analog images and in digital mode for minicomputer processing. The digital images were formed in both 64 x 64 and non-interpolated 128 x 128 matrices, and displayed with software-controlled levels of color on a 19-inch (diagonal) color video monitor.

Eight cases have been studied: agenesis of the right pulmonary artery (2), pulmonary infarction, bronchiectasis, pneumonia, lung abscess and tuberculosis. One patient post pneumonectomy was also studied to assess chest wall radioactivity contribution on time/activity curves. In agenesis of the right pulmonary artery the LCS shows no PAP but excellent visualization of the systemic circulation to that lung. Pneumonia of one week duration showed absence of both pulmonary and systemic circulations to the area of the lesion. Long-standing tuberculosis showed absence of PAP with visually obvious systemic circulation. The lung abscess showed diminished PAP and no obvious systemic increase. Pulmonary infarction showed diminution of both PAP and systemic flow.

Lesions immediately adjacent to the cardiovascular structures were not well seen from the anterior view due to the presence of the bolus in these structures. Thus a pneumonia in the medial basal segment of RLL and bronchiectasis in RML were poorly visualized.

MEASUREMENT OF PULMONARY VASCULAR PERMEABILITY BY EXTERNAL RADIOFLUX DETECTION. A.B. Gorin, J. Weidner, and N. Staub. Cardiovascular Research Institute, San Francisco, CA.

Using a new, noninvasive method, we measured the permeability of vessels in lungs of sheep to In-113m labelled transferrin (MW=76,000). We compared the externally monitored interstitial accumulation of tracer protein (corrected for intravascular content using an independent measure of regional blood volume) to the accumulation in lung lymph. Lymph was obtained by cannulating the caudal mediastinal lymph node efferent duct. Relative regional blood volume was determined using autologous Tc-99m labelled red blood cells.

Studies were done under baseline conditions (10), after Pseudomonas bacteremia, which increases pulmonary vascular permeability (6), and in the presence of elevated left atrial pressure (3). At time zero, we injected 5 mCi of each isotope. We counted the γ-emissions of the 2 radiolabels in the lung using a 3-inch NaI crystal, focussed to a field 4cm in diameter and 14cm inside the chest. In all 19 studies, interstitial accumulation of tracer protein by external radioflux detection correlated well with the accumulation rate in lymph (r>.9). The pulmonary vascular permeability coefficient markedly increased after bacteremia.

Pulmonary Vascular Permeability Coefficient
Measured Directly and by External Radioflux Detection

	Direct	ERD
Baseline	.00271 ±.0006 (s.d.)	.00267 ±.0007 (s.d.)
Bacteremia	.01025 ±.0053 (s.d.)	.00895 ±.0059 (s.d.)

This new, noninvasive method reliably measures pulmonary vascular permeability. We are currently using it in patients to diagnose, and assess therapy, in noncardiogenic pulmonary edema.

SIGNIFICANCE AND MECHANISM OF CHANGING PATTERN OF PULMONARY PERFUSION IN PULMONARY EMBOLISM. Toshiyuki T. Tanaka and Donald E. Tow. V.A. Hospital, West Roxbury and the Joint Program in Nuclear Medicine, Harvard Medical School, Boston, Ma.

Resolution of pulmonary emboli is frequently characterized by changes of perfusion pattern on serial lung scans. This phenomenon has been ascribed to (1) lysis of the clot and subsequent migration downstream of the fragments, (2) recurrent embolism, albeit small, or (3) differential lysis of the larger clot and thereby unmasking the coexisting smaller one. This study was undertaken to study the necessary mechanism and effect of a second embolization on the primary defect. Serial externally detectable pulmonary emboli were created through a catheter in 12 dogs with long-lived radio-labelled non-metabolizable carbonized microspheres. The perfusion defects were followed by serial Tc-99m MAA scans over a period of 2 weeks. Results are summarized in Table. Seven dogs showed decrease in the size of primary perfusion defect after the second lesion was placed, while 3 dogs showed no change and one revealed an increase in the size of the initial defect. In 1 dog, only one lesion was created and this was followed with serial scans for 2 weeks; no changes were observed over this period. No pulmonary arterial hypertension was observed during catheterization and after the embolization. There was also evidence to suggest obscuration of the second lesion by the pre-existing embolism. The data suggest that (1) successive and co-existing emboli mutually affect the perfusion pattern, (2) this effect can be attributed to changes in local vascular resistance alone without concomitant pulmonary arterial hypertension, and (3) careful scrutiny of the evolving scintiphotographic pattern must be made in order to detect the subtle signs of recurrence.

EVALUATION OF PHARMACOLOGIC RESPONSE OF DRUGS AFFECTING THE UPPER RESPIRATORY TRACT. Robert M. Beihn*+, George A. Digenis*, Mary F. Reed*, George Zarocostas*, Frank H. DeLand*+, University of Kentucky*and VA Hospital+, Lexington, Kentucky.

Objective evaluation of the pharmacologic response of drugs affecting the upper respiratory tract has been difficult. A method has been developed for evaluating the patency of the nasal passages and paranasal sinuses by direct visualization of Xe-133 accumulation and rate of washout during normal respiration. We have used this method to demonstrate the decongestant action of phenylpropanolamine-HCl and desoxyribonuclease for promoting drainage in sinusitis. Following the initial image performed on the congested subjects, 2 tab-

lets of the drug (25 mg of phenylpropanolamine HCl and 5 grains of aspirin per tablet) were administered orally to each of them. Scintigraphy was then repeated at 0.5, 1, 2 and 4 hours. On subjects with sinus infections initial scintigraphs were taken followed by administration of the desoxyribonuclease. Imaging was repeated 24 hours later. Dynamic sinus scintigraphy was performed in the anterior position using a scintillation camera with a computer system for dynamic data collection and processing. The Xe-133 was administered with a single nasal inspiration, followed by normal breathing. Following drug administration sequential scintiphotographs showed a decongestant effect as exhibited by accumulation and decreased resistance to the washout of 133 Xe. The objective evaluation of pharmacologic response of drugs affecting the upper respiratory system was significantly enhanced using sinus scintigraphy.

EFFECT OF HYPOXIA ON THE REGIONAL DISTRIBUTION OF CARDIAC OUTPUT IN THE DOG. Haruhiko Adachi, H. William Strauss, Hironobu Ochi and Henry N. Wagner, Jr. The Johns Hopkins Medical Institutions, Baltimore, Md.

Severe hypoxia is a stimulus to the cardiovascular system which results in increased cardiac output and marked changes in vascular resistance of various organs. We have studied the changes in regional perfusion caused by moderate and severe hypoxia in the intact anesthetized dog using the microsphere (MS) distribution method. While breathing room air at fixed tidal volume, 21 dogs received 50μ Sr-85 MS via catheter in the left ventricle. The dogs were then made hypoxic by ventilation with either 10% oxygen (10 dogs) or 5% oxygen (11 dogs) and Ce-141 MS administered in the LV. Brachial artery blood samples were drawn at the time of tracer administration to calculate cardiac output. The animals were then sacrificed and activity in each organ determined as a % dose/organ and as cc/100gm/min. Table I has the data expressed as change in flow compared to the control state.

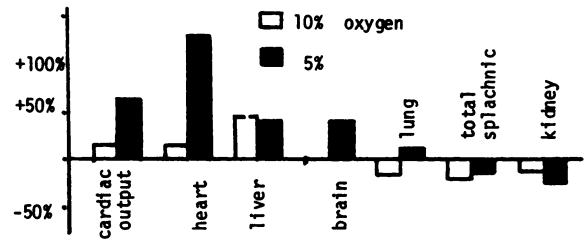

These data indicate that hypoxia markedly alters the distribution of regional perfusion.

WHOLE BODY RETENTION OF RADIOXENON. Herbert Susskind, Harold L. Atkins, Stanton H. Cohn, Kenneth J. Ellis and Powell Richards. Brookhaven National Laboratory, Upton, New York.

Long term whole body retention of xenon-127 was studied in order to refine dosimetry calculations. The photon emissions of Xe-127 are suitable for quantitative measurement in a whole body counter whereas the low energy photons of Xe-133 are not useful for this purpose.

Volunteer subjects (7 male, 4 female), ranging in age from 29 to 61 years and in weight from 110 to 306 lbs., breathed a mixture of air and Xe-127 in a closed system for 10 minutes. Three subjects repeated the study, breathing the mixture for 30 minutes. Constant volume of the system was maintained. Radioactivity in the chest region and in recirculating air was monitored during rebreathing and in the first 5 minutes of the immediate washout period. A calibrated sample volume of the gas mixture was obtained just prior to washout. Subjects were counted at intervals in a whole body counter until background levels of activity were reached in about 72 hours.

Up to 5 components of xenon clearance could be determined. The longest of these had a $T_{\frac{1}{2}}$ of 7.6-17.0 hr and comprised 1.03-17.6% of the total lung activity at start of washout. The $T_{\frac{1}{2}}$ correlated highly with % body fat. Other components of clearance had $T_{\frac{1}{2}}$'s of about 30 sec., 2 min., 0.4 hr and 2.6 hr. The ratio of xenon in the long term component of whole body retention to xenon in the lungs at start of washout varied between 0.01 and 0.18. The range of radiation dose from this component was 0.48-19 mrad for Xe-127 and 0.55-22 mrad for Xe-133 for 1 millicurie in the lungs at start of washout.

WEDNESDAY, 2:00-3:30 BALLROOM A

HEMATOLOGY 1

Chairman: Thomas G. Rudd
Co-Chairman: R. Edward Coleman

RADIOIODINATED PLASMINOGEN: AN IMAGING AGENT FOR PRE-EXISTING THROMBI. S.S.L. Harwig, J.F. Harwig, L.A. Sherman, R.E. Coleman, and M.J. Welch. Mallinckrodt Institute of Radiology, St. Louis, MO.

Several agents have recently been developed for imaging thrombi which are actively propagating. Localization of older thrombi in which net fibrin deposition has slowed is more difficult. To detect such pre-existing thrombi, fibrinolytic agents such as urokinase and streptokinase have been investigated, with variable results. The use of these activators is based solely on the theory that the prime factor in fibrinolysis is the intrinsic plasminogen trapped during thrombus formation. Our approach is based on evidence from immunofluorescence studies that there is a considerable increase in the plasminogen content of older thrombi. We have prepared radioiodinated plasminogen and studied its physicochemical properties, in vivo clearance, and thrombus incorporation. Canine plasminogen is isolated by affinity chromatography using lysine-Sepharose 4B columns and is iodinated with I-131 by the conventional iodine monochloride technique. The iodinated plasminogen retains its full enzymatic activity and clears in dogs with a $t_{\frac{1}{2}}$ of 28-32 hr. SDS gel electrophoresis reveals a single band corresponding to non-labeled plasminogen and containing 90% of the applied radioactivity. Thrombus:blood activity ratios of 9.6 ± 1.8:1 were obtained in dogs when labeled plasminogen was injected 48-144 hr after induction of femoral vein thrombosis. Much lower and variable thrombus:blood ratios were obtained for 24 hr old thrombi, which appears to be related to thrombus retraction and plasminogen release. In 4 out of 5 dogs with 48-144 hr old femoral vein thrombi, good images were obtained with I-131 labeled plasminogen, despite the small size (5-25 mg) of these thrombi. These results indicate that plasminogen labeled with I-123 may be applicable to imaging pre-existing thrombi in patients. (N.I.H. Grant 1 P17 HL 14147-05.)

LABELING OF HUMAN FIBRINOGEN WITH Hg-197. Gopal B. Saha, Peter K. Girschek, and Paul A. Farrer. Royal Victoria Hospital, McGill University, Montreal, Quebec, Canada.

The purpose of the present study was to establish optimal physiochemical conditions for labeling human fibrinogen with Hg-197.

Commercially available human fibrinogen with a concentration of about 10 mg/ml either in acetate buffer or normal saline, was labeled with Hg-197 by adding 1 ml of Hg-197-chloride containing a certain amount of Hg-197 radioactivity The mixture was adjusted to a certain pH by adding 0.5N NaOH and then incubated at a temperature of 0°, 22°, or 37°C for a certain period of time. Labeled fibrinogen was precipitated by adding 3 ml of 4M ammonium sulfate and redissolved in phosphate buffer for radioassay. The effect on the labeling efficiency due to changes in the following parameters were investigated: (1) pH, (2) incubation time, (3) temperature, (4) presence or absence of buffer.

No significant difference in labeling efficiency was observed whether the fibrinogen sample was prepared in acetate buffer or saline solution. The labeling yield increased with increases in pH up to a pH of about 7.0 and then reached a maximum of 90% above pH 7.0. The fibrinogen precipitated at pH greater than 7.0 did not dissolve in

phosphate buffer, while it dissolved at pH less than 7.0. Maximum labeling (about 90%) was achieved when incubation was carried out at 37°C for a period of 15 - 30 minutes. The firmness of labeling was checked by repeated salting-out which showed a loss of only 2 - 5% label after each salting-out step, indicating a firm bonding between Hg and fibrinogen, probably the -SH group of the latter.

The simplicity and firmness of labeling of human fibrinogen with Hg-197, allied with its suitable physical characteristics make Hg-197-fibrinogen a potentially useful agent for the detection of thrombi in patients.

CORRELATION OF ENDOTHELIAL DAMAGE WITH I-125 FIBRINOGEN ACCUMULATION. Milo M. Webber, Eric W. Fonkalsrud, Ramesh C. Verma, Pratiba K. Sansi, and Beth Gleghorn. University of California, Los Angeles, Calif., and Olive View Medical Center, Van Nuys, Calif.

Endothelial damage and thrombosis may be consequences of the ischemia and perfusion with solutions in transplanted organs. This study was designed to correlate this damage (gauged by scanning electron and light microscopy) to the deposition of I-125 fibrinogen. An in vivo animal model was used consisting of arterial segments perfused with 10% dextrose or rendered ischemic (hence anoxic).

Fibrinogen was isolated from dog plasma by NH_4SO_4 precipitation and labeled with I-125 by a modified Bale-Helkamp method. Segments of femoral artery were isolated between two bull dog clamps and perfused with 10% dextrose at the rate of 60 ml/hr for 6 hours. Forty-eight hours before the animals were sacrificed, 125-150 uCi of I-125 fibrinogen were administered intravenously. Multiple specimens were punched out from different parts of the resected perfused segment, the ischemic segment and a distant normal artery. The remaining portion of the segments were weighed and counted individually in a well counter. The radioactivity deposited on the resected segments and in a sample of blood was expressed in cpm/gm of tissue. On comparing the cpm/gm of tissue in various segments, increased uptake of I-125 fibrinogen correlated well with the endothelial damage demonstrated by the scanning electron microscope. The correlation with light microscopy was difficult because of diffuse inflammatory changes in and around the vessel wall. (Supported by USPHS Grant 2-R01-GM17113-04 and ERDA Contract E-(04-1) GEN-12.)

RISA AND I-125 FIBRINOGEN ACCUMULATION IN SITES OF FORMING AND FORMED THROMBI. Ramesh C. Verma, Milo M. Webber, and Beth Gleghorn. University of California, Los Angeles, Calif.

This study was designed to evaluate the differences in the accumulation of I-125 labeled RISA and Fibrinogen (RFIB) in sites of forming and preformed thrombi. A modified Wessler technique was used to induce thrombi in the marginal ear veins of 60 rabbits.

In Group I (30 rabbits), the thrombi were induced one hour after and in Group II (30 rabbits), 24 hours prior to intravenous administration of 100 uCi of the agents. The test and control (opposite ears) were counted daily up to 7 days using a special ratemeter with a 1 cm hole collimator. Counts over the control ear were subtracted from those over the site of thrombosis to give the net counts attributable to the site of thrombosis. The mean net increase in counts in the various groups was plotted against time.

In Group I, both RISA (15 rabbits) and RFIB (15 rabbits) achieve peak counts soon after injection of the tracers. However, the accumulation in Group II (Preformed thrombi) is relatively slower and achieves peak counts approximately 6 hours following administration of the agents. The maximal counts for RISA and RFIB in Group II were approximately 25% of that in Group I. Slower clearance of the tracer from the sites of thrombosis was noted in both groups with RFIB showing a more gradual fall than RISA. The latter is the only apparent difference between the two agents. RISA shows an uptake like RFIB in this experimental model and may, therefore, be a good alternative for thrombosis detection—obviating problems of hepatitis antigen screening which is necessary with RFIB. (Supported by USPHS Grant 2-R01-GM17113-04 and ERDA Contract E-(04-1) GEN-12.)

ACCUMULATION OF Cr-51 PLATELETS, I-125 FIBRINOGEN AND Tc-99m SULFUR COLLOID (TSC) IN THE LUNGS FOLLOWING ENDOTOXIN ADMINISTRATION. Robert E. Henry, Mary M. Somogyi, Lynn R. Hendershott, Dennis J. Klos, Erica A. George and Robert M. Donati. St. Louis VA Hospital and St. Louis University School of Medicine, St. Louis, Mo.

Abnormal lung accumulation of TSC occurs in patients with sepsis or malignancy and has been produced in animals by endotoxin administration. Accumulation of TSC in fibrin deposits in rejecting renal transplants and the in vitro interaction between TSC, platelets and fibrinogen suggested that the coagulation system might play a role in pulmonary accumulation of TSC. Cr-51 labeled platelets and I-125 labeled fibrinogen were given to endotoxin-treated (1/3 LD 50) rabbits. TSC or saline was given 24 hrs thereafter and the distribution of the tracers determined. Cr-51 and I-125 lung activity was 2 fold, and TSC lung activity was 7 fold control values. TSC administration did not augment platelet or fibrinogen accumulation in the lung. The blood clearance and body distribution of platelets, fibrinogen and TSC was determined in rats for the first 72 hrs following endotoxin administration. Endotoxin accelerated the blood clearance of platelets and fibrinogen. The lung accumulation of platelets and fibrinogen had significantly increased by 12 hrs, peaked at 24 hrs and returned toward normal at 72 hrs. These changes were paralleled by similar changes in lung uptake of TSC. Microscopic radioautographs of rat lung 24 hrs post-endotoxin and 30 min post-TSC administration revealed TSC activity in proliferating alveolar septal capillaries in association with endothelial hyperplasia and non-occlusive mural fibrin thrombi. Thus, in the animal model, TSC accumulates in the lung in association with fibrin deposition. These data support the hypothesis that the coagulation system may be involved in the deposition of TSC in the lung of patients with cancer or sepsis and may reflect hypercoagulability or intravascular coagulation.

LUNG UPTAKE OF TECHNETIUM-99m MICROAGGREGATED ALBUMIN IN THE RATS AFTER IMMUNIZATION WITH MACROAGGREGATED ALBUMIN. Hajime Murata, Kenichi Kitani, Masahiro Iio, Hideo Yamada, Kazuo Chiba, Kengo Matsui and Shinichiro Kawaguchi. Tokyo Metropolitan Geriatric Hospital and Metropolitan Institute of Gerontology, Tokyo, Japan.

During the study of liver uptake of Tc-99m human serum albumin(Tc-HSA) in the sensitized dogs, one of authors recognized and reported the occasional occurrence of lung uptake of the Tc-HSA. As a possible cause of lung visualization, pulmonary microembolization of intravascular aggregated albumin was proposed. The purpose of the present study is to verify this hypothesis and to investigate the exact mechanism involved in this phenomenon by using Tc-99m microaggregated albumin (Tc-MIAA).

Wiater rats were immunized by two subcutaneous injections of 5 mg of HSA or human macroaggregated albumin(MAA) in incomplete adjuvant at two weeks interval. Two weeks after the second injection of antigen, lung and liver scannings were performed using Tc-MIAA, Tc-HSA and Tc-sulfur colloid. MIAA was prepared by the sonication of MAA. The particle size was assessed microscopically and by organ distribution studies in the control rats.

As the results, in all rats immunized with MAA, Tc-MIAA were markedly accumulated in the lungs with similar or greater activity than in the liver. However, no lung was visualized in the same group when rats were injected Tc-sulfur colloid or Tc-HSA. On the other hand, in the group which was immunized with HSA, there was no visualization of the lung by Tc-HSA, Tc-MIAA or Tc-sulfur colloid.

Increased deposition of Tc-MIAA in the lung of the rats after immunization with MAA strongly suggested that the mechanism for lung visualization in the present study was due to microembolization of clumping particle(antigen-antibody complex).

WEDNESDAY, 2:00-3:30 BALLROOM B

DATA ANALYSIS 2

Chairman: James Carlson
Co-Chairman: Sidney A. Johnston

RECONSTRUCTION AND ANALYSIS OF DATA FROM A DYNAMIC POSITRON IMAGING DEVICE. C.J. Thompson, Y.L. Yamamoto,

and E. Meyer. Montreal Neurological Institute, Montreal, Quebec, Canada.

Coincidence data from 32 detectors in a 40 cm ring are acquired in a mini computer from cross sections through the brain of a patient who has absorbed Ga-68 or Kr-77. This data can be reconstructed into an image by inversion of the Radon Transform or a convolution technique. The only movement of the detector ring is a to and fro rotation of 5°. The high counting efficiency allows short counting times per frame so that dynamic studies can be performed.

The data from pairs of detectors which face each other along parallel chords represent a "projection" of the isotope distribution. These projections are convolved with a filter function and back-projected from 32 angles onto a 40 X 40 grid where each pixel represents one square cm. The reconstruction of each frame takes 30 sec. on a PDP-12 computer.

Sets of static images may be combined before reconstruction to produce a low noise image in which areas of interest may be defined. The concentration is plotted as a function of time in these areas. Regional cerebral blood flow is computed from the regression line through a selected group of points plotted on a semi log scale.

The device has a FWHM of 2.5 cm axially and 4 cm in the slice. With a 10 μ.Ci. injection, time resolution of 10 seconds is possible in dynamic studies in patients.

COMPUTED EDGE DELINEATION APPLIED TO VENTRICULAR REGIONAL CONTRACTION PATTERNS. Denny D. Watson, Warren J. Janowitz, Peter J. Kenny and Albert J. Gilson. Mount Sinai Medical Center, Miami Beach, Florida.

Evaluation of left ventricular (LV) contraction patterns from ECG gated end-systolic and end-diastolic imaging is a valuable adjunct to the conventional radionuclide angiocardiographic (RAC) study. An alternative method has been developed which simplifies the clinical procedure and improves the definition of LV margins. The images are formed by a commercial data processing unit from the single pass levo phase of the standard RAC study. End-systole, end-diastole, and integration time intervals are determined by the count rate curve from a region-of-interest encompassing the LV (Auto-gating). The images are then formed by retrospective summing over the selected time intervals. An edge delineation process is then applied to the images which are printed on a dimensionally calibrated hard copy unit. The process is a modified second spatial derivative which objectively delineates the ventricular margins and largely eliminates interference and distortion caused by non-constant extra-ventricular background and overlying right heart activity. Phantom and patient studies have been performed. Patient studies have been compared to results from cardiac catheterization, ultrasound, and Thallium-201 studies. The auto-gated edge delineated (AGED) images provide improved and objective definition of LV borders, better dimensional accuracy in comparison to conventional gated RAC images, and do not require prolonged immobilization of the patient or special ECG and phono gating.

EXTENDED NUCLEAR UTILITY: A MODULAR PROGRAMMING SYSTEM FOR SCINTIGRAPHIC DATA ANALYSIS. Bruce R. Line, Renee G. Dunham, Gerald S. Johnston, and James J. Bailey. National Institutes of Health, Bethesda, Md.

The Extended Nuclear Utility (ENU) system consists of 165 program modules written in FORTRAN II and extends the HP 5407 minicomputer software so that large combinations of analysis routines can be efficiently managed and executed. Without being an expert programmer the user can apply ENU to a wide variety of processing tasks. An interactive mode of operation allows a user to generate an analysis procedure by linking modules into sequences (macros) and examining the function of these combinations as they operate. A command editor and macro file manager are provided to allow procedures designed interactively to be changed, stored, and run at a later time under a batch mode of operation. Modular functions include routines for data collection (HP), framing of images (HP), image display, and integer or real arithmetic functions on scalers, one dimensional (1*160), and two dimensional (64*64) arrays. In addition, modules are provided for parametric mapping, time-function extraction, automatic area-of-interest definition and conditional processing control. These conditional control modules test and respond to the state of the data under analysis and may branch to a new macro file or command sequence as needed. Finally, ENU provides a simple mechanism by which new program modules may be incorporated into the system library.

The ENU system has demonstrated its value by greatly reducing the programming time necessary to generate new, efficient analysis procedures for renograms, myocardial images, and automated regional ventilation-perfusion relationships in the lung.

NUCLEAR MEDICINE APPLICATIONS OF THE POCKET CALCULATOR, Peter M. Ronai and Dennis L. Kirch. Univ. of Colorado Medical Center and The Denver VA Hospital, Denver, Colorado.

Because many Nuclear Medicine laboratories cannot afford a computer, this investigation was undertaken to develop programs for the new generation of programmable pocket calculators to perform Nuclear Medicine computations many of which have previously been thought to require a computer. Miniature magnetic cards, each holding 100 program steps, are passed through a slot in the calculator to record or load programs. The major limitation is that relatively few memory registers are available for data storage. This problem can be minimised with ingenuity (eg. using program cards to store data). Multi-card programs are possible. The following programs illustrate the versatility of this device: 1) Radioactive decay: given any 3 of: activity at time t, original activity, half-life and t, computes the 4th. Computes volume of desired patient dose given in addition original volume and desired patient dose. 2) Compton Scatter Correction: corrects lower energy isotope counts for Compton events from higher energy isotope in double label studies. 3) Vitamin-B12 Absorption(double label): computes Co-58 Vitamin-B12 excretion, Co-57 Vitamin-B12/Intrinsic Factor excretion and Co-57: Co-58 ratio. 4) Curve Fitting: fits linear or exponential curves (eg. red cell survival, iron kinetics), computes Y intercept, slope, half-time, correlation coefficient and any point on best-fit line. Components can be stripped from multiexponential curve without plotting curve. 5)Radioimmunoassay: performs logit-log transformation on standard sample data. Determines line of best fit and correlation coefficient by linear regression. Standard curve is thus stored in calculator and antigen concentration of unknown sample can be read out given bound C.P.M. of sample. 6)Modulation Transfer Function: Computes MTF at any frequency from symmetrical or asymmetrical Line Spread Function using exact Fourier Transform including real and imaginary terms. Time taken to run above programs is 2 - 5 minutes.

WEDNESDAY, 2:00-3:30 BALLROOM C

GASTROINTESTINAL 1

Chairman: Thomas P. Haynie
Co-Chairman: George A. Wilson

COMPARISON OF NUCLEAR IMAGING, GRAY SCALE ULTRASONOGRAPHY AND COMPUTED AXIAL TOMOGRAPHY OF THE LIVER. Z.D. Grossman, P. Brian, M. Dinn, J.G. McAfee, B. Wistow and D. Bassano. Upstate Medical Center, Syracuse, N.Y.

To compare three hepatic imaging methods for detection, localization and sizing of lesions, patients were studied initially by any one method and re-examined within one week by either or both of the other two. Nuclear imaging utilized Tc-99m sulphur colloid and high resolution collimators; for computed axial tomography, an Ohio-Nuclear Delta scanner was used; and for ultrasonography, a Unirad Sono II with a G.Z.D.

Nuclear imaging has not failed as yet to disclose intrahepatic lesions detected by C.A.T., while several small lesions have been observed on hepatic scintigrams and not by C.A.T. Bowel gas, surgical clips and ribs produce artefacts on C.A.T. scans which sometimes obscure liver lesions. The difference in attenuation coefficients between tumor and

normal liver tissue unfortunately is often small. Lower attenuation by amebic abscess and fatty infiltration has been observed. Current contrast materials do not significantly improve C.A.T. hepatic images. C.A.T. is helpful in delineating adjacent structures including the spleen, pancreas, spine, kidneys and retroperitoneal space.

Gray scale ultrasound often clarifies indentations observed on nuclear images created by adjacent organs and is distinctly superior to radionuclide scanning for visualization of dilated ducts, the porta hepatis, gall bladder, portal vein, and the thin portion of the left hepatic lobe. For certain very large hepatic lesions and for the lateral portion of the right lobe, nuclear imaging is superior to sonography.

The combination of ultrasound and nuclear imaging more accurately assesses focal hepatic lesions than either modality alone. C.A.T. hepatic imaging appears to be a valuable adjunct to diagnosis only occasionally.

THE COMBINED USE OF GALLIUM SCANNING AND ULTRASOUND IN THE DIAGNOSIS OF INTRA-ABDOMINAL ABSCESSES
J. Ryan, M. Isikoff, C. Nagle, and M. Cooper. University of Maryland Hospital, Baltimore, Maryland.

The combination of scanning using Gallium-67 citrate and B-mode gray scale ultrasound (G.S.U.S.) was evaluated in 6 patients with suspected abdominal abscess.

Gallium-67 scans were obtained following a Tc-99m colloid liver scan at either 6 hrs or 48-72 hrs after injection. G.S.U.S. was performed within 6 days of the scintiscan. In 5 of the patients there was an abnormal focal accumulation of Ga-67 in the abdomen but in only 2 out of 5 of these did G.S.U.S. show a mass at the abnormal Ga-67 site. In one of these cases the mass was cystic and surgery revealed a perinephric abscess, while in the other case the mass was solid, not characteristic of abscess, and at surgery lymphoma involving retroperitoneal nodes without abscess was found. Of the remaining 3 patients, abnormal by Ga-67 scan but without focal lesions on G.S.U.S., 2 had abscesses which were drained surgically and 1 patient with an amebic abscess of the liver responded to medical therapy.

In one of the 6 patients G.S.U.S. revealed a cystic mass, while Ga-67 did not accumulate at the site of the mass. A pancreatic pseudocyst was demonstrated subsequently.

Ga-67 scanning appears to be more sensitive than G.S.U.S. in the detection of intra-abdominal abscesses, but it is nonspecific because of the other known causes of abnormal Ga-67 uptake. When abnormal masses are detected, G.S.U.S. provides definition of their structural characteristics. The combined use of these two studies in patients with suspected abdominal abscesses allows a greater diagnostic accuracy than either study alone.

THE COMBINED USE OF TC-99m HIDA AND ULTRASOUND IN DIFFERENTIAL DIAGNOSIS OF JAUNDICE.
J. Ryan, M. Isikoff, C. Nagle, M. Loberg, E. Buddemeyer, and M. Cooper. University of Maryland Hospital, Baltimore, Maryland.

In the differential diagnosis of obstructive jaundice, it is of value to know if bile duct dilation is present and whether or not the biliary tract is patent. Dilation is revealed by high resolution B-mode gray scale ultrasound (G.S.U.S.). Bile duct patency is demonstrated by transhepatic transport of Tc-99m HIDA into the gut. Ten clinically jaundiced patients with bilirubin levels between 1.9 and 18 mg/dl have been studied using both techniques.

By G.S.U.S., 4 of 10 showed obstruction. Two with complete common duct obstruction due to tumor were also diagnosed with Tc-99m HIDA. The other two patients were thought to have biliary obstruction due to gallstones. Subsequent Tc-99m HIDA studies showed the biliary tract to be patent and it was assumed the obstructing stones had dislodged. One of these two had multiple gallstones in the gallbladder and common duct at surgery, and the other, without surgery, improved clinically but had no change in bile duct dilatation by G.S.U.S. 6 weeks later.

Six of ten patients showed no evidence of obstruction by G.S.U.S. Tc-99m HIDA studies were in agreement in five. However, the sixth patient with intrahepatic cholestasis and no obstructive changes by G.S.U.S. was completely obstructed to Tc-99m HIDA.

The combined use of these two techniques has proven of value in deciding the medical or surgical management of patients with obstructive jaundice. Together, they provide a high degree of accuracy in the differential diagnosis of jaundice which is superior to the use of either technique alone.

AN EVALUATION OF Tc-99m LABELED HIDA DERIVATIVES AS HEPATOBILIARY AGENTS IN EXPERIMENTAL ANIMALS.
Brian Wistow, Gopal Subramanian, John G. McAfee, Robert Hall, George Gagne and Robert Henderson. The Upstate Medical Center, Syracuse, New York

Recent work by Van Heertum et al. (JNM, Vol. 16, No. 6, June 1975, p. 577) provided a means of evaluating several new Tc-99m labeled hepatobiliary agents and comparing these to the classical agent, rose bengal. A baboon model with T-tube bile collections, as well as blood and urine samples was used. Images in rabbits and dogs also were evaluated. Pyridoxal leucine was judged the best of the agents tested.

This study, using a similar model, compares other radiopharmaceuticals including the iminodiacetic acid derivative of lidocaine (HIDA), and related analogues.

It has been shown that increasing the molecular weight of a compound can improve its biliary excretion. Therefore, several new HIDA analogues were synthesized with the substitution of ethyl and ethoxy groups, as well as iodine, on the benzene ring. These new compounds were formulated as instant kits containing the stannous ion as the reducing/complexing agent for labeling with Tc-99m. Analytically, these new radiopharmaceuticals contained negligible colloid or free pertechnetate.

These new agents reached a higher bile concentration than rose bengal in the first 30 minutes but not after 1 hour. During the first 5 minutes blood clearances were faster than that of rose bengal, but not thereafter. Their urinary excretion was also greater. Significant differences in biliary and urinary excretion were observed between the various compounds.

These new radiopharmaceuticals appear to be superior hepatobiliary agents. Because they are labeled with Tc-99m and become highly concentrated in bile, visualization of the biliary tree on serial images is excellent.

WEDNESDAY, 4:00-5:30 BALLROOM A

NEUROLOGY 2

Chairman: Kenneth A. McKusick
Co-Chairman: Frank DeLand

IN VIVO DISTRIBUTION OF ORALLY ADMINISTERED Br-82$^-$ IN TUBERCULAR MENINGITIS.
H. Da Costa, A. Borkar and M. Loken. Radiation Medicine Centre, Bhabha Atomic Research Centre, Tata Memorial Hospital, Bombay, India.

In 1929 Walter administered stable bromide orally and demonstrated that the normal serum to C.S.F. ration was greater than 2 at 48 hours and that ratios below 1.6 were linked with tubercular meningitis (T.B.M.). Using Br-82 0.6 uc/kg orally in 163 patients, we too find a similar correlation. Repeat studies during anti-T.B.M. therapy correlate rising ratios with clinical improvement and lack of change or a decline with a poor prognosis. Because of the necessity of repeat spinal taps, technical simplification is now sought by serial externa[illegible]s over the heart, head and thigh at 4, [illegible] 48 hrs.; counts are expressed as blood: C.S.F. ratios at each interval. T.B.M. patients exhibit a higher C.S.F. permeation initially with a more precipitous decline than non-T.B.M. patients. Ratios obtained by our in vivo counting method appear to

correlate well with the more classical plasma to C.S.F. ratios. Work is in progress to study Br-82 distribution in a variety of other neurological diseases. A paralled trial to evaluate the behaviour of intravenously administered Tc04-99m- in progress.

BRAIN IMAGING USING Ga-68-DTPA AND A MULTIWIRE PROPORTIONAL CHAMBER POSITRON CAMERA. R.S. Hattner, C.B. Lim, S.J. Swann, D. Chu, L. Kaufman, and V. Perez-Mendez. University of California, San Francisco, California.

A dual detector positron camera based upon multiwire proportional chambers using lead channel converters has been constructed and its imaging performance characterized. Preliminary clinical application of the instrument to brain imaging is described.

Ten patients with brain lesions (primary neoplasms, 8; abscess, 1; metastases, 1) were studied 1.5-2 hours after the administration of Ga-68-DTPA. One hundred-200K coincidence events were recorded over approximately 30 minutes. A single positioning with sagittal plane perpendicular to the detectors was used. Serial frontal images were reconstructed from the data set by determining the intersection of the annihilation vectors in planes separated by 1 cm after field uniformity correction, thresholding, and a single smoothing. The images were displayed on the computer's storage oscilloscope, and photographed. Corroborative data included x-ray section scanning (CAT), conventional Tc-99m-DTPA scintigraphy, and surgical pathology in all patients.

The lesions were well visualized in eight patients. One glioma was poorly seen, and another glioma (the first study) escaped detection because of poor camera performance. The positron images demonstrated superb tomography, mitigating the problem of interference of superficially increased activity from craniotomy in determining the presence of intracranial lesion in conventional Tc-99m-DTPA scans, corroborated by CAT. Central necrosis of lesions shown in CAT, not evident in the Tc-99m-DTPA scans, was observed in the positron images. Lesion extent appeared occasionally underestimated in conventional scans compared to the positron images and CAT. In these patients the positron images, although crude, often provided more information than conventional scans.

EVALUATION OF POSITRON EMISSION TOMOGRAPHY FOR STUDY OF CEREBRAL HEMODYNAMICS IN A CROSS SECTION OF THE HEAD USING POSITRON EMITTING GALLIUM 68-EDTA AND KRYPTON-77. Y.L. Yamamoto, C. Thompson and E. Meyer. Montreal Neurological Institute and McGill University, Montreal, Canada.

It is well recognized that positron annihilation coincidence detection offers the basic advantage of depth independent and depth equal responses by back to back emission of 511 Key gamma as compared to the photon detecting system. A ring of 32 scintillation detectors was initially constructed at Brookhaven National Laboratory about 14 years ago. Following extensive modification of the hardware of this device and the analytical method, this system is now relocated at the Montreal Neurological Institute for further modification of the system and clinical investigation. In contrast to other tomographic devices, including the hexagonal positron device, gamma tomography and EMI scanner, all of which require a number of rotations of the detecting system to obtain the final image, while our system is stationary and is therefore most suitable for cerebral hemodynamic studies.

We have been investigating cerebral hemodynamics in subcompartments of the cross section of the head using the inhalation technique of the positron emitting inert gas, ^{77}Kr and the intravenous injection of nondiffusible ^{68}Ga-EDTA. This tomographic dynamic study has the capability of studying the territorial blood flow or perfusion rate of the cerebral arteries as well as the sub-compartments of the internal capsule or thalamic area without any interference from other territorial blood flow. Preliminary studies on stroke, arteriovenous malformations and brain tumors in correlation with the results from the gammacamera dynamic studies and the EMI scans were performed in over 50 cases. This study indicates that the tomographic dynamic study is particularly useful for determination of the hemodynamics of the posterior cerebral circulation and subcortical nuclei as compared to the other techniques,Fig.1-3

COMPARATIVE EVALUATION OF CEREBRAL FLOW AND IMAGING AND COMPUTERIZED AXIAL TOMOGRAPHY. Richard W. Arnold, L. M. Erickson, B. V. Evans, D. D. Lawrence and H. E. Duggan, Foothills Hospital, Calgary, Alberta.

This investigation was undertaken to compare the diagnostic sensitivity and accuracy of computerized axial tomography to cerebral flow and imaging studies.

All nuclear medicine studies consisted of an anterior or posterior flow, followed by four view static images done immediately and at 3 hours. Additional views were obtained if required. Skull radiographs were present. These studies were all interpreted and reported prospectively without knowledge of other neurodiagnostic procedures. The C.A.T. scans were performed on an EMI scanner, usually within 24 hours. Data from 770 cases, including history, cerebral flow, static images, C.A.T. scans with and without infusion, and other neurodiagnostic studies were analyzed. Surgical, pathological, and clinical information was reviewed.

The C.A.T. studies, besides their value in diagnosing of ventricular enlargement and cerebral atrophy, were clearly more sensitive in diagnosing porencephaly, intracerebral hematomas, and low grade astrocytomas. Cerebral flow and imaging studies were often superior in the diagnosis of cerebrovascular disorders, subdural hematomas, postoperative recurrences, highly vascular tumors, and meningitis. The majority of clinically significant space-occupying lesions were demonstrated by both techniques..

WEDNESDAY, 4:00-5:30 BALLROOM B

INSTRUMENTATION 2

Chairman: Paul H. Murphy
Co-Chairman: James C. Ehrhardt

COMPARATIVE PERFORMANCE STUDY OF THE LARGE FIELD SCINTILLATION GAMMA CAMERAS. Chun B. Lim, Paul B. Hoffer, David Palmer, Polly Chang and David Rollo, University of California, San Francisco, Ca.

The purpose of this study was to compare the performance characteristics of two 15 in. diameter field of view gamma cameras (Searle LFOV and Ohio-Nuclear Model 110) with regard to imaging in the 140 keV energy range. Specific parameters studied were: 1) intrinsic sensitivity and resolution, 2) collimator sensitivity and resolution, 3) count rate capability and influence of count rate on resolution, 4) energy resolution, 5) field uniformity.

One production model of each instrument was tested. Both instruments were interfaced with identical PDP 11 computer units for resolution measurements to insure uniformity of comparison. The concise results of the comparison were as follows:

	LFOV	ON
Intrinsic resolution (140 keV FWHM)	7.4 mm	6.5 mm
Max. count rate (20% window)	145 k/sec	73 k/sec
Count rate at 10% data loss	70 k/sec	55 k/sec
Energy resolution	15%	15%

Field uniformity and sensitivity with both instruments was similar. Collimator resolution studies revealed that the two sets of parallel hole collimators available for both instruments were distinctly different, preventing a direct comparison. The LFOV collimators offered a broader spectrum of sensitivity and resolution capabilities.

Both instruments offered significant improvements in field size and count rate capabilities over current 10 inch cameras at the cost of decrease in intrinsic resolution.

PERFORMANCE OF A SCINTILLATION CAMERA WITH DYNAMIC UNIFORM FIELD CONTROL. R.D. Petrocelli, D.B. Sodee, J.L. Besett, and M.L. Sowinski. Hillcrest Hospital, Mayfield Hts.,Oh., and Ohio Nuclear, Inc., Solon, Oh.

With inherent need of quality control of a scintillation camera, evaluation was undertaken of a newly developed system which incorporates dynamic uniform field control (DUFC) and automatic peak tracking (APT).

Integral uniformity was determined from slice profiles with and without DUFC. APT was evaluated. Bar phantoms were utilized to establish the improvement of image quality obtained with DUFC and APT.

Results revealed dramatic improvements in the integral uniformity from ± 13.2% to ± 5.6% utilizing DUFC. The usefulness of APT was demonstrated. Overall field uniformity can be controlled to ± 6% without substantially effecting counting rate statistics.

This newly developed camera system compensates for photomultiplier tube irregularities, collimator imperfections as well as operator variance. A high degree of scintillation camera control can be maintained. Dynamic uniform field control is done on an event by event basis rather than retrospectively, which is a marked advance over the use of extrinsic computer system.

The demonstrated advances of this new scintillation camera will provide clinical assurance that nuclear medicine imaging is free of system artifact to a level of ± 6%.

BRAIN SCINTIGRAPHY WITH THE ANGER TOMOGRAPHIC SCANNER: EVALUATION BY MEANS OF RECEIVER OPERATING CHARACTERISTIC (ROC) CURVES. D.A. Turner, E.W. Fordham, J.V. Pagano, A.A. Ali, M.V. Ramos, P.C. Ramachandran, and T. Aiden Ferry. Rush University Medical Center, Chicago, Ill.

The Anger tomographic scanner was compared with the Anger scintillation camera for brain scintigraphy, in terms of observer performance. Two experiments were performed: In "experiment A", 43 abnormal and 58 normal patients were re-examined with the tomographic scanner because of confusion of superficial and intracranial foci of activity on the camera scintigram, resulting in uncertainty regarding the normality of the intracranial contents. In "experiment B", 36 abnormal and 73 normal patients were selected without known bias from those referred for brain scintigraphy and examined with both the camera and the scanner. Scintigrams in exper. B were each divided into 6 "search areas", yielding 47 abnormal and 607 normal search areas. Images were interpreted independently by observers with varying experience in nuclear medicine. Observers recorded their confidence that intracranial contents were normal or abnormal by means of a 5 category rating scale. Observer performance ("accuracy") was then expressed as ROC curves. Re-examination with the tomographic scanner greatly improved observer performance when there was difficulty distinguishing intracranial lesions from superficial foci of activity by camera scintigraphy alone. In the general population, the scanner has a small advantage over the camera which is proportional to the fraction of cases in which there is difficulty differentiating intracranial from superficial foci of activity by camera scintigraphy.

THE CLINICAL POTENTIAL OF CLINICAL POSITRON TOMOGRAPHY. Paul V. Harper, Heiko Fill, Michael Buchin, and Violet Stark. University of Chicago, Chicago, IL. and Searle Analytic Inc., Des Plaines, IL.

Exploratory clinical studies using an improved version of Angers positron camera configuration (JNM 16:653) have shown substantial promise. Coincidence count rates up to 4000 c/s have been achieved in clinical situations using Rb-81, N-13 ammonia and Cs-130 in the myocardium and Ga-68 EDTA in brain. A resolution of approximately 10 mm FWHM has been achieved over the entire volume of tissue in the field of view. Four tomographic planes are produced with adjustable depth, separation, and depth of focus. Collection of data in list mode permits any number of planes to be reconstructed off line. The system sensitivity is very high (200 c/s/μCi) permitting one million counts to be collected in a myocardial image using a 1-2 mCi dose of N-13 ammonia. Normalization to a transmission image corrects the data for variable attenuation in tissue and the marked radial variation of sensitivity, in principle making the image truly quantitative. Correction for random coincidence events is accomplished by displacing the time windows appropriately. Images of excellent quality have been produced in a variety of situations. Interference from extraneous gamma radiation is minimal. Several options exist for the use of this device as the primary detector for reconstructive imaging. At the present time the place for this device appears to be in connection with investigational studies of uptake and as an adjunct in difficult diagnostic problems. Twenty-one heart studies and 5 brain studies have been carried out to date with the nuclides mentioned above. The anatomic features of the images are clearly defined and complement the conventional studies. (Supported in part by. N1 1 HV-52980, 18940-03, H1-17648, E(11-1)-69, and 1-F05 TW-02200-01.)

GALLIUM-67 CITRATE SCANNING, A CLINICAL COMPARISON BETWEEN A DUAL 5 IN. SCANNER AND A LARGE FIELD GAMMA CAMERA WITH MOVING TABLE. Paul B. Hoffer, Robert A. Schor, Dillu A. Ashby, Robert S. Hattner, David C. Price, David M. Shames, David L. Lilien, and Hirsch Handmaker. University of California, San Francisco, Ca. Charles Metz, University of Chicago, Chicago, Ill.

Improvements in equipment resolution and sensitivity do not always result in improved detection of clinically significant lesions. We have compared a new clinical instrument specially adapted for Gallium-67 citrate imaging with the standard instrument used for this purpose to determine if any improvement in clinical diagnosis could be achieved.

Twenty-one patients with a variety of clinical indications for Gallium-67 citrate scan were studied. Rectilinear scans were performed with an Ohio Nuclear dual 5 in. scanner and middle energy collimator with a single window including the 93 keV and 184 keV Gallium-67 citrate peaks. Gamma camera images were performed with a Searle LFOV camera equipped with middle energy collimator and moving table and with 3 individual windows set on the 3 major Gallium-67 peaks. 3.5 to 5 mCi of Gallium-67 citrate was administered 24 to 96 hours prior to imaging and bowel preparation was performed when possible. Rectilinear and gamma camera scans were obtained within 1 hr of each other and scan time with both instruments was approx equal. 40 sites on the 2 sets of scans were selected for evaluation based on the availability of definitive evidence that the site was positive (16 sites) or normal (24 sites). Scans were evaluated by 4 observers and scored for ROC curve evaluation.

There was a distinct improvement in performance of the observers as a group with the gamma camera images versus those obtained with the rectilinear scanner. These data indicate that the improvement in sensitivity achieved with the large field gamma camera is reflected in improvement in the ability of experienced observers to detect lesions on Gallium-67 citrate scans.

COMPARISON OF DUAL PROBE AND TOMOGRAPHIC SCANNING USING INDIUM-111 BLEOMYCIN. Neal L. Horn, and Leslie R. Bennett. University of California, Center for Health Sciences, Los Angeles, California.

Indium-111 bleomycin (InBLM) has been shown to concentrate in a wide range of tumor types and inflammatory conditions. This prospective study was undertaken to determine whether tomographic scanning could enhance the diagnostic capability of the conventional anterior and posterior views when using InBLM.

Both 5-inch diameter dual probe (Ohio-Nuclear) and tomographic scintigraphy (Pho-Con by Searle) using InBLM were performed within 24 hours of each other on 38 patients referred to the UCLA Nuclear Medicine Clinic. Thirty-three patients had malignancies while five had benign disease. Scintigraphic findings were correlated with histopathologic

data, roentgenographic studies, conventional liver/spleen, brain and bone scans as well as the physical and laboratory findings.

A total of 42 combination studies using both the dual probe and tomographic scanners were performed on these 38 patients. Twenty-seven of the studies were of equal diagnostic value while the tomographic scan was superior in 10 cases and the dual probe scan in five. Twenty-five foci of abnormal isotope deposition were demonstrated by the tomoscanner while 24 abnormal foci were demonstrated with the dual probe instrument.

In addition to localizing one abnormal para-aortic isotope collection not detected with the dual probe scanner, both normal anatomic structures as well as pathologic isotope collections were more frequently better visualized with the tomoscanner. We conclude that with the isotope InBLM, tomographic scintigraphy is a useful adjunct to conventional anterior and posterior views, especially when questionable abnormal foci of uptake are present which must be differentiated from physiologic isotope deposition. (Supported by USPHS Grant 5-T01-GM01920-07.)

WEDNESDAY, 4:00-5:30 BALLROOM C

BONE/JOINT 2

Chairman: Robert E. O'Mara
Co-Chairman: James Woolfenden

DISTRIBUTION AND EFFECT OF P-32 EHDP IN NORMAL AND BONE TUMOR BEARING DOGS. Marion D. Francis, Candice L. Slough and Andrew J. Tofe. Miami Valley Laboratories, The Procter & Gamble Company, Cincinnati, Oh.

Previous work in our laboratories revealed that EHDP (ethane-1-hydroxy-1,1-diphosphonate) is selectively taken up and held by mineralized tissue in amounts proportional to the bone turnover activity. The purpose of this paper is to describe the effects of intravenously administered, high specific activity (97% radiochemical purity) P-32 EHDP in 20 normal beagle dogs (0.029 to 0.29 mCi/kg) and in five dogs with spontaneous osteosarcomas (0.013 to 0.19 mCi/kg).

In normal dogs only the highest EHDP dose 0.29 mCi P-32/kg), showed a significant reduction in the level of circulating lymphocytes and platelets with maximum depression occurring 21 days after dose, and recovery occurring by 42 days. All other blood parameters (serum chemistry and hematology) were essentially normal. Osseous retention in normal dogs was highest in areas of high bone activity such as the ends of long bones (mean bone/soft tissue ratio was 260/1).

In tumor bearing dogs P-32 EHDP produced an increase in mobility and in one dog a decrease in alkaline phosphatase. Histological evaluation of these osteosarcoma tumors has shown the primary tumor to have extensive coagulation or liquefaction necrosis and hemorrhagic foci. Calcified metastatic tumors, for example, in the lung, if present, consistently showed areas of liquefaction after dosing.

The P-32 EHDP safety studies and distribution data in conjunction with the proven ability of Tc-99m-Sn·EHDP skeletal imaging agent to delineate sites of high primary or metastatic tumor activity all suggested the potential of the radiolabeled EHDP as a palliative agent for the treatment of osseous tumors.

COMPARATIVE DISTRIBUTION OF P-32 AND Tc-99m DIPHOSPHONATES IN PATIENTS WITH OSTEOGENIC SARCOMA. Rodney E. Bigler, Gerald Rosen, Andrew J. Tofe, Gerald A. Russ, Marion D. Francis, Richard S. Benua, Helen Q. Woodard and Jeffrey A. Kostick. Memorial Sloan-Kettering Cancer Center, New York, New York 10021 and Miami Valley Laboratories, The Procter & Gamble Company, Cincinnati, Ohio 45239.

The comparative tissue distributions of ethane-1-hydroxy-1 1-diphosphonate (EHDP) labeled with phosphorus-32 or with technetium-99m have been investigated in 10 patients with osteogenic sarcoma. Simultaneous intravenous administrations of both radiopharmaceuticals were carried out 24 hrs prior to previously scheduled surgery. Blood samples were drawn at ½,1,3,6 and 24 hrs. Total-body retention was estimated by urine collection for up to 4 days. Tissue samples made available at surgery were analyzed for both Tc-99m and P-32. Blood clearance of P-32 EHDP was more rapid than Tc-99m EHDP. Total-body retention of P-32 EHDP was significantly greater than Tc-99m EHDP. Relative concentrations (administered dose fraction/gm-tissue/gm-body wt) of P-32 were higher than Tc-99m in primary tumor, metastatic lung tumor and other calcified tissues. At 24 hrs the following ratios of concentrations of radionuclides in tumor to other tissues were observed in a representative patient.

Tissue	P-32 Ratio	Tc-99m Ratio
Tumor to trabecular bone	4:1	5:1
Tumor to cortical bone	18:1	22:1
Tumor to yellow marrow	30:1	110:1
Tumor to muscle	*	550:1
Tumor to blood	*	180:1

*Muscle and blood activity below P-32 limit of detection.

The high uptake of P-32 in EHDP in calcified tumor tissue relative to normal tissue observed in this study suggests this radiopharmaceutical may be of value as an adjuvant to present methods of managing osteogenic sarcoma. (Supported by ERDA Contract E(11-1)-3521 and NCI Grant CA 08748-10).

P-33 EHDP AND P-32 (EHDP, PPi, and Pi) TISSUE DISTRIBUTIONS IN CONSIDERATIONS OF PALLIATIVE TREATMENT FOR OSSEOUS NEOPLASMS. Andrew J. Tofe, Marion D. Francis, Candice L. Slough, Arlette K. Merritt and William J. Harvey. Miami Valley Laboratories, The Procter & Gamble Company, Cincinnati, Oh.

Palliative treatment of osseous neoplasms has previously been limited to P-32 orthophosphate either with or without hormonal stimulation to increase uptake of the isotope.

The purpose of this paper is to evaluate the specificity of other potential palliative agents, P-32 or P-33 radiolabeled EHDP(ethane-1-hydroxy-1,1-diphosphonate) and P-32 pyrophosphate (PPi) compared to P-32 orthophosphate (Pi) in Sprague-Dawley rats.

Phosphorus labeled compounds were administered intravenously. Following sacrifice at 3 and 24 hours tissue samples were assayed by scintillation counting. P-32 and P-33 EHDP had an identical biological distribution in all osseous and nonosseous tissues. All three phosphorus compounds produced similar uptake in bone while bone marrow retention for the labeled EHDP, PPi and Pi were 0.04, 0.56 and 0.94% dose per gram respectively at 24 hours.

The bone (femur) to skeletal muscle ratios at 24 hours for radiolabeled EHDP, PPi and Pi were 1115, 7, and 8, respectively, and reflect the role of inorganic phosphate in muscle metabolism. At 24 hours the bone to blood ratios were 216, 117, and 12, respectively, for the same tagged materials.

These investigations of distribution combined with high tumor specificity strongly suggests that phosphorus tagged EHDP in humans would give significantly lower radiation exposure using EHDP than either PPi or Pi. A further reduction in exposure could be affected by the use of P-33 rather than P-32 because of the lower energy beta particle and hence shorter path length into the marrow.

PHOSPHORUS-32 EHDP CLINICAL STUDY OF PATIENTS WITH PROSTATE CARCINOMA BONE METASTASES. M. Potsaid, R. Irwin, F. Castronovo, G. Prout, W. Harvey, M. Francis and A. Tofe. Massachusetts General Hospital, Boston, Mass. and Miami Valley Laboratories, The Procter & Gamble Company, Cincinnati, Oh.

The strong chemisorptive properties of P-32 EHDP for bone suggested its use for palliation of pain from osseous metastases. Extensive preclinical animal studies supported clinical trials. In this study we investigated the use of P-32 EHDP in proven stage IV prostate carcinoma to determine safe dose levels.

Hematological, biochemical, EKG, x-ray, bone scan and clinical parameters were followed for two months after intravenous administration of P-32.

Five patients were treated: two received three doses of 3 mCi a week apart and three patients received a single 3 mCi dose. P-32 EHDP chemical purity on all doses was greater than 95 percent.

One patient at the highest dose level (total 9 mCi) had no change in the course of his disease while the other patient had a profound drop in peripheral WBC and platelets, but made a good recovery from his bone marrow

depression and had relief of bone pain. Two patients given the lower dose (3 mCi) had no change in any parameters monitored and had no relief of bone pain. One patient at the lower dose had a profound drop in blood WBC and platelets which corresponded with the worsening clinical condition.

The difference in hematological and palliative response at the higher dose of P-32 EHDP combined with the unexpected blood response in one patient at the low dose, suggests that with this highly specific bone agent, marrow competence must be assessed prior to attempted palliation. Current studies directed at assessing marrow competence may suggest a possible resolution of the above clinical problems.

I-125 7-IODO-6-DEOXY-6-DEMETHYLTETRACYCLINE: ITS USE IN THE STUDY OF BONE MINERALIZATION. B.M. Bowen, E.S. Garnett, J.K. Porter, F.W. Teare. McMaster University Medical Centre, Hamilton, and University of Toronto, Toronto, Ontario, Canada.

Tetracyclines have been used to localize and mark sites of active mineralization in bones. Sequential doses of the drugs have been used to estimate the amount of bone growth during the interval between doses. Biopsies are necessary for this determination. We have prepared I-125 7-iodo-6-deoxy-6-demethyltetracycline to study mineralization of bone by external methods. The compound has been shown to be useful in the study of fracture union, accumulating only when mineralization is occurring. Studies are in progress to determine whether the amount of I-125 tetracycline accumulated bears a direct relation to the amount of mineral laid down by osteoblasts in the bone. If this relation is established, the use of the drug will be expanded to the study of generalized metabolic bone disease.

A MODEL OF LOCAL ACCUMULATION OF BONE SEEKING RADIOPHARMACEUTICALS. Michael A. King, Robert W. Kilpper, and David A. Weber. University of Rochester Medical Center, Rochester, N.Y.

The present controversy over the role played by various factors in producing abnormal bone images stimulated work on a mathematical model capable of predicting local tracer accumulation in disturbed states. In this model, blood delivering tracer to one gram of bone is treated as a compartment separate from the remainder of the circulation. This allows one to observe the changes in local tracer accumulation produced by variations in blood flow and capillary permeability. Bone is modeled as two compartments. One compartment represents exchangeable bone and extracellular fluid; the other corresponds to deposition by long-term exchange and accretion.

With data from the literature, analog computer simulations of the kinetics of an isolated segment of bone were developed for Ca-47 and F-18 using the blood level as a forcing function. For a given percentage change above or below its "normal fit" value, blood flow had the greatest influence on deposition of F-18. Progressively smaller effects were observed for variations in volume of the exchangeable bone pool, V_{BE}, and a constant, K, which allows for uptake by accretion and long-term exchange. Changes in permeability showed little effect for F-18. V_{BE} produced the greatest alteration in local accumulation of Ca-47, followed by blood flow, K, and permeability.

Apparent confirmation of the predicted influence of decreased blood flow on F-18 deposition was obtained by measuring F-18 uptake by bone and blood flow assayed by Rb-86 clearance following partial ligation of the right femoral artery in rabbits.

The analog computer model developed in this study provides a direct method by which various rate limiting factors in tracer uptake and clearance can be tested.

THURSDAY, JUNE 10, 1976

THURSDAY, 8:30-10:30 BALLROOM A

IN VITRO 2

Chairman: Henry N. Wagner
Co-Chairman: M. A. Razzak

DEVELOPMENT OF RADIOIMMUNOASSAY SPECIFIC FOR 3-O-METHYLDOPAMINE. Bahjat A. Faraj and Vernon M. Camp. Department of Radiology (Division of Nuclear Medicine), Emory University School of Medicine, Atlanta, Ga.

Immunologic methods for assaying and obtaining metabolic information for many hormones have been reported by several investigators. In a previous report from this laboratory (Faraj et al Proc. Soc. Exptl. Biol. Med. 149, 664, 1975), it was shown that specific antibodies can be elicited to a sympathomimetic amine, tyramine. The ongoing program has been directed to developing radioimmunoassays (RIA) which are specific for the various catecholamines and their metabolites. The present study demonstrated the preparation of antibodies (Ab) against a metabolite of dopamine (3-O-methyldopamine, MD) by conjugating it to hemocyanin (H). The antigen was prepared as follows: p-aminohippuric acid was coupled to H using a carbodiimide reagent. The amino group was diazotized and attached to the aromatic ring of MD. The immunogen (2 mg) in Freund's complete adjuvant was injected into rabbits. The specificity of the resulting Ab was determined by RIA. Using random-labeled MD-^{3}H (s.a. 6.7 ci/mMole), MD, catecholamines and their metabolites, sympathomimetic amines and certain amino acids were evaluated by competitive binding assay. With this technique, 4 ng of MD inhibited the binding of MD-^{3}H by 50%. Cross-reactivity was found only with 3,4-dimethoxyphenethylamine and 3,4-dimethoxy-N-methyl-phenethylamine. The anti-3-O-methyldopamine serum offers a possible sensitive (lowest amount 400 pg) and specific technique for the measurement of MD in body fluids. The diagnostic application of this RIA is being evaluated by determining plasma and urine levels of MD in patients with neurocrest tumors (pheochromocytoma and neuroblastoma) and other disease categories. (Supported in part by a grant from the Pharmaceutical Manufacturers Association Foundation).

AUTOMATED CURVILINEAR ANALYSIS IMPROVING FIT OF RIA BINDING CURVES. George H. Barrows and Ellis Samols. Nuclear Medicine Service, V. A. Hospital and Departments of Pathology and Medicine, University of Louisville, School of Medicine, Louisville, Kentucky.

Most current methods of automated radioimmunoassay analysis utilize transformation of RIA binding data to logit (or expressions such as probit or arc sine) and plot ligand binding versus logarithm of concentration by linear regression. Frequently rectilinear curves generated by these methods depart from standard curves, particularly in high and low ranges of concentration. An automated curvilinear approach using multiple regression by least squares was evaluated for different clinical radioimmunoassays. The experimental data was found to correlate best with the 1/2 power (square root) of standard concentrations in a third order polynomial expansion. The resultant polynomial expression usually gave a better fit than rectilinear logit-logarithm plots or hyperbolic plots. In addition, experimental error appears to be evenly distributed over the experimental range. Appropriate selection of standard values enhances curve fit over a wide range; increasing the number of standards improves curve fit because of

the flexibility allowed by third order equation. Visual interpretation is markedly improved since the curve is not compressed by logarithmic expression of standard concentrations. Analysis was carried out on consecutive clinical assays including T_4, T_3, TSH, HGH, cortisol, renin, glucagon and dilantin. The curvilinear approximation using the polynomial regression was in general superior to all other fits tested for covering a variety of clinical assays.

SIMULTANEOUS MEASUREMENT OF TRIIODOTHYRONINE AND THYROXINE IN UNEXTRACTED SERUM SAMPLES USING A DOUBLE ISOTOPE RADIOIMMUNOASSAY METHOD. M. L. Brown, T. Hannah, G. Stephens, and D. A. Podoloff, and R. F. Carretta. Wilford Hall USAF Medical Center, Lackland AFB, Texas.

Methodology for the simultaneous measurement of triiodothyronine and thyroxine in a 0.040 ml of unextracted serum is presented. Antibodies were prepared by immunizations of rabbits with triiodothyronine and thyroxine human serum albumin conjugates. Bound and free labeled hormones are separated using the double antibody technique. 8-anilino-1-napthalene sulfonic acid has been used to inhibit binding of the two hormones to thyroxine-binding globulin. The validity of the assay using I-125 T-3 and I-131 T-4 is demonstrated by the excellent recovery of T-3 and T-4 added to serum, and by production of a curve obtained by various dilutions of a hyperthyroid serum which is parallel to the standard curves. In all clinical states, serum triiodothyronine and thyroxine values obtained using the double isotope radioimmunoassay method afford excellent agreement with those obtained by separate radioimmunoassay techniques. The combined T-3, T-4 method appears to be accurate, sensitive and specific making the assay highly desirable as a technical time saver.

A RADIOIMMUNOASSAY FOR BLEOMYCIN. Michael K. Elson, Martin M. Oken, and Rex B. Shafer. V.A. Hospital, Minneapolis, Minnesota.

The antineoplastic properties of bleomycin are limited by its pulmonary and cutaneous toxicity. In order to monitor patients receiving chemotherapy, we developed a radioimmunoassay for bleomycin.

Specific antisera for the radioimmunoassay were produced in rabbits immunized with a bleomycin-bovine serum albumin conjugate. Bleomycin was coupled to albumin using a water soluble carbodiimide. Each assay tube contained 25 µl of standard or sample serum. A Co-57 bleomycin chelate was used as the radioactive tracer. Antisera and tracer were premixed and pipetted together to simplify the assay. Polyethylene glycol (mw 6000) was used to precipitate the antibody-bleomycin complex. This assay detected less than 0.05 µg bleomycin per ml of serum. Specificity studies showed less than 0.1% cross-reactivity with cyclophosphamid, prednisone, procarbazine and vincristine - all drugs likely to be present during cancer chemotherapy. Serum concentrations of bleomycin measured by this assay correlated well with microbiological assay data. Bleomycin excreted in the urine was also measured and showed similar correlation.

The bleomycin radioimmunoassay has specific application in kinetic studies of bleomycin clearance and tissue distribution. Routine assay of serum drug levels will permit more precise dosage for patients undergoing bleomycin therapy. Detection of endogenous antibody to bleomycin in patients on chronic therapy is possible by omitting antisera from the assay. The radioimmunoassay for bleomycin, more specific, sensitive and facile than the microbiological assay, expands the scope of clinical investigations of bleomycin toxicity.

DNA IN THE SERUM OF CANCER PATIENTS AND THE EFFECT OF THERAPY. S. A. Leon, B. Shapiro, and D. M. Sklaroff. Albert Einstein Medical Center, Philadelphia, PA.

A radioimmunoassay for nanogram quantities of DNA was developed. I-125-iododeoxyuridine-labelled DNA was used as the antigen, and the serum of a lupus erythematosus patient served as the source of antibody. The level of free DNA in the serum of 173 patients with various types of cancer, and 55 healthy individuals, was determined by this radioimmunoassay. DNA concentration in the normal controls had a range of 0 to 100 ng/ml with a mean of 13 ng/ml ± 3 (SEM). For comparison purposes, the range of 0 to 50 ng/ml was designated (arbitrarily) as normal, and then 93% of the controls were found in this range. In the cancer patients, the DNA concentration ranges from 0 up to microgram levels, with a mean of 180 ng/ml ± 38 (SEM). Fifty percent of the patients' values were found between 0 to 50 ng/ml; the other 50% were between 50 and 2000 ng/ml. No correlation could be seen between DNA concentrations and stage of the disease (presence or absence of metastases) or the size of the primary tumor.

After radiation or chemotherapy, in lymphoma, lung, bladder, and prostate tumors, the levels decreased in 66%-90% of the patients, whereas in glioma, breast, colon and rectal tumors, the DNA levels decreased only in 16%-33% of the patients. Generally, the decrease in DNA concentration correlates with improvement of the clinical situation (such as decrease of tumor size, reduction of pain). On the other hand, when the DNA levels increased or remained unchanged, a lack of response to the treatment was noted. Out of 15 patients who died within a year, 8 showed DNA levels that remained high or unchanged during treatment.

We conclude that the DNA level in serum may be of little diagnostic value; however, it may be an important tool for the evaluation of therapy.

QUANTITATIVE RADIOMETRIC ASSAY OF BACTERIAL METABOLISM. E. Buddemeyer, R. Hutchinson, and M. Cooper. University of Maryland Hospital, Baltimore, Maryland.

The purpose of this paper is to introduce a new automated, radiometric technique for the quantitative measurement of the growth and the inhibition of growth in replicating populations of bacteria. In a two-compartment scintillation vial, suspensions of bacteria were cultured with labelled Glucose and the released C-14 tagged carbon dioxide measured continuously, cumulatively, and automatically in a liquid scintillation counter modified to maintain sample temperature at 37C. The system is sensitive enough to track the metabolism of bacterial populations through their early phase of exponential growth with good precision. From an analysis of the exponential portion of the cumulative activity vs time curves, cell replication rate can be defined in units of time. Fine shades of response to growth inhibitors can be measured by noting the relative prolongation of replication in the presence of antibiotics.

In the 36 determinations of uninhibited growth rate completed to date with 4 species of bacteria, the radiometrically-measured replication time was found to be representative of the species and practically independent of the size of the inoculum. In 48 determinations of sensitivity (4 species against 4 antibiotics each, in triplicate), the measured relative inhibition was precise and in agreement with the standard, qualitative, zone-diffusion technique of Kirby and Bauer.

The method described is quantitative and independent of a number of common experimental variables (vial-to-vial variations in counting efficiency, imprecise pipetting of the substrate or the bacteria, etc.) that do not effect the slope of the exponential portion of the growth curve. The method shows promise in the quantitative analysis of bacterial growth and inhibition.

SIMPLE RADIOMETRIC TECHNIQUES FOR RAPID DETECTION OF HSV-1 IN WI-38 CELL CULTURE. Nancy L. D'Antonio, Min-Fu Tsan, Patricia Charache, Steven M. Larson, and Henry N. Wagner, Jr. The Johns Hopkins Medical Institutions, Baltimore, Md.

Radiometric detection of bacterial growth has been used to facilitate certain clinical microbiological procedures. The present study was designed to extend the radiometric method to the detection of viruses.

Two radiometric techniques were evaluated for detecting the presence of herpes simplex virus type 1 (HSV-1) in stationary monolayers of the diploid cell line WI-38. The time of detection was compared to that obtained from visual examination for cytopathic effects in the same cell line. Glucose-1-14C oxidation and DNA synthesis of infected and uninfected cells were monitored by

$^{14}CO_2$ production measured by an ion chamber and 3H-thymidine incorporation measured by scintillation counting, respectively. HSV-1 ($10^{6.5}$ $TCID_{50}$) infected cells showed a 23 to 26% reduction in glucose-1-14C oxidation and a 355 to 498% increase in 3H-thymidine incorporation 4 to 6 hours postinfection as compared to uninfected control cells. Virus induced cytopathic effects could not be identified until 1 day postinfection. The increase in 3H-thymidine incorporation was completely inhibited by viral neutralization with specific antiserum. The addition of three common bacterial skin contaminants had no effect on 3H-thymidine incorporation by virus infected or control cells. Increased incorporation was observed 5 hours postinfection with 10^4 $TCID_{50}$ units of virus and 20 hours postinfection with $10^{2.8}$ $TCID_{50}$ units.

These radiometric methods, particularly the measurement of 3H-thymidine incorporation, are simple, rapid, and objective, and may be applicable to the detection and typing of viruses in clinical medicine.

C-13-BREATH TEST AS THE EXTENTION OF C-14-BREATH TEST, Y. Sasaki, H. Oh-hara, T. Maeda, K. Someya, St. Marianna University School of Medicine, Kawasaki, Japan and M. Sano, Daiichi Seiyaku Co. Ltd., Tokyo, Japan.

C-14-breath test consisting of sereal collection of CO_2 after administration of C-14-labeled compounds such as glycine-cholate is a useful diagnostic test. The use of stable isotope expands the applicability of the test to pregnant women, infants, young adults and mass survey of healthy population. The purpose of this study is to validate the C-13-breath test.

C-14- or C-13-glycine(G) and glycine cholate(GC) were given i.v. or p.o. to rats. Vials were attached to the outlet of the Rodent respirator and CO_2 in the breath was collected by neutralization of alkaline solution. For the collection of CO_2 in the breath in human subjects the apparatus previously reported was used. C-14 and C-13 specific activity in CO_2 was measured in a liquid scintillation counter and a mass spectrometer, respectictively.

When C-14-G(1μCi) and C-13-G(50mg/kg) were simultaneously given i.v. or p.o. to rats, C-14-CO_2 curves and C-13-CO_2 curves agreed very well. When trace dose of C-14-G and loading dose (16.5mg) of C-13-G were given with 2 hours interval, the shape of the curves were similar but the excretion rate of C-13-CO_2 was significantly lower (15.2%/6 hrs.) than that of C-14-CO_2 (18.9%). C-14 and C-13-GC was given p.o. to rats with jejunocolostomy. C-13 and C-14 curves agreed well with sudden increase of radioactivity at 6 hrs. In a patient with blind loop and malabsorption C-13 and C-14 breath test after oral simultaneous administration of labeled GC gave a positive result with area under curve 31/6 hrs(nl. 3.1+1.8).

In conclusion C-13-compounds are suitable to be used for breath test in place of C-14-breath test. Loading dose of C-13 compounds may cause different quantitative results from the tracer dose of C-14-compounds.

THURSDAY, 8:30-10:30 BALLROOM B

COMPUTED TOMOGRAPHY

Chairman: David E. Kuhl
Co-Chairman: William L. Rogers

TRANSVERSE SECTION RECONSTRUCTION WITH POSITRON EMITTERS AND THE MGH POSITRON CAMERA. J. A. Correia, D.A. Chesler, B. Hoop Jr., B. Ahluwalia, T. Walters and G.L. Brownell. Physics Research Laboratory, Massachusetts General Hospital Boston, MA

Transverse section images have been obtained in man, animals and phantoms using the MGH positron camera and short-lived positron emitting isotopes. The reconstructions were generated using the filtered backprojection method. Transmission measurements were made in the same geometry as the emission measurements and were used to correct the emission data point by point for absorption in the source.

In order to obtain higher resolution, various combinations of linear detector motion and camera rotation were studied. Furthermore, a Hanning weighted filter was used to reduce ripple in the reconstructions. As a result images of phantoms have been reconstructed at 1.2 cm resolution with minimum distortion.

Transverse section reconstructions of N-13 labelled NH_3 and O-15 labelled CO_2 have been obtained in the brain in man. The CO_2 was administered by constant inhalation to an equilibrium distribution. NH_3 was administered by intravenous injection. In both cases 3D images was possible because the distributions were effectively static. Preliminary animal studies using a Ga-68 labelled aerosol in the lung and intravenously injected Rb-82 in the myocardium have also been made.

This work demonstrates the feasibility of transverse section reconstruction using compounds of several positron emitting isotopes as well as the ability to achieve high resolution with low ripple and distortion. Further studies are underway to evaluate the clinical significance of these techniques.

This work has been supported in part by NCI Contract #NO1-CB-53913

RADIONUCLIDE EMISSION COMPUTED TOMOGRAPHY WITH A SCINTILLATION CAMERA. Ronald Jaszczak, Diane Huard, Paul Murphy, John Burdine. Searle Analytic Inc. & Searle Radiographics Inc., Des Plaines, Ill., and Baylor Coll. Med., St. Luke's Episcopal-Texas Children's Hospitals, Houston, Tex.

Transmission computed tomography has had a growing impact on diagnostic imaging within the recent past. Emission tomography has been attempted but has had limited success primarily due to the specialized nature of the instrumentation employed. A tomographic system incorporating a light weight scintillation camera head has been developed to investigate the potential applicability of this technique in brain imaging. Data is collected for periods ranging from 2-20 min. after the IV injection of 15-20 mCi of ^{99m}Tc pertechnetate as used in routine brain imaging. Typically 4M counts are collected for a complete study. During data collection, the detector head rotates at a constant angular velocity 360° around the patient who is supine in a comfortable and immobile position. Scintillation data is deposited on videotape continuously with data on detector orientation each 4° for subsequent off-line image reconstruction. The reconstructed image consists of 9 contiguous sections, each 16 mm thick. Lesion visibility was judged qualitatively by comparing section images to standard camera views, and quantitatively by comparison of lesion-to-background ratios for the two types of images. An increase in image contrast of approximately 2 is generally observed in comparison to the best view from the static scintiphotos.

Increased lesion contrast in these preliminary results suggest that emission tomography has the potential of a similar impact on imaging as has transmission tomography because of the more physiologic basis of the radiopharmaceutical localizing mechanisms. Using a light weight camera as the detector both routine scintiphotography and tomography in multiple planes is possible.

DYNAMIC SCANNER, AN IMAGING SYSTEM EMPLOYING FLYING SPOT X-RAY MICROMEAM. Yukio Tateno, Hitoshi Tanaka, and Eiji Watanabe. Chiba University Hospital, Chiba, and JEOL Ltd., Tokyo, Japan

An imaging system employing a flying spot X-ray microbeam generator has been developed. This system provides 1) computerized transverse axial tomography, 2) computer-controlled dynamic measurement, and 3) plain scanning images. In this system, unlike conventional computerized tomographic systems, a high-energy electron beam is electromagnetically controlled and focused to generate an X-ray microbeam, which can be directed to any portion of a patient by means of an on-line computer or a built-in control system, thereby permitting images of the designated portions to be obtained. In this system the main imaging apparatus has an imaging chanber, which is cylindrical and measures 700mm in diameter. Inside the chamber a small table is set to accommodate the patient. The X-ray generator and the detectors, a 16"-diameter scintillation detector for plain scanning images and a line shaped scintillation detector for transverse axial tomography, are

rotated around the chamber by a digital servo-drive system and brought to the designated imaging position. In this system, the computer plays a very diversified role such as designation of X-ray microbeam projections, instantaneous on-line evaluation of imformation from the irradiated point, control of main imaging apparatus, control of display, image processing and reconstruction, and data filing.

THE HUMONGOTRON - A GAMMA CAMERA TRANSAXIAL TOMOGRAPH. John W. Keyes, Jr., Nicolae Orlandea, William J. Heetderks, and Patrick F. Leonard. University of Michigan Medical Center, Ann Arbor, Mich.

Efforts in our laboratory focussed on the development of an emission CAT system have produced a very practical unit for this purpose. This device, the Humongotron, utilizes a standard gamma camera detector interfaced to a commercial small computer system for data acquisition and control. It permits both tomographic imaging and all conventional camera studies. The camera is mounted on a cantilevered C-arm which permits full 360 degrees rotation about a special patient table mounted on the axis of rotation. In and out movement of the detector is permitted in any rotational position and counterweights maintain neutral balance regardless of detector position.

Thorough testing in a clinical setting has proven this system to be practical for both tomography and all routine imaging procedures. As the patient is totally passive, the system actually simplifies the imaging of very ill or partially immobilized patients. Minor modifications would also permit whole body scanning with the system making it a truly universal device.

We conclude from our experience that it is both economically and practically feasible to add CAT capability to a standard gamma camera and that further development of systems of this type is warrented.

(This work was supported in part by NIH grants GM 20129 and GM22678.)

COMPARATIVE STUDY OF RADIONUCLIDE STUDIES AND COMPUTERIZED AXIAL TOMOGRAPHY IN THE DIAGNOSIS OF CENTRAL NERVOUS SYSTEM DISEASES. James H. Christie, Hirofumi Mori, Raymundo T. Go, Steven H. Cornell, University of Iowa Hospitals and Clinics, Iowa City, Iowa.

The increasing role of Computerized Axial Tomography (CT) scanning demands re-evaluation of radionuclide brain imaging (RN). The purpose of this paper is to assess the accuracy of radionuclide studies in comparison with CT scans.

During the first 18 months of experience with the EMI scanner, 635 cases had both CT scans and radionuclide brain scans within reasonable intervals. These cases were retrospectively reviewed. Dilated ventricles, porencephaly and/or brain atrophy, which are detected only by CT scans, were eliminated from the study. Radionuclide studies were performed using $^{99m}TcO_4^-$ with a scintillation camera. Dynamic, 10 min. and 2 hr. static images were routinely obtained; 4 hr. images and/or posterior stereoscanning were taken when indicated. The technique of the CT scan with the EMI scanner is essentially the same as in previous reports. In later cases, I.V. injection of Renografin-60 was given selectively after review of the CT scan.

The retrospective study showed discrepant diagnosis in 38 cases. In 18 cases, CT scans were negative, but radionuclide studies showed abnormalities. In 20 cases, radionuclide studies were negative, but CT scans showed abnormalities. The diagnostic accuracy of the radionuclide studies and CT scans in the 115 cases with neoplastic lesions was the same in both studies (RN - 83%, CT - 83%,combined 90%). In 86 cases with non-neoplastic lesions (CVD, vascular anomalies, CNS infection and trauma) the accuracy was almost the same (RN - 66%, CT - 67%, combined - 83%). These two procedures are complementary. The combination of these two non-invasive studies provides a higher diagnostic accuracy.

COMPUTERIZED TRANSAXIAL TOMOGRAPHIC BLOOD POOL AND PERFUSION IMAGING IN HUMAN VOLUNTEERS AND PATIENTS. Michael E. Phelps, Edward J. Hoffman, R. Edward Coleman, Michael J. Welch, Marcus E. Raichle, Edward S. Weiss, Burton E. Sobel, Michel M. TerPogossian. Hospital of the University of Pennsylvania, Philadelphia, Pa. and Washington University School of Medicine, St Louis, Mo.

A whole body positron transaxial tomograph(PETT III) was used to image N-13,ammonia,(perfusion)and C-11,CO-hemoglobin(blood pool)cross sections in brain and heart of volunteers and patients with selected pathology. Images were obtained subsequent to intravenous injection or inhalation of tracers. Studies were performed to determine uptake of N-13, ammonia(typically >50% extraction)and tissue clearance rates ($t-\frac{1}{2}$ ~70min). Ratio of N-13,ammonia uptake in superficial cortex,cerebellum and brain stem to subcortical white matter was found to be 3.3,3.2,and 2.8,respectively. Taking into account the 1 cm resolution of PETT III,these values are in excellent agreement with measured ratios of perfusion of 3.6, 3 and 3. Good anatomical delineation is shown between N-13,ammonia images and brain slices from corresponding levels. Cerebral lesions demonstrated by angiography and flow studies to have high(metastases)and low(stroke) blood flow showed corresponding high and low uptake of N-13,ammonia. Small vessel and/or large vessel involvement are clearly delineated with ammonia and CO images. Ga-68 EDTA was used to show impairment of blood brain barrier. Perfusion and blood pool images of human heart show clear delineation of left and right ventricle,ventricular chambers,atrium and aorta. Levels of heart from superior to inferior in 1.5 cm increments are shown. A transmural anterior myocardial infarct in a patient was clearly demonstrated in degree and extent. Effective combination of positron transaxial tomography and positron labeled compounds provide a noninvasive method for quantitately imaging hemodynamic and physiological functions with high tomographic image quality.

TRANSVERSE SECTION IMAGING OF THE MYOCARDIUM. Thomas F. Budinger, Grant T. Gullberg, Brian R. Moyer, John L. Cahoon, and Ronald H. Huesman. Donner Laboratory, University of California, Berkeley, Calif.

The myocardium of animal and man has been imaged in transverse section from multiple views from the gamma camera using Cs-129, Tl-201, and Se-75 methionine. By incorporating EKG signals images have been prepared of the beating myocardium in transverse section.

Four patients with known myocardial disease were examined using an iodine medium collimator for Cs-129 and a technetium collimator for Tl-201 (Hg x-rays) and the Anger 16-inch camera. Patients were rotated in the sitting position with arms overhead on a rest, and data were taken at 5° or 10° increments and digitized in a 64 x 64 frame for each angle. Projections for the transverse sections were prepared by selecting from each of the frames 3 rows of data corresponding to a particular transverse level through the patient. Reconstruction was performed using both iterative least squares and Fourier transforms. Attenuation compensation was performed using attenuation coefficients measured by a transmission transverse section study.

For a study incorporating EKG signals, data were obtained in list mode along with a computer word designating the occurrence of the R-wave. Data were reconstituted by framing all those data representing each of eight 100 msec periods within the cardiac cycle for each projection. In order to gain adequate statistics for 20% uncertainty it is necessary to collect 3.6×10^5 events per section. Studies involve 1 to 4 hours of patient time, and 30 seconds for computational reconstruction, but 24 hours of small computer time for data reorganization for heart motion studies. Left ventricle myocardium is revealed with 1.5 cm resolution on these transverse sections. These studies point the way to new instrument development which will minimize patient imaging time and computation procedures. A motion picture of the myocardium beating in vivo was prepared.

THE EFFECT OF ATTENUATION ON RECONSTRUCTION AND STATISTICAL NOISE. Sing C. Pang and Sebastian Genna. Boston V.A. Hospital and Boston University Medical Center, Boston, Mass.

In order to reliably reconstruct the transaxial emission distribution from the projected measured counts (PMC), the attenuation distribution of the cross section must be considered. In an earlier work (J. Nucl. Med. 6, 529, 1975), we presented the noise propagation of positron emitters in the presence and absence of attenuation. Since Tc-99m (140 keV) and positron emitters (pair photon coincidence) are most commonly used, the effect of their differences in energies and attenuation path length on reconstruction are treated here. A phantom similar to a section of brain is simulated (by computer) with a disc and a surrounding ring

having the attenuation of water and bone. Then for each of the two emitters, different emission source distributions are studied separately. The uncorrected simulated PMC is reconstructed. The distortion due to attenuation is shown to be more severe for the positron emitter than for Tc-99m. When the PMC is corrected for attenuation, the effect of attenuation on the count statistics are shown by the reconstruction of the variance of each cell. The variance is greater for the positron emitter.

The phantom simulation involves 64 views/section and 64 cells/view with dimensions of 3.2 cells/cm. Convolution and back projection techniques are used for reconstruction.

THURSDAY, 8:30-10:30 BALLROOM C

PEDIATRICS

Chairman: Philip O. Alderson
Chairman: Gary F. Gates

THE SENSITIVITY, SPECIFICITY AND ACCURACY OF RADIONUCLIDE IMAGING OF MECKEL'S DIVERTICULUM. James J. Conway, and the Pediatric Nuclear Club of the Society of Nuclear Medicine. The Children's Memorial Hospital, Chicago, Il.

Meckel's diverticulum is the most frequent congenital malformation of the gastrointestinal tract in man. Gastric mucosa is present in less than 20% of all cases but is in the majority of those with complications. Roentgenographic detection is notoriously poor and thus the technique of localization with 99m-Tc pertechnetate has been received with enthusiasm by many since 1970. A review of the literature and a collation of patient data from members of the Pediatric Nuclear Club and other cooperative hospitals attest to the efficacy of this procedure.

Gamma camera imaging at 10-15 minute intervals during the first hour following intravenous injection of 100 uCi/lb. of 99m-Tc pertechnetate is essential for success. Potassium perchlorate is not given. False positives which occur are usually also of surgical significance and include abscess, appendicitis, peptic ulceration, hemangioma, and gastric mucosa in duplications. False negatives are more difficult to explain but include insufficient gastric mucosa and necrosis of the Meckel's diverticulum.

The results of surgically proven Meckel's diverticulum are as follows:

Patients	True+	True-	False+	False-
114	43	46	11	14

The calculated parameters of this technique are specificity, 79%; sensitivity, 75%; accuracy, 78%.

The speed, simplicity, and safety of this procedure warrants its routine use in the diagnostic workup of the patient with rectal bleeding.

DIAGNOSIS OF MECKEL'S DIVERTICULUM BY SCINTIGRAPHY:CLINICAL AND PATHOLOGICAL CORRELATION. M.J. Gelfand,E.B. Silberstein and J.Cox, Radioisotope Laboratory, General Hospital, and Department of Surgery, Children's Hospital,Cincinnati,Ohio

Fifty-two children were studied for Meckel's diverticulum (Meckel's) by scintigraphy with Tc-99m-pertechnetate. Patients were two weeks to nineteen years old with a median age of two years. No potassium perchlorate was given.

Eight patients, who had laparotomy for hematochezia or melena were found to have Meckel's with gastric mucosa. Six of these children had clearly positive scintigraphic evidence of Meckel's, one had equivocal images, and one had negative images. A positive study was characterized by a small round area of intense radionuclide uptake appearing at 15 to 30 minutes, and persisting until one to three hours after injection. Images were read as equivocal if the area of activity was of low intensity or of short duration.

Laparotomy was performed on seven other patients. A child with negative images had the incidental finding of Meckel's with no inflammation and only a few microscopic foci of gastric mucosa. Four other children with negative images had no Meckel's at laparotomy. One patient with a very large intense area of pertechnetate uptake in the abdomen had ulcerative colitis. At surgery 31 months later, no Meckel's was found. A child with equivocal images had ileitis at laparotomy.

Five children with equivocal images had no surgery.Early gastric emptying prevented interpretation of four cases.

The eight patients with Meckel's who had laparotomy for hematochezia or melena had evidence of significant blood loss. Of 37 other patients with hematochezia or melena,only 11 had signs of significant acute or chronic blood loss. Despite 33 barium enema and 30 contrast upper gastrointestinal examinations, a reasonably certain cause of the rectal bleeding was found in only nine cases.

Scintigraphic imaging of Meckel's is a useful clinical technique of acceptable sensitivity and specificity.

MECKEL'S DIVERTICULA-SERIAL MULTIPLE VIEW IMAGING. Elisabeth Kilburn, David L. Gilday and Judith Ash. The Hospital for Sick Children, Toronto, Ont.

Abdominal imaging with Tc-99m pertechnetate has gained a mixed reputation due to a significant number of erroneous diagnoses. We have evolved a technique while examining over 170 children, with unexplained rectal bleeding or abdominal pain, which minimizes the potential false positive and false negative results.

The child should be fasting and not have had any intestinal irritants such as barium, laxatives or aspirin for at least 3 days. Patients are injected with Tc-99m pertechnetate (maximum dose 15 mCi.) while lying supine. Serial anterior images are taken with the gamma camera from 1 to 15 minutes. The child is not moved during this time. After 15 minutes right lateral and posterior views are taken: the three views are repeated at 30 minutes.

Accumulation of radionuclide in a Meckel's diverticulum parallels that of the stomach, and persists as a focal area; if present, it should be visualized by 15 minutes and is best seen at 10 to 15 minutes. A Meckel's diverticulum may move during the study, but usually activity which moves is more likely in the gut or urinary tract. Multiple views facilitate the differentiation of these areas which can lead to false positive interpretations.

Of 170 children, 151 had normal scans and none have had a lesion discovered. Eleven confirmed Meckel's diverticula had positive scans; 3 had abnormal scans for other entities. The 5 erroneous diagnoses were; a true false negative, a false negative but with no gastric mucosa in the diverticulum, 3 false positives, 2 of which would be eliminated by our current technique.

Our technique has improved our accuracy for detecting Meckel's diverticula and other abnormalities. The important considerations are patient preparation, early and serial imaging with multiple views.

TESTICULAR IMAGING FOR TESTICULAR TORSION IN PEDIATRIC SURGERY. David L. Gilday, David Hitch, Barry Shandling and Judith Ash. The Hospital for Sick Children, Toronto, Ont.

The infant or small boy with a swollen, painful testis presents a diagnostic enigma as testicular torsion can only rarely be distinguished from acute epididymo-orchitis. Until recently the only accurate means of differentiation was surgical exploration. Therefore some children without testicular torsion underwent unnecessary operations. For some children, with testicular torsion, the often disastrous "wait and see" approach was employed.

Introduced for adults in 1973, scrotal imaging has allowed a precise evaluation of perfusion of scrotal contents thus refining the criteria for operation. Our experience with children (45) has been so dramatic that in all but the most obvious cases this study preceeds surgical exploration.

Using a gamma camera with a high resolution collimator, images of the scrotum, placed on a lead shield, with the penis taped superiorly out of the field of view, were obtained during the vascular phase following an injection of Technetium-99m pertechnetate or albumin. We have correctly diagnosed 11 patients with testicular torsion, 8 with an infection and consequent hyperemia, and categorized 12 patients as being normal. Of 9 children clinically felt to have torsion of the appendix, 4 had hyperemia on the scan and 5 had normal scans.

Two studies are classified as false negative although in one child the testis spontaneously rotated back to normal (the "Bell-Clapper deformity" was found bilaterally) and in the other a 360° rather than 420° rotation of the testis was found at surgery with an intact arterial supply but impaired venous drainage.

A boy with a swollen testis, should be scanned immediately to determine whether it is viable or not.

THE DIAGNOSTIC AND PROGNOSTIC VALUE OF BRAIN SCANNING IN PERINATAL ASPHYXIA. Judith Ash, David Gilday, John O'Brien and Karen Pape. The Hospital for Sick Children, Toronto, Ont.

The purpose of this study is to assess the diagnostic and prognostic value of the brain scan in neonates considered to have perinatal asphyxia.

For optimum visualization of hypoxic change, brain scans (using 8.3 millicuries of Tc-99m pertechnetate per metre squared) were performed between 4 and 8 days post-natally. If abnormal, they were repeated between 3 to 4 weeks of age. Further studies were done only if scan abnormalities persisted.

Ninety-two of 189 neonates studied by brain scanning in the past 2 years were clinically suspected of having suffered perinatal asphyxia. Of the 56 patients with normal scans all have developed normally or another diagnosis established, except in 2 patients. The remaining 36 neonates had abnormal studies: 3 were secondary to subdural hematomas; 3 demonstrated perfusion abnormalities alone; and 30 had brain scan changes showing increased activity attributable to significant cerebral hypoxia in 5 distinct patterns: 1) Watershed area, 2) infarction, 3) laminar cortical necrosis, 4) periventricular increase, 5) diffuse increase. Seven infants demonstrated mixed patterns.

To date 43 infants have been followed anywhere from 6 to 18 months of age. The duration of brain scan abnormalities correlated better with neurological outcome than did any specific pattern. Reversion of the scan to normal by 3 to 4 weeks resulted in a good prognosis with minor or transient neurological deficits, whereas infants with a persistently abnormal study remained grossly abnormal clinically.

The brain scan has proven useful in deciding whether or not significant cerebral hypoxemia has occurred, and in predicting future neurological sequelae.

THE "HOT JOINT"-INCREASED DIAGNOSTIC ACCURACY USING COMBINED ^{99m}Tc-PHOSPHATE AND ^{67}Ga CITRATE IMAGING IN PEDIATRICS H.Handmaker, S.T.Giammona. Children's Hospital of San Francisco, San Francisco, CA.

The febrile child with a painful joint is a difficult pediatric diagnostic problem since the commonest causes have widely variant treatments. Septic arthritis, osteomyelitis and toxic synovitis are the commonest causes of this symptom complex, and our early experience with 10 such patients is the subject of this report. Following initial experience with normal bone scans and xrays in patients with early acute hematogenous osteomyelitis, the authors began evaluating these children with ^{67}Ga citrate as well. 10 patients were studied in this manner. 4 patients were subsequently confirmed as acute septic arthritis (3 S.aureus, 1 H.influenza). The bone scans in these patients were normal, but gallium scans markedly abnormal. 3 patients were found to have acute hematogenous osteomyelitis (S.aureus); (2 femoral head, 1 proximal tibia). 2 of the 3 had normal or decreased phosphate distribution, but all 3 had markedly positive gallium scans, with later positive bone scans in the same areas. 2 patients were studied with normal bone scans and ^{67}Ga scans, and at aspiration were confirmed as toxic synovitis, a self-limited disease requiring no antibiotic therapy. 1 patient with an abnormal bone scan and normal ^{67}Ga scan proved to have pain resulting from an old fracture (4 mo) in the ischium, confirmed on late xrays by demonstration of callus formation. The combination of normal xrays, normal bone scans and abnormal ^{67}Ga scan makes the likelihood of septic arthritis much greater and should prompt joint aspiration. Abnormal xrays, bone and ^{67}Ga scans may be seen in osteomyelitis with or without septic arthritis. These frequently coexist.

Diagnostic accuracy of this approach exceeded that of the bone scan alone in 8 of our 10 patients with fever and joint pain and seems rational in the workup of these patients.

JOINT SCANNING IN JUVENILE RHEUMATOID ARTHRITIS. Edwin P. Hutsal, David L. Gilday and Mark Greenberg. The Hospital for Sick Children, Toronto, Ont.

A prospective study using a single injection of methylene disphosphonate to produce immediate blood pool and delayed bone images has been carried out in children suspected of being juvenile rheumatoid arthritics.

The joint images were tempero-mandibular, cervical spine, shoulder, elbow, sacro-iliac, hips, knees, hands and feet. The results were correlated with the patient's symptomatology, laboratory tests, and eventual diagnosis.

We found that with the two images we were more confident in our diagnosis especially in minimal cases, and we obtained two results with one injection - namely vascularity and bony uptake. The images in children with juvenile rheumatoid arthritis almost universally showed increased vascularity if the delayed images were positive. Patients with arthralgia due to whatever cause and some juvenile rheumatoid arthritics under symptomatic treatment usually showed normal or minimally abnormal scans. The dual image method of scanning was also helpful in following patients both for regression and progression of disease.

We found the single injection with both immediate and delayed images provided us with more information and saved the patient two examinations.

XENON-133 LUNG VENTILATION-PERFUSION STUDIES AND RADIONUCLIDE ANGIOGRAMS IN PATIENTS WITH D-TRANSPOSITION OF THE GREAT ARTERIES Salvador Treves, M.D., Marlene Rabinovitch, M.D., D.S. Ahnberg, Amnon Rosenthal, M.D., Robert M. Sade, M.D., Alexander S. Nadas, M.D. and Aldo R. Castaneda, M.D. Children's Hospital Medical Center, Boston, Massachusetts

Nineteen patients (pts) aged 2 mos to 20 yrs (mean 5.5 yrs) with D-transpostion of the great arteries (DTGA) underwent Xenon-133 (Xe) lung scans to assess changes in pulmonary ventilation (V) and perfusion (Q) pre and post-operatively, and technetium-99m (Tc) radionuclide angiograms to evaluate intracardiac shunting or atrial baffle obstruction. Nine pts (Group A) had simple DTGA and 10 (Group B) complex DTGA. Prior to Mustard procedure V inequalities between right (R) and left (L) lung (>10%) were noted in none of Group A and 2 of 10 in Group B. Q imbalance (>10%) and V/Q abnormalities (<0.8>1.2) were present in 3 of 9 in Group A and 6 of 10 in Group B ($p<0.05$). In Group A pts with demonstrated Q abnormalities excessive flow was directed to the R lung; of those abnormal in Group B, increased flow was directed to the L lung in pts with pulmonary artery band and to the site of the shunt in pts with aorto-pulmonary anastomoses.

Ten pts were studied after Mustard repair. V abnormalities were present in 2 and Q and V/Q imbalance in 5. Tc angiograms showed absence of intracardiac shunting in all but 1 pt and atrial baffle obstruction in 4 pts. Findings were confirmed in each case by cardiac catheterization. We conclude that Xe-133 lung scan is useful in quantitating V/Q imbalance before and after Mustard repair, and that Tc angiograms can detect significant residual intracardiac shunts and baffle obstruction in pts with DTGA. Moreover, these studies can be performed at any age because pt cooperation is not required.

QUANTITATIVE RADIONUCLIDE ANGIOCARDIOGRAPHY (RAC) IN PREMATURE INFANTS WITH PATENT DUCTUS ARTERIOSUS (PDA) AND RESPIRATORY DISTRESS SYNDROME (RDS). S. Treves, R. Collins-Nakai, D.S. Ahnberg, and P. Lang. The Children's Hospital Medical Center and Harvard Medical School, Boston, Mass.

Respiratory distress syndrome and hemodynamically significant PDA in premature infants is a serious and potentially lethal combination. Quantitation of left-to-right shunting through the PDA utilizing a technique which does not further jeopardize the life of these ill infants is imperative if early surgical interruption of the PDA is to be performed. Portable gamma cameras have permitted such quantitation in premature infants with RDS and PDA with considerable benefit in the clinical management of these patients.

Radioangiocardiograms were performed in 17 infants ranging in age from 4 to 98 days (mean=21) and in weight from 1040 to 2050 grams (mean=1296) utilizing either a mobile gamma camera and computer or a portable probe. Three to five mCi of ^{99m}Tc as pertechnetate was given

intravenously and recorded in the computer at 4 frames per second.

Twenty-six RAC's were done in 17 premature infants. Of the 15 preoperative studies, seven infants were found to have left-to-right shunts greater than 3.0 (Qp:Qs); in 4 infants the Qp:Qs was between 1.8 and 3.0, and in 4 infants the Qp:Qs was less than 1.8. Nine infants had surgical interruption of the PDA, and postoperative RAC in 3 of the 9 infants revealed a Qp:Qs less than 1.3. In 1 patient, Qp:Qs by RAC was 2.9 and was confirmed by cardiac catheterization. We contend that quantitation of left-to-right shunting through a PDA by RAC is an accurate, rapid, and reliable method of assessing the Qp:Qs in the face of pulmonary problems which make the other techniques such as cardiac catheterization less reliable and more dangerous.

NON-INVASIVE DETECTION OF LEFT-TO-RIGHT SHUNTS BY INHALATION OF OXYGEN-15 LABELED CARBON DIOXIDE. Denny D. Watson, Dolores M. Tamer, Warren R. Janowitz, Peter J. Kenny, Henry Gelband and Albert J. Gilson, Mount Sinai Medical Center and the University of Miami, Miami, Florida.

Oxygen-15 labeled carbon dioxide was used to develop a totally non-invasive method to detect and quantitate left-to-right intracardiac shunts. A bolus of labeled carbon dioxide is inhaled. The oxygen-15 label quickly exchanges to water in the pulmonary venous blood and is carried directly into the left heart. Radionuclide indicator-dilution curves are subsequently recorded by external detectors placed over the heart and lung. A new analytic method is used for shunt quantitation. A prospective study was undertaken in 42 patients to define the value of carbon dioxide inhalation in the detection and quantitation of left-to-right shunts in children age 2-16 years admitted for elective cardiac cathetorization (CC). 18 patients had no evidence of a left-to-right shunt at the time of CC by oximetry or angiography. None of these patients had a positive inhalation study. 22 of 24 documented shunts were detected by the inhalation method. Two false negatives occurred in shunts of less than 20% of pulmonary blood flow. Quantitative correlation was good (r=0.9) with a standard deviation confidence interval of ±10% about the calculated percent shunt flow. This technique is non-invasive, repeatable, safe, and correlates well with oximetry values obtained at CC. Thus it is a valuable new method for the detection, quantitation and follow-up of left-to-right intracardiac shunts.

AN IMPROVED OSMIUM-IRIDIUM GENERATOR FOR RADIONUCLIDE ANGIOGRAPHY. D. J. Hnatowich, S. Kulprathipanja, and S. Treves. Massachusetts General Hospital and Children's Hospital Medical Center, Boston, Mass.

Indium-191m is a potential tracer for use in radionuclide angiography and may be of particular value in the evaluation of children with congenital heart disease. The radionuclide possess a short half life (4.9 sec.), suitable photon energy (129 keV) and may be obtained as a generator product by decay of its long lived (15.3 day) parent Osmium-191. An Osmium-Iridium generator capable of providing 15 mCi of Ir-191m in 1.5 ml of eluant is described. The separation of Iridium from Osmium is achieved by absorbing Osmium Hexachloroosmate on an anion exchange resin and eluting with a solution of 8.7% NaCl at pH 2.2. The generator employs an additional resin column which is replaced periodically to reduce Osmium breakthrough. The breakthrough is less than 0.01% over a period of at least one month and after multiple elutions.

Radionuclide angiocardiograms were obtained in two anesthetized rhesus monkeys with a gamma scintillation camera-computer system equipped with a low energy converging collimator. The radioactivity was seen as it circulated through the superior vena cava, right heart, pulmonary artery, lungs, left heart, aorta, and kidneys. Using the decay corrected pulmonary dilution curve, it was possible to interpolate a gamma variate function and estimate the pulmonary-to-systemic flow ratio in the primates. Approximately thirty radionuclide angiograms were obtained in each primate using three different generator systems. There were no observable toxic or pharmacologic effects.

Tc-99m PYRIDOXYLIDENEGLUTAMATE-QUALITY CONTROL AND CLINICAL ASPECTS IN PEDIATRIC NUCLEAR MEDICINE. Robert G. Brown, David L. Gilday and Judith M. Ash. The Hospital for Sick Children, Toronto, Ont.

As an alternative to the traditional I 131 Rose Bengal scans for the demonstration of biliary tree patency, Tc-99m pyridoxylideneglutamate (Tc-99m PYG) has been investigated in our laboratory as a diagnostic agent in pediatric nuclear medicine.

Prior to use extensive chromatographic analysis was conducted to establish the quality control parameters necessary for all radiopharmaceuticals. During the synthesis of the pyridoxylamino acid Tc-99m complex there is the possibility of the formation of pyridoxal Tc-99m complex as an impurity. This material is excreted in a different manner than the Tc-99m PYG and thus its production must be minimized. At the same time high levels of free pertechnetate must be avoided. Development of paper chromatograms in an acetone solvent will demonstrate bound and free pertechnetate ion only, but utilizing silica-gel chromagrams complete resolution of Tc-99m PYG, pyridoxal Tc-99m, and free pertechnetate is possible. Modifications of these techniques allows a rapid pre-injection evaluation of the agent.

To date 7 children have been investigated utilizing this agent. A dose of 100 uCi/kg was administered intravenously and sequential anterior, posterior and lateral images were obtained at time intervals up to 4 hours. The variety of positions is necessary to distinguish between right renal and gallbladder accumulation of the activity. Bowel activity is normally evident in 30 minutes.

In our experience Tc-99m PYG is a useful diagnostic agent in children without the inherent radiation dose and poor imaging quality of I 131 Rose Bengal. Optimum quality control can be maintained with simple chromatographic assays.

THURSDAY, 2:00-3:30 BALLROOM A

CARDIOVASCULAR 3

Chairman: Paul M. Weber
Co-Chairman: Norman D. Poe

DETERMINATION OF LEFT VENTRICULAR EJECTION FRACTION AND REGIONAL WALL MOTION FROM FIRST-PASS RADIONUCLIDE ANGIOCARDIOGRAMS USING A COMPUTERIZED MULTI-CRYSTAL SCINTILLATION CAMERA. R.C. Marshall, G.S. Freedman, J.C. Costi, L.S. Cohen, A. Gottschalk and B.L. Zaret, Yale University School of Medicine, New Haven, CT.

Quantitative first-pass radionuclide angiocardiograms (RA) were performed in 22 patients (pts) undergoing biplane left ventricular (LV) contrast angiography (CA). Studies were performed using a computerized multi-crystal scintillation camera. Two views (Ant and LAO) were obtained following sequential peripheral venous injections of Tc-99m colloid and pertechnetate. Dead-time corrected precordial activity was recorded at .05 sec. intervals with count rates averaging between 35,000 and 150,000 counts/sec for each injection. Counts within the LV area of interest were summed over 3-6 cardiac cycles. The resulting data were used to form a high count rate high frequency LV time activity curve (TAC) beginning at end-diastole (ED) and forming a single representative cardiac cycle. Background frames were selected from the preliminary TAC at a point just before the bolus entered the LV, and were subtracted from the "representative" cardiac cycle such that LV counts in ED (averaging 1,000 to 4,000 C/.05 sec) and end systole (ES) were obtained. A computer generated end-diastolic perimeter was superimposed on the ES image to evaluate regional wall motion (RWM) in each view.

Repeated studies of LVEF correlated well in terms of either LAO vs Ant position (r=.97), mean Ant = 55.6%, mean LAO = 52.2%) or first study vs second study (r= .95, mean LVEF1 = 54.9, mean LVEF2 = 52.9). Average RAEF from both views correlated well with biplane CAEF (r= .95), as did RA-LAO EF (r= .97), and RA-Ant EF (r= .92). RWM abnormalities were noted in 10/11 pts with CA abnormal RWM.

Thus, quantitative RA using a computerized multi-crystal scintillation camera represents a new approach for accurately and reproducibly determining LVEF and RWM.

LEFT VENTRICULAR CONTRACTILITY AS ASSESSED BY NORMALIZED EJECTION VELOCITY UTILIZING QUANTITATIVE RADIONUCLIDE ANGIOCARDIOGRAPHY AND A COMPUTERIZED MULTI-CRYSTAL SCINTILLATION CAMERA. R.C. Marshall, G.S. Freedman, H.J. Berger, J. Wolberg, L.S. Cohen, A. Gottschalk, B.L. Zaret, Yale Univ. Sch. of Med., New Haven, CT.

Quantitative first-pass radionuclide angiocardiograms (RA) were utilized to determine normalized left ventricular ejection velocity (LVEV), an index of LV contractility, in 28 patients. Studies were performed using a computerized multi-crystal scintillation camera. A high count-rate, background corrected LV time activity curve (TAC) was formed by summing counts (C) within the LV area of interest over 3-6 cardiac cycles starting at end-diastole and subtracting an equal number of background frames taken from a point just before the bolus entered the LV. The data over the ejection phase of the representative LV TAC were fitted to a straight line using a least squares program and a value for normalized LVEV expressed as dC/dt/C average was calculated.

LVEV was compared to LV ejection fraction (EF) calculated from the same RA. LVEV averaged (±SEM) 1.25±0.15 sec-1 in pts with abnormal EF <60% and 3.27±0.12 in pts with normal EF >60%. Overall, LVEV correlated well with EF (r=.94). However, with abnormal LVEF<60% r=.94 (n=10) while abnormal LVEF>60% r=.47 (n=18).

In three normal subjects isoproterenol infusion resulted in LVEV increases averaging 58% while LVEF increased by only 12% and heart rate (HR) increased 35%. The independent effect of HR on LVEV was studied in one clinically normal subject in whom 5 minutes of atrial pacing increased heart rate by 65% but resulted in an increase of LVEV of only 9%.

Thus, normalized LVEV, a new contractility index, can be readily calculated from quantitative RA. This new independent parameter of LV function correlates well with EF, but under varying physiologic circumstances can be dissociated from both EF and heart rate.

ASSESSMENT OF LEFT VENTRICULAR FUNCTION BY A SINGLE RADIONUCLIDE TRANSIT THROUGH THE HEART. Robert H. Jones W. Robin Howe, and Jack K. Goodrich. Duke University Medical Center, Durham, N. C.

Left ventricular wall motion and chamber volume changes occurring during each cardiac contraction provide important indices of left ventricular function. Blood pool images obtained at defined phases of the cardiac cycle with a gamma camera gated by the EKG contain sufficient counts to evaluate left ventricular wall motion. Recognized disadvantages of this approach include the time required for patient study and the activity present in structures adjacent to the left ventricle, particularly the left atrium. This study describes use of a high count rate gamma camera which provides digital counting rates greater than 350,000 counts/sec. following intravenous injection of 25 mCi technetium-99m. Using this instrument, radionuclide angiocardiograms were obtained with 50 msec. counting intervals in 52 patients before and after operation for acquired valvular or coronary artery disease. Optimal images were achieved by adding counts detected during several cardiac contractions while retaining phasic relationships of the cardiac cycle. The resulting images reflect high spatial and temporal resolution because of the large number of counts obtained at discrete phases of cardiac contraction. In addition to these images which permit assessment of left ventricular wall motion, count changes reflect actual left ventricular volume changes during the cardiac cycle. In the 52 patients studied, radionuclide assessment of left ventricular function correlated closely with the left ventriculogram obtained by cardiac catheterization. Moreover, clinical observations documented the usefulness of radionuclide assessment of left ventricular function in preoperative assessment and sequential evaluation of patients with a variety of cardiac disorders.

CALCULATION OF EJECTION FRACTION FROM FIRST TRANSIT RADIONUCLIDE DATA: A COMPARISON OF SEVERAL METHODS WITH CONTRAST ANGIOGRAPHY. Glen W. Hamilton, W. Douglas Weaver, David L. Williams, James L. Ritchie, James Caldwell, and J. Ward Kennedy. Veterans Administration Hospital, Seattle, Wa.

First pass time activity curves following the intravenous injection of 25 mCi of Tc-99m albumin were obtained in 55 patients with various cardiac diseases. Information was recorded in the left posterior oblique position with a scintillation camera and stored in list mode on a computer with the ECG R wave signal. Quantitative contrast angiography was performed within 48 hours in all patients.

Two methods of defining the left ventricle (LV) region were explored: addition of all data and addition of only end-diastolic data over 5-7 consecutive heart cycles. Time activity curves were generated non-gated at 25 frames per second, and as a single summed heart cycle reconstructed from the ECG R wave. EF was calculated from the mean end-diastolic and -systolic counts (EDC, ESC) averaged over 5-7 heart cycles. EDC and ESC were obtained by visual assessment, summation of absolute maximum and minimum counts and by the root mean square method. Calculations with and without background subtraction were made in all. The comparisons to contrast EF were also analyzed to detect the effect of heart rate changes between the two studies.

The LV region was larger and more easily defined from the gated end-diastolic than from the non-gated images, but change in calculated EF was minimal. Analysis of the non-gated time activity curves by the three methods produced little change (r = .90, .91, and .93) and no single method was clearly superior. The summed, R wave gated single cycle reconstruction analysis correlated most closely with the contrast angiogram (N = 27, r = 0.95). In all groups, radionuclide-contrast angiographic comparisons were improved by eliminating patients in whom there was greater than 10% change in heart rate.

REPRODUCIBILITY OF THE EJECTION FRACTION MEASURED BY FIRST TRANSIT RADIONUCLIDE STUDIES. W. Douglas Weaver, Glen W. Hamilton, David L. Williams, Gene B. Trobaugh, and James L. Ritchie. Veterans Administration Hospital, Seattle, Wa.

Noninvasive measurement of the ejection fraction (EF) by analysis of the first transit left ventricular (LV) radionuclide time-activity curve correlates well with the EF measured by contrast angiography. As a basis for measurement of serial EF or following interventions, we have measured the reproducibility of this technique over several days in 21 patients with various cardiac diseases. Several different methods of analysis and the effect of heart rate changes were assessed. EF was measured from the mean end-diastolic and end-systolic counts (EDC and ESC).

The determination of EF from maximum-minimum counts over 5-7 cycles by visual assessment or the root mean square method were the least reliable (r = .84 and .77, respectively, from study 1 to study 2). Definition of the LV region, by ECG gating only diastolic events, improved the correlation (r = .88). Construction of a single composite time activity curve from the ECG gated events over 5-7 cycles was the most reproducible method (r = .97). Using this technique, EF-1 was .44 ± .03 and EF-2 was .44 ± .03. Heart rate changes in the gated single analyses between study 1 and 2 were minimal (<10% in 93% of cases), and no improvement in correlation was found by elimination of patients with heart rate changes.

Radionuclide determination of EF is a very reproducible technique and is enhanced by measures which decrease observer variation (end-diastolic gating of LV image and ECG construction of a composite curve). This technique appears suitable for serial studies of LV EF.

SELECTION OF APPROPRIATE FRAME RATES FOR RADIONUCLIDE ANGIOGRAPHY. Glen W. Hamilton, David L. Williams, K. Lance Gould. Veterans Administration Hospital, Seattle, Wa.

Radionuclide time-activity curves recorded over the left ventricle (LV) are commonly used to measure ejection fraction (EF). Selection of an appropriate frame rate for initial recording or reformation is critical: low frame rates cause loss of high frequency signal content and excessively high frame rates result in large statistical uncertainties. Frame rate considerations based on sample theory and applied to contrast cineradiography are not directly applicable due to the long sample period employed with radionuclide studies (sample periods for radiographic studies are in the .001 sec range; radionuclides are usually .01 to .10 sec range).

First, the effect of sample period was studied by calculating relative system frequency response from the Fourier transformation of the sampling function at various sample periods. Sample periods in the ranges used for radiography (.001-.004 sec) are essentially flat with no amplitude loss to 25 Hz. Sample periods of .1 to .04 sec (corresponding

to frame rates of 10 and 25 frames/sec) caused significant amplitude loss above 3 and 7 Hz, respectively. Next, 100 frame/sec angiographic LV volume curves were reduced to frame rates of 50, 25, 20, 16, 12, 10, and 6 frames/sec with the sample period equal to the reciprocal of the frame rate and EF calculated from the reduced data. At heart rates of 62 to 105, there was minimal (<3%) decrease in EF down to frame rates of 25/sec. Below 20 frames/sec, decreases in EF were unacceptable (>5%) and the phase relationship between sampling and volume changes caused further random error.

Based on this data, we conclude the frame rates of 20-25/sec are required for EF studies at heart rates encountered in adults.

COMPARISON OF NUCLEAR METHODS OF MONITORING LEFT VENTRICULAR FUNCTION IN MAN. H. N. Wagner, Jr., R. Wake, T. K. Natarajan, E. Nickoloff, H. W. Strauss, and B. Pitt. The Johns Hopkins Medical Institutions, Baltimore, Maryland.

We have designed, built and carried out preliminary evaluation of a new instrument called a "nuclear stethoscope" that permits continuous monitoring of left ventricular function at the bedside. Since the original description by Dodge, et al, left ventricular systolic and diastolic volumes and ejection fraction (LVEF) have been derived from contrast ventriculography, which remains the standard against which newer methods must be judged. In previous studies, we compared the results of measurement of LVEF by contrast ventriculography with the use of the gated scintillation camera and found a correlation coefficient of 0.92. Correlation of the results of the nuclear stethoscope method of recording LVEF with the scintigraphic method in 44 patients yielded a correlation coefficient of 0.75.

After injection of Tc-99m albumin, the nuclear stethoscope builds up a real time image of the amount of radioactivity within the cardiac chambers during successive intervals within the heart cycle. A collimated detector is hand-held over the chest wall to measure the activity at intervals of approximately one hundreths of a second after the electrocardiographic QRS complex. A multichannel memory provides real time display of the ventricular volumes on a small TV monitor. End systolic and diastolic volumes, stroke volume, cardiac output, pre-ejection period, left ventricular ejection time, and rates of ventricular emptying and filling can be observed.

Problems under investigation have included: (a) collimator design; (b) background correction; and (c) validation by comparison with a simulated biventricular heart. Experience to date suggests that the camera-computer method is more accurate, but that the nuclear stethoscope has great promise for studies at the bedside.

AN ECG-GATED SCINTILLATION PROBE-MINICOMPUTER SYSTEM FOR REAL-TIME CONSTRUCTION AND ANALYSIS OF HIGH TEMPORAL RESOLUTION LEFT VENTRICULAR VOLUME CURVES. Stephen L. Bacharach, Michael V. Green, David R. Redwood, Gerald S. Johnston. National Institutes of Health, Bethesda, Md.

A system comprised of a small, collimated, non-imaging NaI probe, ECG-trigger and minicomputer is described that permits the variation of left ventricular (LV) volume over a complete, average cardiac cycle to be plotted and displayed in real-time. The LV time-activity curve accumulated with the probe in its "optimal" position over the LV is background corrected and analyzed to yield estimates of LV ejection fraction and other functional parameters.

Optimal probe position is defined as that location over the left chest which gives the largest value of the ratio (N1-N2)/N1, where N1 and N2 are the gross end diastolic and end systolic counts respectively, observed in the time-activity curve at that location. Each position tested is attained solely by translation of the probe, which is fixed in a modified left anterior oblique orientation with respect to the patient. LV background is estimated by the average of two probe measurements obtained by translating the probe from its optimal position to the first lateral and first apical positions respectively, at which the associated time-activity curves just become flat.

Results obtained in a preliminary patient study and by simulation suggest that LV time-activity curves obtained with this method do not differ significantly from those obtained with the scintillation camera (J. Nucl. Med. 16: 95-98,1975)in which the location of the LV is precisely known.

The gated probe system is assembled from inexpensive components and can be made portable for use in an emergency room or catheterization laboratory. This system is of potential value in the measurement of a patients response to medication or in continuous LV function monitoring.

COUNT RATE MEASUREMENT OF LEFT VENTRICULAR EJECTION FRACTION FROM GATED SCINTIGRAPHIC IMAGES. Michael V. Green, William R. Brody, Margaret A. Douglas, David R. Redwood, James J. Bailey, Gerald S. Johnston. National Institutes of Health, Bethesda, Md.

Thirty-six patients (coronary artery disease (CAD)-18, aortic/mitral regurgitation-9, asymmetric septal hypertrophy-9) were studied by left ventricular (LV) contrast angiography and by computer-based ECG-gated scintigraphy (J. Nucl. Med.16: 95-98, 1975). Scintigraphic left ventricular ejection fraction (LVEF) was calculated from 50 msec. (modified left anterior oblique) end diastolic (ED) and end systolic (ES) gated images by integration of counts in the LV region at ED (N1) and at ES (N2). LV background (BKG) was estimated by appropriate area scaling of the integral of counts in a hand-drawn semi-annulus outside and around the ES ventricular profile. LVEF was calculated with the relation: LVEF=(N1-N2)/(N1-BKG).

Absolute ED and ES volumes were obtained from right anterior oblique angiographic studies in the same patients by planimetry of the opacified ventricle at ED and ES. LVEF was calculated from these data in the usual manner.

There was excellent correlation between LVEF measured scintigraphically and LVEF measured angiographically (all patients: r=0.83, P<.0001, N=36; patients with CAD: r=0.86, P<.001, N=18). These results suggest that the count-based scintigraphic method, which is a simple non-invasive, readily repeatable technique independent of ventricular geometry, provides reliable information concerning systolic function of the left ventricle in patients with heart disease.

RADIOCARDIOGRAPHY: RECOVERY OF PURE TIME-ACTIVITY FUNCTIONS FROM ANGER CAMERA STUDIES. M.I. Friedman, R.N. Pierson, Jr., J. Dagan, St. Luke's Hosp. Center, Columbia Univ., NYC, NY.

Quantitation of cardiac hemodynamic parameters from analysis of gamma camera regional (chamber) time-activity (TA) curves has eluded solution, chiefly because of significant overlap of chamber-based regions-of-interest (ROI). A method has been developed to determine ROI crosstalk arising from both anatomic and scatter overlap. A contamination matrix (CM), determined independently for each study, is used to separate out TA curves for each cardiopulmonary chamber, stripping off effects of activity in other chambers. Analysis yields cardiac chamber volumes, mean transit times (MTT), cardiac output (CO), left ventricular ejection fraction (EF), end-diastolic and systolic volumes, dV/dt, and systolic ejection time.

CM elements are determined based on two physiologic assumptions: 1)Tracer injected into the right atrium during ventricular systole is well mixed upon reaching the right ventricle, and 2)temporal resolution implies that no tracer appears downstream until ejection from the proximal upstream chamber (barring shunts). Postulating a constant linear combination of true chamber TA functions observed as ROI TA curves, the assumption of temporal resolution is used to define and eliminate upstream contaminants by least squares determination of upstream coefficients. Extrapolating chamber washouts according to some (exponential, gamma variate, etc.) function allows similar least squares determination of downstream CM elements. The precision with which CM elements are determined may be evaluated during the least squares process, and is reflected in the precision of the reported cardiac parameters, of which EF, left ventricular MTT, and chamber-by-chamber CO are most sensitive to error.

This CM formulation was applied to 52 patient studies in right and left views, 10 with simultaneous catheterization, allowing quantitation of all listed hemodynamic parameters.

THURSDAY, 2:00-3:30 BALLROOM B

RADIOPHARMACEUTICAL SCIENCE 3

Chairman: Alfred P. Wolf
Co-Chairman: Michael Welch

C-11-LABELED AMINO ACIDS FOR PANCREAS VISUALIZATION. Lee

C. Washburn, Tan Tan Sun, J. J. Rafter, and R. L. Hayes. Oak Ridge Associated Universities (ORAU), Oak Ridge, Tn.

Carcinoma of the pancreas is the fourth leading cause of cancer deaths in the U.S. and there is currently no suitable radiopharmaceutical agent for imaging of this organ. Since several naturally occurring amino acids are known to concentrate in the pancreas, we have been studying the synthesis of C-11-labeled amino acids for use as external visualization agents for the pancreas.

We have used early (15 min-1 hr) tissue distribution studies of the analogous C-14-labeled amino acids in the hamster, rat, rabbit, and dog to assess the value of C-11-labeled amino acids for pancreas imaging. C-11-Carboxyl-labeled DL-valine, DL-leucine, and DL-tryptophan appear to have the greatest potential. Pancreas-to-liver concentration ratios of up to 13:1 were obtained at 30 min.

Radiochemical synthetic methods for the above three amino acids as well as several others under development have been devised by using a high-temperature, high-pressure, Strecker technique developed for C-11-carboxyl-labeled 1-aminocyclopentanecarboxylic acid. The appropriate aldehyde or ketone is heated with $(NH_4)_2CO_3$, NH_4Cl, and labeled KCN at 210°C for 10 min in a stainless steel pressure vessel to give the hydantoin, which is then hydrolyzed with NaOH at 210°C for 10 min. Purification is by anion exchange followed by cation exchange chromatography. Yields of 40-55% are obtained except for DL-tryptophan, where competing side reactions lower the yield to 12%. Labeled DL-valine and DL-leucine are 30-40% decarboxylated within 2 hr in the rat, compared to only 7% for DL-tryptophan.

Considerations of synthetic yields, tissue ratios, and decarboxylation loss factors indicate that C-11-labeled DL-valine is the most promising C-11-labeled amino acid for pancreatic imaging. (This work was supported by USPHS Research Grant CA-14669 from NCI. ORAU is under contract with the US ERDA.)

ENZYMIC SYNTHESIS OF C-11 CITRIC ACID. L. Spolter, C.C. Chang, D. Bobinet, M.B. Cohen, N.S. MacDonald, A. Flesher, and J. Takahashi. VA Hospital, Sepulveda, Calif. and Univ. of Calif., Los Angeles, Calif.

Procedures for rapid enzymic synthesis and purification of C-11 citric acid were developed and the metabolic distribution of this substance in rabbits was determined.

C-11 CO2 produced in the UCLA Biomedical Cyclotron in a (p,α) reaction, was reacted with methyl magnesium bromide to form C-11 acetic acid. The latter was converted to C-11 acetyl phosphate, then to C-11 acetyl CoA, and finally to C-11 citric acid (in the presence of acetate kinase, phosphotransacetylase, and citrate synthase, respectively).

A second synthetic procedure involved the reaction of C-11 CO2 with phosphoenolpyruvate (PEP), to form C-11 oxaloacetic acid, followed by reaction with acetyl CoA to yield C-11 citric acid (in the presence of PEP carboxylase and citrate synthase, respectively).

C-11 citric acid was separated from C-11 CO2 or C-11 acetic acid on an ion-exchange column (AG 1-X8). C-14 CO2 and C-14 acetic acid were used to establish reaction conditions and the C-14 citric acid formed was characterized by paper and column chromatography and by paper electrophoresis.

Relatively large amounts of tracer were found in rabbit blood, kidney, and various other organs in both scintigraphic and tissue distribution studies. It appears thus that C-11 citric acid would not be useful as an organ imaging agent. While citric acid is metabolized in the tricarboxylic acid cycle throughout the body, it is also an important agent for acid-base regulation by the kidney. This latter role suggests that C-11 citric acid would be a valuable tool for the in vivo study of renal acid-base regulation. C-11 acetyl CoA and C-11 citric acid may also be utilized to synthesize other substances, such as various acetylated compounds and TCA cycle intermediates.

PREPARATION OF N-13 BCNU AND ITS TISSUE DISTRIBUTION IN RATS. William A. Pettit*, Roy S. Tilbury°, George A. Digenis+, Morris S. Zedeck°, Lawrence R. Helson°, Gerald R. Russ°, and Richard H. Mortara*. *Neurosurgery Dept., VA Hospital, Lexington, Ky., °Sloan-Kettering Cancer Center, N.Y., N.Y., +College of Pharmacy, University of Kentucky, Lexington, Ky.

Bis(2-chloroethyl)nitrosourea (BCNU) has been used experimentally in humans for the chemotherapy of neoplasms, especially brain tumors. In order to determine its tissue distribution and its potential for localization of tumors, we have prepared this material labeled in the nitroso group with the short-lived radionuclide, N-13. N-13 nitrate was prepared by the p,α reaction on water. Following evaporation of the water, the nitrate was reduced to nitrite by acetic acid and copper dust in the presence of a small amount of carrier nitrate. The nitrous acid produced reacts with bis(2-chloroethyl)urea to form the labeled agent. N-13 BCNU prepared by this method was demonstrated to be 99+% radiochemically pure by TLC. The drug was prepared for injection by extraction into chloroform, evaporation and dissolution in ethanol-saline. A radiochemical yield of 25-40% (corrected for decay) was obtained in a synthesis time of 15-20 min. Rats were injected via the femoral vein and subsequently visualized by sequential gamma camera imaging and/or sacrificed. Selected organs were excised and assayed for radioactivity. Results were expressed as relative concentrations and as organ/blood ratios. Sequential imaging demonstrated a changing organ distribution of activity with time and correlated with the relative organ counts obtained by autopsy. Radionuclide concentration in neurogenic and non-neurogenic tumors was compared. In rats no increased activity was observed in primary liver or colon neoplasms after administration of N-3 BCNU. However, radionuclide concentration in a human neuroblastoma (grown in nude mice) was three times that of normal brain.

AN O-15 WATER FACILITY FOR THE STUDY OF EXCHANGE REACTIONS OF OXIDATIVE PHOSPHORYLATION. R. Jerome Nickles, Sheldon M. Schuster and Henry A. Lardy. University of Wisconsin Medical School and Enzyme Institute, Madison, Wis.

A facility has been developed to produce oxygen-15 labeled water for in vitro studies of fundamental biochemical processes, in particular oxidative phosphorylation. Two minute O-15 is produced on a Tandem accelerator by deuteron irradiation of nitrogen, and is continuously transmitted 500 meters to the UW nuclear medicine radiopharmacy through a "tuned" gas pipeline. Hydrogen and carrier oxygen are added and quantitatively converted to water in a platinum catalytic reactor (1). Activities saturate in excess of 20 mCi/uA, captured in liquid volumes selectable by the user. Similarly, O-15 labeled inorganic phosphate is formed by the hydrolysis of water vapor on phosphorous pentoxide, permitting tracer access to both reactants in the studies.

The solubility of the ammonium molybdate complex of inorganic phosphate in organic solvents was used to facilitate the rapid separation of phosphate and water. This allowed us to rapidly measure the rate of the exchange of O-15 from water into inorganic phosphates catalyzed by the enzymes associated with oxidative phosphorylation on beef heart submitochondrial particles. There was a protein concentration and time-dependent exchange of label from water into phosphate. This exchange was nearly totally abolished by the addition of uncouplers or inhibitors of oxidative phosphorylation. The speed and reproducibility with which this type of oxygen exchange data can be obtained make this technique potentially valuable for studies of the mechanism of ATP synthesis.

1. West JB, Dollery CT: Absorption of inhaled radioactive water vapor. Nature 189: 588, 1961.

F-18-DAST: A NOVEL FLUORINATING AGENT. Maria G. Straatmann and Michael J. Welch. Mallinckrodt Institute of Radiology, St. Louis, Mo.

A new F-18-fluorinating agent was developed by incorporation of F-18 into diethylaminosulfurtrifluoride (DAST), a reagent capable of replacing hydroxyl and carbonyl oxygen with fluorine. This reaction occurs under mild conditions and should be applicable to labeling a wide variety of biological molecules. The DAST was synthesized using sulfur tetrafluoride and trimethylsilyldiethylamine in freon-11 solvent at -78°C, and purified by reduced pressure distillation. Labeling was then accomplished by exchange with F-18-HF; >60% of the available activity was incorporated into the DAST as shown by percent of activity distilling with DAST at 46° and 10 mmHg.

DAST (50 µl) in 0.5 ml methylene chloride was frozen in a trap attached to a circulating system of the cyclotron. Neon + 15% hydrogen was bombarded with deuterons in a nickel coated target chamber with the gas mixture passing through the trap in liquid nitrogen. At the end of bombardment, the trap was removed, shaken for 5 min. with an additional 1.5 ml methylene chloride; the compound to be labeled was added and shaking continued for 1 min. Any excess reagent was destroyed by dilute base. As model compounds, F-18-methyl fluoride, F-18-ethyl fluoride and F-18-2-fluoroethanol were prepared from methanol, ethanol and ethylene glycol in 20%, 25% and 12% yields respectively.

Any hydroxyl or carbonyl-containing compound that can be solubilized in inert organic solvents such as methylene chloride, freon-11 or acetonitrile should be a candidate for labeling with F-18 DAST.

COPPER-62: A SHORT-LIVED, GENERATOR PRODUCED, POSITRON EMITTING RADIONUCLIDE FOR RADIOPHARMACEUTICALS. G. D. Robinson, Jr. University of California, Los Angeles, Calif.

Routine use of short-lived, positron emitting radiopharmaceuticals is limited to institutions having on-site accelerators. Copper-62 ($T^1/_2$ = 9.2 min) is an easily obtainable, generator produced positron emitter which may be used to prepare radiodiagnostic agents in clinical centers without such on-site facilities.

The zinc-62 parent ($T^1/_2$ = 9.8 hr) is produced at a rate of 1 mCi/µAhr by the Cu-63(p,2n)Zn-62 reaction when a thin copper target is bombarded with 22 MeV protons. The target is dissolved in 25 ml of concentrated nitric acid and copper and zinc are converted to complex chlorides by addition of 25 ml of concentrated HCl with subsequent evaporation to dryness. The residue is taken up in 25 ml of 2 N HCl. Zinc is isolated on a 2 cm dia x 7 cm "Dowex 1-8x" resin column which is eluted with 50 ml of 2 N HCl. Radiozinc is removed from the column by elution with 50 ml of distilled water. After the resulting solution is evaporated to dryness, the Zn-62 residue is taken up in 3 ml of 2 N HCl and is applied to the 1 cm dia x 2 cm "Dowex 1-8x," 200-400 mesh, generator column. When the generator is eluted with 3 ml of 0.1 N HCl containing 100 mg/ml NaCl and 1 µg/ml Cu(II) carrier, over 85 percent of the available Cu-62 is recovered. Zn-62 levels in the eluate are less than 1 µCi/mCi Cu-62.

Several simple Cu-62 radiopharmaceuticals, including: Cu-62 sulfide for RES imaging; Cu-62 sulfide or hydroxide aggregated with HSA for lung perfusion imaging; and the Cu-62 chelate of trans-1, 2-diaminocyclohexanetetraacetic acid (DCTA) for renal studies, have been quickly and efficiently prepared using reagent kits. In each case rapid organ uptake was observed in experimental animals. Cu-62 DTPA and EDTA were found to be unstable in vivo. Agents for direct imaging of regional brain perfusion are being developed.

THURSDAY, 2:00-3:30 BALLROOM C

GASTROINTESTINAL 2

Chairman: Naomi P. Alazraki
Co-Chairman: Lynn R. Witherspoon

THE VALUE OF BOWEL PREPARATION IN GALLIUM-67 CITRATE SCANNING. Robert Zeman and Thomas Ryerson. Northwestern University Medical School, Chicago, Il.

The ability of Ga-67 citrate to localize inflammatory and neoplastic lesions has been well documented. Colonic excretion of Gallium has rendered interpretation of the 72 hour scan difficult, and can give rise to false positive interpretations. The use of various combinations of cathartics has become established practice in preparing the patient for the Ga-67 scan. To evaluate this practice, we retrospectively analyzed 200 randomly selected 72 hour Ga-67 scans done from 1973-75, and compared the extent of bowel activity in two groups of patients: those receiving a bowel preparation consisting of Dulcolax tablets and Magnesium Citrate (BOPREP) and those receiving no preparation (NOPREP). The populations were studied with regard to their age, sex, ambulatory status, pathology, and preparation. Scans were evaluated on a five point scale, ranging from no discernible colonic activity to intense activity throughout all segments of the colon. An indeterminate category was included for those cases where technical defects or abdominal pathology might have obscured colonic activity. Scans with detectable colonic activity were repeated at 96 hours. Our data reveals the following: in the BOPREP and NOPREP groups respectively, 44% and 34% of patients were scanned to diagnose Hodgkin's Disease or lymphoma, 24% and 22% were scanned to study other malignancy, 14% and 17% to rule out abcess, and 18% and 27% for other pathology. 6% of patients in each group were out-patients. A three way analysis of variance, prep x age x sex, showed no influence of these parameters on colonic activity. We conclude that bowel preparation yielded no significant reduction in bowel activity ($P > .1$). It is recommended that patients not receive cathartics prior to Ga-67 scanning. If colonic activity is present, delayed 96 hour scanning may be indicated.

AUTORADIOGRAPHIC STUDIES OF DISTRIBUTION IN THE STOMACH OF Tc-99m-PERTECHNETATE. Tapan K. Chaudhuri, and Joseph J. Polak. V.A. Center and Eastern Virginia Medical School, Hampton, Va.

The purpose of this paper is to report our observation on the exact cellular site of distribution of Tc-99m-pertechnetate in the stomach of different animal species; namely, mouse, rat, cat and dog. Following overnight fasting, animals were injected intravenously with 10 mCi of Tc-99m-pertechnetate. Stomach sections (from the corpus part) were taken 15 to 20 min. post-injection. Multiple tangential and horizontal slices (5-10 µ thick) were autoradiographed using Kodak NTB3 liquid emulsion. The results indicated that Tc-99m-pertechnetate localized predominantly in the mucus-secreting cells. Heavy silver grain concentration was observed at the mucous lining. Little or no grains were detected in the parietal and chief cells. There was no species difference observed at least between mice, rats, cats and dogs. These findings are enable to explain the following facts: (1) Why in Barrett's esophagus, gastric tissue without parietal cells (Amer. J. Roentg. 123: 401, 1975) accumulates Tc-99m-pertechnetate and (2) Why an isolated gastric antrum devoid of parietal cells (Gastroenterology 65: 697, 1973) secrete Tc-99m-pertechnetate. In conclusion, gastric secretion of Tc-99m-pertechnetate is a function mainly of mucus-secreting cells of the surface mucosa of the stomach. There exists very little or no role of parietal and chief cells on gastric secretion of pertechnetate.

QUANTITATION OF GASTROESOPHAGEAL(GE) REFLUX BEFORE AND AFTER THERAPY USING THE GE SCINTISCAN. Leon S. Malmud, Robert S. Fisher, Ira Lobis, Willis Maier. Temple University Hospital, Philadelphia, Pa.

Therapeutic modalities employed to treat GE reflux(GER) include change in body position, bethanechol, antacids, antacid-alginate compounds, or fundoplication. This study was designed to quantitate the effectiveness of these modalities on GER using the GE scintiscan(GES). Five groups of 10 patients were studied before and after each modality. The GES was compared to the patient's symptomatology and to the acid reflux test. The surgical group had pre-and post-operative fluoroscopy. The GES was performed by orally administering 300 mCi Tc99m sulfur colloid in 300 ml water and obtaining 30 sec. gamma camera images as the GE pressure gradient was increased from 10 to 35 mm HG at 5mm Hg increments using an inflatable abdominal binder. Data was processed using a digital computer. Any reflux Greater than 4% was visible without data processing and was considered abnormal. Reflux was reduced by change in position from recumbent to upright, and by the use of subcutaneous bethanechol, oral antacid, or oral antacid-alginate compound. Only fundoplication reduced reflux to less than 4%. Preoperatively, only 6 of 10 patients had reflux by fluoroscopy, although all had symptoms, positive acid reflux test, and positive GES. Postoperatively, 1 patient had reflux by fluoroscopy, symptomatology, a positive GES, a

positive acid reflux test and this was a surgical failure.

The GES is more sensitive than fluoroscopy, correlates well with clinical symptomatology, and is a reliable and convenient technique for the quantitation of GER before and after therapy.

SCINTIGRAPHIC, ANGIOGRAPHIC AND HISTOLOGIC CORRELATION IN 5 CASES OF HEPATIC ADENOMA AND FOCAL NODULAR HYPERPLASIA. C.M. Kim, F.F. Ruzicka, and S. Goldfarb. University of Wisconsin Hospitals, Madison, Wisconsin.

The incidence of hepatic adenoma and focal nodular hyperplasia (FNH) have been reported to be related to long term use of sex hormones. In a short period of 2 1/2 years we have found 5 cases occuring in women taking oral contraceptives for long periods.

All patients were studied with a Tc-99m SC LS, hepatic angiography and were operated with a histopathologic diagnosis obtained.

Patients with adenomas demonstrated reduced radiocolloid concentrations consistent with the histologic findings of absent reticuloendothelial cells. All of the adenomas were large averaging 12 cm in the longest dimension.

One patient with 2 separate adenomas had one showing premalignant histologic changes but no patient had a diagnosis of hepatic malignancy. Since hepatocytes are present in the adenomas, but no bile ducts, an I-131 RB scan showed delayed uptake and prolonged retention suggesting cholestasis.

FNH contains bile ducts as well as hepatocytes and reticuloendothelial cells and are usually much smaller than adenomas. In one patient the FNH presented as a small bulge below the anteroinferior surface of the liver with normal radiocolloid concentration. In another patient 3 areas of FNH were not demonstrated on the Tc-99m SC scan and were found incidentally at surgery.

When interpreting abnormal liver scans performed on women receiving birth control pills, this entity should be considered in the differential diagnosis and the Tc-99m SC scan should be followed by a delayed I-131 RB scan.

A DOG MODEL FOR PANCREATIC SCANNING USING RETROGRADE INJECTION OF TECHNETIUM-99m. Paul F. Varley, Stephen E. Silvis, and Rex B. Shafer. Veterans Administration Hospital, Minneapolis, Minnesota.

Present methods of pancreatic imaging are less than optimal. With widespread acceptance of endoscopic retrograde pancreatography (ERP), a new means of injecting a radionuclide into the pancreas became available. This procedure would add parenchymal visualization to the already well-demonstrated ductal anatomy of the ERP.

Prior to studying retrograde imaging in humans, a dog model was developed to determine resolution and toxicity. Both normal animals and those with induced acute pancreatitis were studied. After surgically cannulating the main pancreatic duct, technetium-99m labelled material (including pertechnetate, pyrophosphate, sulfur colloid and microspheres) was injected and followed serially for up to 24 hours. The images obtained show homogeneous parenchymal activity with both ionic and particulate material. The ionic materials were absorbed from the pancreas and redistributed throughout the body, while the particulate materials remained within the pancreatic parenchyma. The dog's pancreas was later examined histologically for evidence of damage to the pancreas from the injected material.

The results show excellent visualization of the pancreatic parenchyma in dogs and suggest the feasibility of this technique in humans. No evidence of tissue toxicity was observed.

HUMAN PANCREATIC IMAGING WITH N-13 L-ALANINE. Marvin B. Cohen, Leonard Spolter, Norman MacDonald, Darrell Bobinet, Chia Chin Chang and Joseph Takahashi. UCLA and V.A. Hospital, Sepulveda, California.

The utility of N-13 L-Alanine for pancreatic imaging was investigated in humans. Radiopharmaceutically pure N-13 L-Alanine was synthesized using columns containing enzymes bound to porous silica beads, followed by column chromotomography. Pancreatic scans were performed in seven human volunteers and eleven patients. Imaging was accomplished using either a scintillation camera (H-P Searle) equipped with a tungsten collimator, a dual 5-inch scanner (Ohio Nuclear) or a dual 8-inch tomographic scanner (Searle) equipped with 511 KEV collimators. Substraction scans were obtained in selected studies. Imaging began immediately after the intravenous injection of 3-8 mCi of N-13 L-Alanine. No special patient preparation was utilized.

Good quality high photon images of the pancreas were obtained with either the scintillation camera or the tomographic scanner, when the pancreas and liver were observed to be anatomically separate. Interfering activity from an overlying liver was only partially eliminated by the tomographic scanner, which also was unsatisfactory for patients with a large abdominal girth. Poor images of the pancreas were obtained in the two patients studied with the dual 5-inch scanner. Computer performed substraction studies removed interfering liver activity from the scintillation camera images, but also accentuated previously unrecognized tracer activity in the kidney, stomach and small intestines, which severely detracted from the quality of the image.

While presently available commercial imaging systems are not optimal for use with positron emitters, N-13 L-Alanine appears to be a very good agent for pancreatic imaging in humans. (Supported by Veterans Administration and Contract between UCLA and ERDA:ET-GEN 12).

FRIDAY, JUNE 11, 1976

FRIDAY, 8:30-10:00 BALLROOM A

HEMATOLOGY 2

Chairman: David C. Price
Co-Chairman: Sally DeNardo

INDIUM-111 LABELED LEUKOCYTES FOR THE LOCALIZATION OF ABSCESSES. Mathew L. Thakur, R. Edward Coleman and Michael J. Welch, Washington University School of Medicine, St. Louis, Mo.

Leukocytes are separated from ∿30 ml of blood which is drawn in a syringe containing 0.6 ml of preservative free heparin. To the blood is added 0.9 ml of 2% (W/V) methyl cellulose solution in 0.9% NaCl. The blood is mixed gently and allowed to stand for one hour. The leukocyte rich plasma is separated and centrifuged for 5 minutes at 450G. The cells are washed twice with 5 ml 0.9% NaCl and resuspended in the same volume of the isotonic saline.

Indium-111 is chelated with 8-hydroxyquinoline and the lipid soluble complex is extracted in chloroform. The chloroform is evaporated to dryness and the residue is dissolved in 100 µl ethanol. The solution is diluted to 500 µl with normal saline, added dropwise to the cell suspension, and the cells are incubated at room temperature for 45 minutes. Labeling efficiency of ∿95% is achieved.

The specificity of the labeled leukocytes has been determined by autoradiography of the labeled cells and by selective cell separation. Approximately 90% of the activity is incorporated with the polymorphonuclear leukocytes. In dogs the indium-111 activity remains in association with the cells for at least 27 hours after administration. The viability of the labeled cells has been demonstrated by the half clearance time of 6 to 9 hours in animals. The tissue distribution of the radioactivity ad-

ministered as labeled leukocytes demonstrated that the radioactivity concentrates mainly in the liver, spleen and induced abscesses. In dogs the abscess to blood activity ratios obtained 24 hours after administration were 70.2±23 compared to 4.5±1.6 with Ga-67 citrate in the same animals. These results plus the suitable characteristics of the radionuclide make the indium-111 labeled leukocytes a desirable agent for the localization of abscesses.

INDIUM-111 LABELED PLATELETS: PREPARATION, FUNCTION STUDIES AND IN VIVO EVALUATION. Mathew L. Thakur, Michael J. Welch, J. Heinrich Joist and R. Edward Coleman. Washington University School of Medicine, St. Louis, Mo.

Platelets have been labeled with a lipid soluble complex of indium-111. The complex is formed with 8-hydroxyquinoline, and extracted in chloroform which is evaporated to dryness. The residue is dissolved in 50 µl of ethanol and diluted to 200 µl with normal saline.

Platelets have been harvested by a differential centrifugation technique from blood drawn in a 50 ml syringe containing 7 ml acid citrate dextrose solution. They are washed twice with Tyrodes solution pH 7.4 and resuspended in 10 ml of the Tyrodes solution. The final platelet concentration is about 3 x 10 to the power of 8 per ml. To the suspension is added the radioactive complex solution and the mixture is incubated at 37°C for 30 minutes. More than 95% of the radioactivity is incorporated with the platelets.

The function of the labeled platelets has been studied by their aggregability using low concentrations of adenosine diphosphate and collagen as the stimulating agents. No adverse effects have been observed.

The labeled canine platelets have been administered to dogs with venous thrombi induced by alteration of the intima by an electric current. The thrombi were detected by imaging 3 hours after administration. Twenty four hours later the thrombi were removed and had 15 times the radioactivity of an equal weight of blood. Accumulation of large amounts of activity in previous surgical wounds has also been observed. Damage of the intima of carotid arteries in animals by a balloon catheter demonstrated 8 to 20 times more activity in the region of damage than in the normal artery. Results indicate that In-111 labeled platelets are a potential agent for evaluating vascular damage.

LABELING OF PERIPHERAL BLOOD LEUKOCYTES BY PHAGOCYTOSIS OF TC-99M MINIMICROSPHERES. Ralph G. Robinson, Diana Bradshaw, David F. Preston, Rolf F. Barth, Norman L. Martin and Buck Rhodes. Kansas University Medical Center, Kansas City, KS.

Phagocytic labeling of human peripheral blood leukocytes with Tc-99m minimicrospheres (MMS) made of human serum albumin was evaluated and compared with another phagocytic label, Tc-99m sulfur colloid. Leukocytes separated from 50 ml of heparinized whole blood by dextran sedimentation were incubated with Tc-99m labeled colloid. The Tc-99m MMS labeled leukocytes were tested in vitro to establish whether cell associated activity was the result of phagocytosis. Following 10 washes, 43% of the initial activity remained cell associated. There was a decrease in labeling when cells were incubated at 4°C rather than 37°C and the cell associated activity was not displaced by varying concentrations of unlabeled MMS. Opsonization by fresh plasma complement was necessary for phagocytic labeling; heat inactivation of complement proteins reduced the cell associated activity by 72%. Preincubation of MMS with fresh plasma increased cell associated activity by 7%. There was no significant difference between cells labeled with autologous and heterologous plasma.

Whole body scans at 1 and 4 hours after injection of Tc-99m MMS and blood disappearance curves were done using 5 normal human volunteers. These scans showed significant compartmentalization of labeled leukocytes in the lungs, liver, spleen, blood and bone marrow at 1 hour after injection. There was a significant shift from the pulmonary compartment to the liver and spleen at 4 hours. The immediate blood clearance was 10 times greater in 5 subjects similarly studied using Tc-99m sulfur colloid labeled cells.

Leukocytes have been labeled by phagocytosis of colloids, the MMS method yielding more Tc-99m per cell than the sulfur colloid method. These studies show Tc-99m MMS can be used as a leukocyte label in humans.

SPLENIC IMAGING WITH DAMAGED TECHNETIUM-99m RED BLOOD CELLS: A COMPARATIVE STUDY. Robert G. Hamilton, Philip O. Alderson, John F. Harwig, and Barry A. Siegel. Armed Forces Radiobiology Research Institute, Bethesda, MD and the Mallinckrodt Institute of Radiology, St.Louis,MO.

This study was performed to compare several previously reported methods for splenic imaging with damaged red blood cells (RBCs) to the results obtained with RBCs damaged by sulfhydryl inhibitors. RBCs from donor animals were labeled with Tc-99m by the electrolytic method of Harwig et al. and damaged by heating (50°C, 15 min), excess acid citrate dextrose (ACD), excess Sn (II) ion, or the sulfhydryl inhibitors, p-hydroxymercuribenzoate (PMB) or N-ethylmaleimide (NEM). The distribution of undamaged and the several types of damaged RBCs was determined in 200-400 g male rats. Imaging studies were also obtained in rabbits.

Splenic localization was greatest with heat damaged (45.4 ± 1.6% dose/spleen) and PMB damaged (38.2 ± 9.0%) RBCs; both results were significantly greater than those with undamaged (1.4 ± 0.3%), ACD damaged (2.6 ± 0.7%), Sn (II) ion damaged (2.8 ± 0.5%), or NEM damaged (19.2 ±9.0%) RBCs. Maximum spleen to liver concentration ratios were observed 2 hours after injection (28.2 heat damaged; 17.5 PMB damaged). Both heat and PMB damaged RBCs resulted in splenic images of high quality.

Heat damaging is the best method for producing splenic localization of Tc-99m RBCs. PMB damaging, which is technically simple and less time-consuming, is an acceptable alternate approach.

A STUDY OF SURFACE FUNCTIONAL GROUPS IN RELATIONSHIP TO THE OXIDATIVE METABOLIC CHANGES WHICH OCCUR DURING PHAGOCYTOSIS IN HUMAN POLYMORPHONUCLEAR LEUKOCYTES (PMN). Min-Fu Tsan, Burlina Newman, Marianne Chen, Kenneth H. Douglass, and Patricia A. McIntyre. The Johns Hopkins Medical Institutions, Baltimore, Md.

The role of plasma membrane in phagocytosis-associated oxidative metabolism in human PMN was evaluated by modifying it in two ways: 1) P-chloromercury benzene sulfonic acid (PCMBSA) (0.1mM) was used to inhibit surface -SH groups and 2) sialidase (0.1lµ/ml) was used to delete membrane sialic acids. Neither 1 nor 2 had any effect on phagocytosis of latex particles. Hexose monophosphate shunt activity (HMS), hydrogen peroxide (H_2O_2) and superoxide (O_2^-) production during phagocytosis were measured in control and treated cells as was the ability of these cells to kill staphylococcus aureus. The results (expressed as % of control values) were:

Latex Particle Stimulated Human PMN

Treatment	HMS	H_2O_2	O_2^-	Killing Staph. aureus
controls	100%	100%	100%	100%
1	33%	7%	87%	94%
2	105%	20%	11%	7%

We conclude that a) superoxide production and HMS activity are under separate membrane control, with -SH groups required for normal HMS, and sialic acid for O_2^-. b) HMS plays an active role in providing NADPH for the generation of H_2O_2 from superoxide, and c) superoxide plays an important role in the killing of staphylococcus aureus.

FRIDAY, 8:30-10:00 BALLROOM B

RADIOPHARMACEUTICAL SCIENCE 4

Chairman: Gopal Subramanian
Co-Chairman: David Allen

A HIGHLY STABLE CONJUGATE OF ALBUMIN WITH A CHELATE OF INDIUM-111 FOR IN VIVO TRACER EXPERIMENTS. David A.

Goodwin, Claude F. Meares, Charles S-H Leung, David J. Silvester, Adrian D. Nunn, and Peter J. Lavender. Vet. Admin. Hospital, Palo Alto, CA, Stanford Univ. School of Med., Dept. of Chemistry, Univ. of Calif. at Davis, and Hammersmith Hospital, London, England.

A conjugate of the bifunctional chelate 1-(p-benzenediazonium) EDTA and human serum albumin was synthesized and indium-111 ions added specifically to the chelating groups. The product (specific activity 0.7 mc/mg) was incubated in human serum under conditions and concentrations appropriate to human diagnostic use. The loss of metal ion from the chelating group to transferrin was less than 3% at one week, and 5% at 2 weeks.

The biological half life of this HSA tracer was followed in rabbit plasma and compared to iodinated HSA I-125 and the conjugate of rabbit albumin with the bifunctional chelate of indium-111. The characteristic immunologic recognition of the foreign protein was demonstrated by a sudden drop of plasma activity on day 6 of HSA with both the iodine-125 and indium-111 labels. This did not occur with rabbit albumin labeled with a bifunctional chelate of indium-111, and the plasma disappearance curve continued unbroken up to day 15.

The plasma disappearance of 1.4mc of indium-111 chelate labeled HSA was followed 16 days in a patient studied by whole body scanning. The biological T 1/2 was 7.4 days, with 85% of the radioactivity still in the albumin by electrophoresis on day 7.

An excellent whole body scan was obtained with the vascular structures visible for 48 hours, and no bone marrow concentration.

The stability of the chelate demonstrated in these experiments provides forceful evidence that this technique has significant applications in labeling other biomolecules for use in nuclear medicine.

In-111 PHENOLPHTHALEXON (PPX):A NEW AGENT FOR EXTENDED CHOLESCINTIGRAPHY. Max S. Lin, V.A. Hospital, Palo Alto, Ca.

In seeking an improved agent for extended cholescintigraphic evaluation of extrahepatic bile duct patency, an In-111 labeled PPX, structurally related to rose bengal (RB), has been formulated and studied preclinically.

In-111 was complexed to PPX, a $-CH_2N(CH_2COO^-)_2$ derivative of phenolphthalein, essentially instantly and quantitatively by mixing acidic In-111 chloride with equal parts of Na_2HPO_4-"buffered" 10-mM PPX to give a mixture at pH 6.0 to 6.5. The preparation was sterilized with 0.22-u Millipore filters (which retained 2-4% of the applied In) and was found to be stable for at least 3 days.

In pentobarbital-anesthetized dogs, gall bladders (GB) and common bile ducts were about maximally visualized 1 h after iv injection. After 3 h, 6%, 25% and 34% doses were recovered in the blood, GB and urine, respectively. At this time, In concentration of the GB bile was 250 and 290 times that of the liver and the blood, respectively. The biliary In entered the gut after the dog awoke from the anesthesia. For the next 2 days, abdominal scintigraphy clearly distinguished intestinal from renal and urinary radioactivities. In rats (no GB), bowel loops were visualized as early as 10 min, and the %dose/organ after 3 h was: intestine 29%, liver 1.3%, kidneys 5.8% and blood 3.4%. No evidence was found in dogs or rats for In translocation in vivo from PPX to transferrin in the first day. The PPX was not lethal to rats in single iv doses of 170 mg (220 umole)/kg (1,700 times expected human dose), and failed to produce clinical or histologic changes when given in several iv doses over 4 wk to a total of 50 mg/kg in dogs and 600 mg/kg in rats. Radiation absorbed dose to the critical organ (lower large intestine) per mCi in anticipated human studies was estimated to be about 1/10 of that for I-131 RB.

In conclusion, a new cholescintigraphic agent, In-111 PPX, has been formulated and shown to exhibit preclinical characteristics that give grounds for its clinical trial.

DETERMINATION OF THE NET CHARGE ON SOME Tc-99m RADIOPHARMACEUTICALS. Azu Owunwanne, Jacob A. Marinsky and Monte Blau. State University of New York at Buffalo, Buffalo, New York.

The chemical nature of most Tc-99m labeled radiopharmaceuticals is not well established. In many cases not even the net charge on the Tc-99m complex is known.

Using the ion exchange distribution method we have studied the charge on Tc-99m-hydroxyethylene diphosphonate (Tc-99m-HEDP) and Tc-99m-glucoheptonate (Tc-99m-GH). This method involves the measurement of the equilibrium distribution, Do, of a trace amount of Tc-99m radiopharmaceutical between an anion exchange resin (AGI,X8, 50-100 mesh) and a bulk electrolyte of known charge (ClO_4^-). When Do is measured as a function of ClO_4^- concentration, the slope of the displacement curve yields the net charge on the Tc-99m complex. The advantage of this technique is that tracer amounts of complex can be studied and the concentrations can be as low as those used in routine preparations of the pharmaceuticals.

To test the validity of the system the charge on TcO_4^- was studied. The measured slope of 0.98 corresponds to the known charge of -1. Technetium-99m-GH had a slope corresponding to a charge of -1 also. The Tc-99m-HEDP complex contained two components; one with a charge of -0.5, the other with a charge of -2.

Attempts to study the charge on Tc-99m-pyrophosphate were unsuccessful. Using our system it was not possible to keep the reduced Tc-99m complex from oxidizing back to TcO_4^-.

Possible structures for these various radiopharmaceuticals are suggested based on the measured net charges.

FRIDAY, 8:30-10:00 BALLROOM C

HYPERTENSION

Chairman: Martin L. Nusynowitz
Co-Chairman: Barry A. Siegel

COMPARISON OF RENAL IMAGING, SARALASIN INFUSION AND RENIN ASSAYS IN THE EVALUATION OF ANGIOTENSINOGENIC HYPERTENSION. J.G. McAfee, F.D. Thomas, Z.D. Grossman, D.H.P. Streeten, and G. Gagne. Upstate Medical Center, Syracuse, N.Y.

Recently, a one-day screening procedure has been developed specifically for angiotensinogenic hypertension based on a fall in blood pressure on IV infusion of the angiotensin antagonist Saralasin (P113) and peripheral venous renin assays by RIA, in a sodium-depleted state (Streeten, D.H.P., New Eng. J. Med. 13/657/1975).

In 162 hypertensive patients screened by this procedure, renal imaging was performed after 15 mCi of Tc-99m glucoheptonate and 200 μCi of I-131 Hippuran IV. Renal vein renin assays, IVP and renal arteriography were performed selectively.

The P113 infusion test proved superior to peripheral venous renin assays for the detection of angiotensinogenic hypertension. Occasionally, however, this type of hypertension occured with bilateral renal disease and/or malignant hypertension. Renal imaging proved valuable in indicating which patients had a unilateral abnormality; nonetheless, the imaging procedure frequently could not distinguish unilateral renovascular disease from unilateral parenchymal disease without angiotensinogenic hypertension.

Twenty-six patients in this series had arteriographic renal artery stenosis of whom 5 had a negative P113 infusion test, 9 had a negative peripheral renin assay and 2 had no imaging abnormalities. Some arteriographic abnormalities were not associated with angiotensinogenic hypertension, as assessed by P113 infusion and by renal vein renin assays.

This study indicates that radioisotopic imaging is a useful procedure for the investigation of hypertensive patients after the initial P113 infusion test has been performed, to detect unilateral or segmented renal or renovascular lesions.

THE RADIOIMMUNOASSAY OF ANGIOTENSIN-I IN HYPERTENSIVE PATIENTS BEFORE AND AFTER BEDREST.

C.Constantinides, M.Mavrikakis, P. Athanasiades, M.Chrisikou and S. Moulopoulos.

Department of Clinical Therapeutics, Medical School, University of Athens, Alexandra Hospital,Athens 611,Greece.

This investigation was undertaken to determine the existance of any relationship between blood pressure reduction and a change in the level of Angiotensin-I in the venous blood of hypertensive patients before and after bedrest.

Twenty-five hypertensive patients were included in this study. Angiotensin-I was determined in venous blood by using the method of radioimmunoassay. Upon admission 12 out of 25 patients (group I=48%) showed an angiotensin-I activity higher than the normal, ranging from 1.33 to 3.06ng/ml/h. 13 patients (group II=44%) showed an angiotensin-I activity within normal limits (0.015-096ng/ml/h). After 72 hours of bedrest the angiotensin-I activity was found lower than the original value in all cases.

The angiotensin-I activity of the patients of group I before and after bedrest was found statistically different ($P<0.001$). The angiotensin-I reduction for the patients of group II was significant too ($P<0.005$). The reduction of angiotensin-I in the group showing high values before bedrest was more significant than that of the group initially showing normal values of angiotensin. The difference between the two groups was statistically significant ($P<0.001$). The correlation of changes in angiotensin-I levels and blood pressure changes shows the greatest change in blood pressure in patients with a small difference in angiotensin-I values before and after bedrest. Furthermore, the largest reduction in blood pressure was seen in patients with originally low angiotensin-I blood levels.

6β-19-NOR-IODOCHOLESTEROL (NP-59): A SUPERIOR ADRENAL IMAGING AGENT IN HUMANS. S. D. Sarkar, E. L. Cohen, W. H. Beierwaltes, R. D. Ice, S. P. Gill, and E. N. Gold. University of Michigan Hospital, Nuclear Medicine and Endocrine and Metabolism Sections, Ann Arbor, Mich.

Adrenal imaging with I-131-19-iodocholesterol (NM-145) has provided a non-invasive method of determining adrenal structure and function in humans. We have reported that NP-59 concentrates in the adrenals of the rat and dog 5 X > I-131-19-iodocholesterol with higher target to non-target ratios (J. Nucl. Med. 16: 1038, '75).

Each of 31 patients was given 2 mCi of NP-59 (sp. act. 1-5 mCi/mg) iv. Adrenal imaging was performed identically as in previous studies with NM-145 at several intervals between 1 and 10 days, using a Searle Radiographics gamma camera mated with a MDS Computer.

NP-59 showed all the desirable characteristics of NM-145, namely: 1) Cushing's Syndrome (16 patients): non-suppressible symmetrical uptake (2 mg dexamethasone/da X 2 da before tracer) in pituitary ACTH excess bilateral hyperplasia; unilateral uptake in hyperfunctioning adenoma with suppression of uptake in normal adrenal, and lack of uptake in adrenocortical carcinoma. (Histopathologic data is incomplete at this date in the following hypertensive states). 2) Primary aldosteronism with dexamethasone suppression (7 patients): early asymmetrical uptake in unilateral tumor and symmetrical uptake in bilateral hyperplasia. 3) Pheochromocytoma (5 patients): lack of uptake in the affected adrenal due to compression of adrenal cortex by tumor.

We also did dexamethasone suppression studies on: a) 2 patients with low renin hypertension, one showing bilateral suppression early and late and another, early bilateral uptake. b) 1 patient with excessive adrenal androgens, showing early bilateral uptake.

NP-59 was superior to NM-145 in that: 1)Diagnostic uptake was present at one day. 2) The adrenal image was brighter. 3) The background activity was less.

FRIDAY, 10:30-12:00 BALLROOM A

CARDIOVASCULAR 4

Chairman: Richard N. Pierson, Jr.
Co-Chairman: S. Treves

AN OPTIMAL APPROACH TO INVESTIGATIVE DIAGNOSIS OF VENOUS THROMBOSIS. Ramesh C. Verma, Milo M. Webber, Lealie R. Bennett, and Norman D. Levine. University of California and Olive View Medical Centers, Los Angeles, Ca.

Currently, there are at least 10 established thrombosis detection procedures utilizing 6 different modalities. This has lead to significant confusion as to their optimal utilization. A practical approach to the investigative diagnosis of thrombosis has been developed following an extensive review of the literature. This approach is based upon presenting clinical problems: A. Prospective: the high risk group; B. Retrospective: those with a documented venous embolism; C. Recurrence: in patients with past history; D. Confirmatory: i) low suspicion with one or more symptoms or signs of thrombophlebitis, and ii) high suspicion with one or more high risk factors plus one or more symptoms or signs.

The tests of choice recommended for each of the above groups are: A. Fibrinogen Uptake Test (FUT); Antithrombin III (Heparin Cofactor) estimation may turn out to be a good test to screen for high risk individuals; B. Radionuclide Venogram (RNV) plus Radiolabelled Particle Entrapment (RPE) Scans (RNV delayed scans, thromboscintiscans, etc.) and Contrast Phlebogram (if extent of thrombus is to be determined and if caval ligation/plication is planned); C. FUT and possibly serial Fibrin Degradation Products (FDP) estimations; D. i) RNV and RPE scans, and ii) RNV and RPE scans followed by FDP or Fibrin Monomer estimations, ultrasonic flow or rheographic studies if ileofemorals are suspected, and FUT if calf veins are suspected, and last of all, Contrast Phlebograms if further confirmation of the diagnosis is needed. When the efficacy of I-123 or Tc-99m Fibrinogen is well proven, they may replace the FUT for groups C and D.

(This study was supported by USPHS Grant 2 R01 GM 17113-04.)

CORRELATION OF Tc-99m MAA THROMBOSIS SCANS TO VENOGRAMS. Ramesh C. Verma, Milo M. Webber, and Michael D. Cragin. University of California, Los Angeles, Calif., and Olive View Medical Center, Van Nuys, Calif.

The affinity of Tc-99m MAA for sites of endothelial damage has been well documented experimentally (Radiology 92:620, 1969). This study was conducted to correlate the TcMAA Thromboscintiscan (MAA Scan) to contrast venography (CV) in patients with suspected thrombophlebitis.

The MAA Scan technique involves application of above ankle and above knee tourniquets (to cause flow through the deep venous system), intravenous injection of 1.5 mCi of Tc-99m MAA separately into each foot and exercising the feet for 5 minutes followed by scanning of both legs. Conventional techniques for CV were used.

Fifty-two patients underwent both studies which were done not more than 7 days apart. No antithrombotic therapy was administered in the interim. Eighty-five percent (17/20) of the patients with documented recent thrombi on CV had positive MAA Scans and 21 of the 32 patients with normal CV also had negative MAA Scans. Of the remaining 16 patients, 11 had "false" positive and 3 had "false" negative MAA scans as compared to CV. The latter are most probably due to poor injection or complete occlusions with good collateral flow (the particles, therefore, do not flow past the thrombus). The etiology of the false positive MAA scans has not been well determined; these may be due to early endothelial damage which is not demonstrated on CV or due to accumulations in the superficial veins which are not evaluated at CV. With an overall accuracy of 76% (true correlations) and a very low false negative rate, the MAA scan is an ideal noninvasive screening procedure for thrombosis detection. (Supported by USPHS Grant 2-R01-GM17113-04 and ERDA Contract E-(04-1) GEN-12.)

RADIONUCLIDE VENOGRAPHY, CORRELATION TO CLINICAL AND RADIOGRAPHIC FINDING. U. Yun Ryo, Mohammad Qazi, S. Srikantaswamy, and Steven M. Pinsky. Michael Reese Hospital and Medical Center, Chicago, Ill.

In order to further evaluate positive findings of the radionuclide venogram (RNV), the RNV with 99mTc-MAA and contrast venography were performed in 23 patients (pts) with clinically suspected thrombophlebitis.

Clinical findings, pain and/or swelling of leg(s) were found to be non specific in 4 pts later by clinical obser-

vations and examinations. All contrast venograms and RNVs from these 4 pts were normal.

In the rest of 19 pts, contrast venogram was abnormal in 11 (58%) and RNV was abnormal in 18 (95%) pts. Eight of 18 pts with abnormal RNV had normal contrast venograms. Five of these 8 pts showed retention of radioactivity in the calf, after a knee joint exercise, as only positive finding and an abnormal collateral flow in addition to the radioactivity retention was noted in 3 patients.

RNV was definitely abnormal in 10 and questionable in 1 out of 11 pts with abnormal contrast venogram. The 1 questionable case showed a slight retention of radioactivity in the abnormal calf. Abnormal findings from the 10 RNVs were ; 1) area(s) of decreased radioactivity corresponding to the region of thrombosis or of obstruction, 2) retention of radioactivity below the area of obstruction, and 3) abnormal collateral flow(s). "Hot spot" or area of radioactivity retention in the calf coincided well with incompetent or prominent valve with some degree of a venous stasis demonstrated by contrast venogram in all cases.

When the retention of radioactivity was ruled out as an evidence of venous abnormality, positive correlation between RNV and contrast venogram became 85%.

Clinical findings, local pain and swelling, correlated better with RNV findings than with contrast venogram.

WHEN RADIONUCLIDE AND CONTRAST VENOGRAPHY DISAGREE. David F. Preston, Kyo Rak Lee, Ralph G. Robinson, Norman L. Martin and Buck A. Rhodes. Kansas University Medical Center, Kansas City, KS.

Radionuclide venography (RNV) is a relatively new test currently undergoing the first blushes of enthusiasm and clinical acceptance. In our experience involving 10 legs in 9 patients having both RNV with Tc human albumin microspheres (HAM) (5mCi) and contrast venography (CV) opinions frequently disagreed. Causes of the differences were sought for each anatomical site and each patient. Five abnormal RNV findings were recorded: 1. apparent obstruction 2. collateral bloodflow 3. immediate hotspot 4. delayed hotspot 5. delayed arrival. In 9 of 10 examinations contrast venography preceded RNV by 1 hour. HAM were injected in divided doses through a butterfly kept open with normal saline. The pelvis, thigh, knee and calf were imaged by scintillation camera in sequence obtaining 15,000 counts per image. 40 individual sites were examined in 10 studies.

		RNV +	RNV -
	+	10	5
	-	7	15
CV	Off Film	3	0

There was disagreement in 2/9 of pelvic, 4/10 of thigh, 3/10 of knee, 3/8 of calf sites. Three studies from 2 patients with clinical pelvic thrombophlebitis accounted for 9 of the 12 disagreements. A superficial saphenous vein was mistaken for a deep femoral vein by RNV. The knee must be marked on RNV. Agitation of the injecting syringe is necessary as up to 1/3rd. of the 5 mCi dose may be recovered from the syringe following apparent total volume injection. Additional correlation between RNV and CV is needed.

RADIONUCLIDE VENOGRAPHY: A SIMPLIFIED APPROACH USING THE GAMMA CAMERA AND WHOLE BODY SCANNING BED. Owen C. Van Kirk, Alan A. Jansen, Mary T. Burry, Donald Barnett, and Steven M. Larson. Portland V.A. Hospital, Portland, Oregon.

A simplified technique for performing the radionuclide venogram has been developed which allows for a more integrated presentation of the data. Basic to this technique is the use of a gamma camera and syncronized whole body scanning bed. Following a posterior ventilation lung scan with xenon-133, the patient is placed supinely on the scanning table and radioactive markers placed on the medial and lateral aspects of the ankles, knees, midthigh, and hips. Exposure is initiated and as the table begins to move, starting at the feet at a speed of 96cm/min., 1-2 mCi of Tc 99m MAA (or microspheres) is injected into the dorsal pedal vein. The procedure is repeated on the opposite leg, and then four views of the lungs are obtained to evaluate perfusion.

Twenty-three patients were studied by this combined approach. There was a 93% correlation between the radiovenogram and the contrast venogram in the 14 patients who had both procedures performed. Seventy-seven percent of the patients with abnormal radiovenograms had perfusion lung scans strongly suggestive of pulmonary embolus. Two-thirds of patients with abnormal lung scans suggestive of pulmonary embolus had abnormal radiovenograms.

In conclusion, the use of the gamma camera and whole body scanning bed provides for a simpler technique for performing the radionuclide venogram. This method is a valuable adjunct in the evaluation of patients suspected of having thromboembolic disease.

A STUDY ON USEFULNESS OF 99mTc-RBC FOR AN EVALUATION OF HAND BLOOD FLOW IN PATIENTS WITH RAYNAUD'S PHENOMENON. U. Yun Ryo, Aslam Siddiqui, Michael H. Ellman, and Steven M. Pinsky. Michael Reese Hospital and Medical Center, Chicago, Ill.

Proper evaluation of Raynaud's phenomenon is difficult without a simple and effective method for a quantitative measurement of a change in the blood flow to the hand.

This study was undertaken to evaluate the usefulness of 99mTc-RBC for measurement of the blood flow change in the hand in response to a cold exposure. Five to 10 ml of autologous RBCs were labeled with 99mTc, 10 to 15 mCi, and reinfused into the patient. A gamma scintillation camera was used to record radioactivity from the hands before and after an application of cold (ice water bag) and after the cold was removed. The study was carried out in 10 volunteers and in 40 patients (pts) with varying degree of Raynaud's symptom.

In the 10 control subjects, the radioactivity count (RC) showed an average of 12% decrease (range: 6-17%) following the cold exposure. The RC returned to the baseline value within 10 min when the cold was removed in all control subjects. Five of 6 pts with SLE (83%), 7 of 8 pts with scleroderma (88%), and 6 of 7 pts with cryoglobulinemia (86%) showed 23% (17-30%), 23% (14-40%), and 25% (15-35%) decrease respectively in the RC following the cold exposure. In all pts with SLE or scleroderma, recovery of the RC after removal of the cold was markedly delayed. The recovery rate of the RC in cryoglobulinemia pts was similar to the value of the control subjects. Six pts with Raynaud's disease and 3 pts with rheumatoid arthritis pts showed 14% (4-20), and 13% (0-22) decrease respectively in the RC from the hand following the cold exposure.

These results demonstrate the usefulness of the hand blood flow study with 99mTc-RBC in evaluation of patients with Raynaud's phenomenon.

THE EFFECT OF INJECTION TECHNIQUE ON RADIOPHARMACEUTICAL BOLUS CHARACTERISTICS. Choong-Man Kim, James E. Holden, Robert E. Polcyn, and R. Jerome Nickles. Dept. of Radiol., University Hospitals, Madison, Wis.

We have studied radiopharmaceutical bolus characteristics as a function of injection technique comparing: 1) simple, rapid basilic vein injection; 2) basilic vein injections followed by a saline flush of 5, 10, 15, 20 and 25 ml volume; 3) non-basilic vein injections (cephalic veins, veins of the hand and wrist) with and without saline flush; 4) the Oldendorf technique. Data from 135 patients are included.

Injected volumes were 0.6 to 1.6 ml representing 5 mCi of Tc-99m sulfur colloid. Pho-Gamma HP and Radicamera II detectors with low energy collimators were used. With each patient positioned with the superior vena cava (SVC) roughly central in the camera's field of view, serial 1 second data frames were recorded in an anterior projection through a dedicated PDP-11-40 computer. Time/activity data from a small region of interest at the junction of the subclavian vein and SVC were fitted to a modified gamma function as described by Kiukka, et al. The first moment of these time distributions or mean transit time (MTT) of each bolus was extracted.

The MTT following simple basilic vein injection was 7 $\pm$ 6 seconds. When a 25 ml flush immediately followed basilic vein injection, MTT was 3 $\pm$ 1 seconds. Since about 25% of patients require injection into other than the basilic vein, it is of particular interest that when a 25 ml flush is used, average MTT values for basilic and non-basilic injection sites are indistinguishable. Saline

flush using smaller volumes, because it less completely displaces the radiopharmaceutical, is inferior to a 25 ml volume. Oldendorf and 25 ml saline flush techniques provide superior bolus delivery into the SVC but the saline flush technique does so more consistently.

RADIONUCLIDE ANGIOCARDIOGRAPHY USING IN VIVO LABELING OF ERYTHROCYTES WITH TECHNETIUM-99m PERTECHNETATE. Ernest M. Stokely, Robert W. Parkey, Frederick J. Bonte, Kenneth D. Graham, Marvin J. Stone, and James T. Willerson. University of Texas Health Science Center and Parkland Memorial Hospital, Dallas, Texas.

Several workers have reported the difficulty of obtaining artifact-free brain scintigrams using technetium-99m pertechnetate following a technetium-99m stannous pyrophosphate (Tc-99m PYP) bone scan on a previous day. The artifacts are apparently caused by blood pools which become visible because of the radioactive tagging of technetium-99m pertechnetate to the red cells. While this phenomenon is a nuisance in the brain scanning of patients who have had a recent Tc-99m PYP bone scan, the in vivo tagging of technetium-99m pertechnetate to red cells might be used to image the great vessels and chambers of the heart in patients and thus provide important noninvasive data regarding left ventricular function.

To test this hypothesis we have imaged 10 mongrel dogs and five patient volunteers by giving technetium-99m pertechnetate 24-48 hrs after a Tc-99m PYP myocardial scintigram. In each of the animals and patients we found good delineation of the LV cavity and the great vessels; red blood cell radioactivity was 8.4-21.6 times higher in erythrocytes than in plasma following the injection of technetium-99m pertechnetate.

Thus the data suggest that myocardial images obtained in this manner can be used to detect left ventricular wall motion abnormalities, or to calculate left ventricular ejection fractions and ventricular volumes if an ECG gating device is employed. This technique should particularly lend itself to more detailed cardiac studies of patients who have had a recent Tc-99m PYP myocardial infarct scintigram.

FRIDAY, 10:30-12:00 BALLROOM B

RADIOPHARMACEUTICAL SCIENCE 5

Chairman: David Allen
Co-Chairman: Mary Ann Leeper

THE STRUCTURE OF STANNOUS DIMERCAPTOSUCCINIC ACID CHELATES. Gary E. Krejcarek, James H. Wicks, Paul E. Heerwald, Karen L. Tucker, Verna M. Kubik, Richard A. Newmark and Robert C. Williams. 3M Company, St. Paul, MN.

This study establishes the formation and structures of Sn+2 mercapto acid chelates. The structure of these chelates may determine the ultimate distribution of the Tc-99m labeled radiopharmaceutical complex.

Dimercaptosuccinic acid (DMSA) forms two distinct complexes with Sn+2, one at low pH, e.g. 1-4, and another at a neutral or alkaline pH, e.g. pH 7 and above. The complex formed under acidic conditions when labeled with Tc-99m, concentrates in the kidneys. The complex formed at alkaline pH, however, is more rapidly excreted in the urine. The DMSA/Sn+2 complexes are interconvertible by changing the pH. After labeling with Tc-99m, pH does not change the properties of the complex.

The stoichiometry of the two DMSA/Sn+2 chelates was determined by difference u.v. spectroscopy. At pH 4 the ratio of DMSA to Sn+2 is 2:1 while at pH 8 it is 1:1. Potentiometric titrations of the 2:1 complex indicates that one mercapto group per mole of DMSA is involved in the chelate. The 1:1 complex involves two mercapto groups per mole of DMSA. There are three possible structures for the 2:1 complex and one possible structure for the 1:1 complex. The infrared spectrum of the 1:1 complex shows no S-H stretch near 2500 wave numbers. The nuclear magnetic reasonance (nmr) spectrum exhibits a sharp singlet at 4.46 ppm which is shifted downfield from the non-chelated DMSA at 3.33 ppm. This is indicative of a five membered chelate ring involving the two mercapto groups of DMSA. The third ligand is probably halide or hydroxide. The nmr of the 2:1 complex also shows a sharp singlet at 4.45 ppm. The structure of the 2:1 complex also contains a 5 membered ring involving two mercapto groups from one DMSA. The third ligand on Sn+2 appears to be a carboxyl of the second DMSA molecule.

DERIVATIVES OF BIOLOGICALLY ACTIVE COMPOUNDS WITH HIGH AFFINITY FOR Tc-99m. W.C. Eckelman, W.J. Rzeszotarski, S.M. Karesh, and R.C. Reba. George Washington Univ., Wash. D.C.

Of the conveniently available radionuclides, Tc-99m has the best nuclear properties for imaging; however the poor chemical properties have limited its use as a label for biochemicals. Labeling of a compound with Tc-99m using functional groups present in the compound itself can be a severe limitation. Therefore a compound chosen to follow a specific biologic pathway will most likely have to be derivatized. The derivative would contain the biologically active compound covalently bound to a chelating agent with a high affinity for Tc-99m. Fatty acids are a class of compounds known to localize in the heart. Four fatty acid derivatives were synthesized by combining long chain fatty acid compounds with DTPA-like compounds. The derivatives were labeled with Co-57 and H-3 and the biological distribution in rabbits 30 min after IV administration was compared to the distribution of the parent compound palmitic acid. The average myocardial uptake of the derivatives was 0.04%/g compared to 0.14%/g for H-3 palmitic acid. The heart to blood ratio at 30 min reached a maximum of 3 for the best chemical analog of palmitic acid (N-(15-carboxy-9-pentadecenyl iminobis (ethylenenitrilo) tetraacetic acid) compared to 30 for the palmitic acid. It is apparent that the chemical analogs produced are not complete biological analogs to act as tracers for fatty acid metabolism in the myocardium. However the synthetic efforts from this work have led to the development of a chelating agent which can be combined with a series of biologically active molecules. The compound N'-(2-aminoethyl) diethylenetriamine-N,N,N'',N'' tetraacetic acid has been synthesized and reacted with various biologically active compounds containing a halogen, a ketone or an epoxide moiety. The development of this chelating agent should allow the derivatization of a cross section of biologically active compounds.

EDDA – A NEW BIFUNCTIONAL CHELATE FOR THE DESIGN OF Tc-99m LABELED RADIOPHARMACEUTICALS. G. Subramanian, J.G. McAfee, R.W. Henderson and M. Rosenstreich. Upstate Medical Center, Syracuse, New York

Ethylenediamine diacetic acid (EDDA) is a good chelating agent and it forms stronger coordination compounds with metal ions than the iminodiacetic acid, a previously suggested bifunctional chelate.

A variety of new compounds each containing symmetrically N-substituted ethylenediamine diacetic acid (R-N (CH2COOH)-CH2-CH2-N(CH2COOH)-R) were synthesized, made into kits and labelled with Tc-99m using stannous ions as the reducing/complexing agent for technetium. Methyl, Ethyl, Dibenzyl and 2,6 dimethyl acetanilide (DMAEDDA) groups were substituted for the iminohydrogen (R) in EDDA. These compounds were found to be stable by the absence of free pertechnetate and colloids as determined by paper and thin layer chromatography in various solvents.

Tissue distribution and imaging studies were performed in mice, rabbits and dogs. Imaging studies in rabbits and dogs showed rapid blood clearance for all compounds with different organ localization. With the increasing molecular weight, the liver concentration increased and urinary excretion decreased. The liver retention also varied with each compound. The largest compound (DMAEDDA) was eliminated from the liver through the bile resulting in excellent visualization of the gall bladder and the intestine. The kidney was only faintly seen. Tissue distribution in mice also demonstrated that Tc-99m-DMAEDDA could be useful as a hepatobiliary agent, substituting for I-131 Rose-Bengal.

These studies demonstrate that EDDA forms strong, stable chelates with Tc-99m and alteration of the R-group substituents changes the biodistribution. These characteristics may be useful in designing new radiopharmaceuticals with metal ions, especially Tc-99m, using this bifunctional chelate.

DEPOSITION OF STRONTIUM-85 AND TECHNETIUM-99m PHOSPHATE IN SURGICAL WOUNDS. Guido Ludwig, Giraud V. Foster, H. William Strauss, and Henry N. Wagner, Jr. The Johns Hopkins Medical Institutions, Baltimore, Md.

In the rat the level of plasma calcium falls significantly following surgical procedures. The following studies were carried out to determine whether Sr-85 can serve as an appropriate isotopic analogue for calcium to study what tissues Sr-85 enters during surgery, and to determine whether it is as effective a marker for damaged tissue as Tc-99m pyrophosphate. A standard midline abdominal laparotomy was performed under light ether anesthesia in 8 rats while an additional 8 rats were anesthetized in an identical manner to serve as controls. Each animal was given 50 μCi Sr-85 and 300 μCi Tc-99m pyrophosphate intravenously and 90 minutes after administration of the isotopes, skin and muscle adjacent to the incision or comparable tissues in controls, and epididymal fat and the right femur from all animals, were removed and the radioactivity in these tissues counted and expressed as % dose/gram. No significant difference in the uptake of Sr-85 and Tc-99m pyrophosphate was observed in skin, fat and bone. However, the uptake of Sr-85 in the muscle adjacent to the wound was three-fold greater than control tissue (0.173 ± 0.015 vs. 0.057 ± 0.003% D/g $p < 0.0005$) comparable to a two-fold increase observed with stable calcium. Radioactivity associated with Tc-99m pyrophosphate was five times greater than from control animals in muscle (0.10 + .01 vs. 0.02 ± 0.001% D/g $p < 0.0005$). We conclude that (1) the ingress of Sr-85 in injured muscle is increased following surgery without significant changes in uptake by skin, bone, and fat, and (2) as an index of muscle damage, Tc-99m pyrophosphate is superior to Sr-85.

IN-VIVO RED BLOOD CELL LABELING USING CONSECUTIVE INJECTIONS OF STANNOUS PYROPHOSPHATE AND TECHNETIUM-99m PERTECHNETATE. A.M. Zimmer, D.G. Pavel, and V.N. Patterson, University of Ill. Med. Center, Chicago, Ill.

Recent evidence has demonstrated red blood cell labeling when technetium-99m pertechnetate was administered to patients that had received technetium-99m stannous pyrophosphate for bone scan imaging in the preceding days.

Our laboratory has attempted the labeling of red blood cells in-vivo by the consecutive short interval injection of stannous pyrophosphate (Mallinckrodt Nuclear) and technetium-99m pertechnetate. The optimum lag time between these injections was experimentally determined in-vitro by incubating Tc-99m pertechnetate with patients blood obtained at various time intervals after stannous pyrophosphate administration. The total activity bound to red blood cells and the chemical state of Tc-99m in plasma was determined. In-vitro data indicated a maximum mean red cell tagging of 88 percent after a lag time of 30 minutes. The remaining activity in plasma was approximately equally divided between Tc-99m pertechnetate and Tc-99m pyrophosphate.

Patients were subsequently injected with 5-15 mCi of Tc-99m pertechnetate 30 minutes after stannous pyrophosphate injection (0.2 mg/kg. body wt.). In-vivo date indicated a mean red cell tagging of 96 percent, five minutes after Tc-99m pertechnetate injection, and the tagging efficiency remained greater than 95 percent up to one hour after injection. The highest peripheral blood concentration was reached 15 minutes after Tc-99m pertechnetate injection and approximately 95 percent of this maximum level was found one hour after injection.

The in-vivo red cell labeling technique outlined is easy to perform and the tagging and stability of the red cell preparation is quite satisfactory for blood pool imaging.

NEW GA-68-LABELED SKELETAL IMAGING AGENTS FOR POSITRON SCINTIGRAPHY. Mrinal K. Dewanjee, R. Beh, D.J. Hnatowich. Tufts Medical School-New England Medical Center and Massachusetts General Hospital, Boston, Mass.

We have synthesized two new gallium chelates, Ga-68-ethylenediaminetetramethylenephosphonate (Ga-EDTMP) and Ga-68-diethylenetriaminepentamethylenephosphonate (Ga-DTPMP). Addition of carrier gallium is not necessary for skeletal uptake. The radiopharmaceuticals were prepared by adding $GaCl_4^-$ complex to 20-50mg. of EDTMP or DTPMP stock solutions and neutralizing to pH 5.5. The solution was then sterilized by membrane filtration. The organ distribution of Ga-67-EDTMP and Ga-67-DTPMP was performed in 30 Sprague-Dawley rats. The results show that (50-60)% of the injected dose accumulates in bone at 1 hour after injection; and (25-30)% is excreted with the urine. Except for the slower blood clearance of Ga-67-DTPMP, the general trends of organ distribution of both the complexes are similar. At 3 hours after intravenous injection the (bone/blood) and (bone/muscle) ratios are 15,70 and 10,47 for 67-Ga-EDTMP and Ga-67-DTPMP respectively.

Ga-68-labeled chelates were used for positron scintigraphy in dogs. Dogs were injected intravenously with 8mCi of Ga-68-EDTMP or Ga-68-DTPMP, imaged and sacrificed at one, two, and three hours post injection. Satisfactory images were obtained after 2 hours with both complexes, however superior images were obtained with Ga-68-EDTMP. The (bone/muscle) and (bone/blood) ratio of Ga-EDTMP in dogs increased from 3 to 10 and 2 to 8 respectively from 1 to 3 hours. At the end of three hours, 35% of the injected dose was in bone, 1% in blood and 50% in urine. Gel filtration studies indicate that like Tc-99m and In-113m-labeled phosphonates the Ga-labeled chelates also bind with serum protein. Due to slower blood clearance of Ga-68-DTPMP, Ga-68-EDTMP appears more suitable for skeletal imaging by positron scintigraphy.

FRIDAY, 10:30-12:00 BALLROOM C

ONCOLOGY 2

Chairman: Frank H. DeLand
Co-Chairman: Andrew T. Taylor, Jr.

TECHNETIUM-99m PHOSPHONATE COMPLEXES: BIOLOGICAL DISTRIBUTION IN A TUMOR ANIMAL MODEL (RC6). Frank P. Castronovo, Majic S. Potsaid and Paul L. Kornblith. Massachusetts General Hospital. Boston, MA 02114.

The development of radiopharmaceuticals utilizing the phosphonate moiety as a handle for Tc-99m has been pursued in our laboratory. We investigated analogs having structual modifications relative to our initial compound, HEDP. These include 3-amino,3-carboxypropyl phosphonic acid (ACPA), 2-aminoethylphosphonate (AEP), aminomethylphosphonate (AMP), 2-aminophosphonobutyric acid (APBA), and 1, 4-dihydroxybutylidene-1, 1-4, 4-tetraphosphonic acid (TPA). After formulation and quality control, each Tc-99m complex was administered IV to adult rats (RT6 tumor). Tissue distribution was determined and the results expressed as $\bar{m}$ %D/org. ± s.d. (N=3) at 4 hours. Relative tumor concentration was expressed as the ratio of %D/gm. tumor to %D/gm. tissue. Similar studies were performed with Tc-99m labeled HEDP, pyrophosphate, trimetaphosphate (TMP) and pertechnetate.

Relative to the HEDP, the phosphonate analogs showed reduced skeletal % uptake per organ (12.72±0.405 to 15.89±1.92 vs. 33.29±3.0) with a concomitant increase in blood concentrations; (0.745±0.74 to 5.92±0.040 vs. 0.195 ± 0.03). A similar distribution was observed with muscle. The highest skeletal uptake was with the PYO (37.62± 2.97). Tumor to brain ratios showed the phosphonate analogs (10.7 to 16.79) to be similar to pertechnetate (13.75), but lower than HEDP (27.62) and TMP (74.5). Tumor to blood ratios showed a similar distribution.

Studies suggest the phosphonate analogs and trimetaphosphate as possible tumor agent.

THROMBOPLASTIC ACTIVITY (TA) AND FIBRINOLYTIC ACTIVITY (FA) OF NORMAL AND NEOPLASTIC TISSUE. Jeffrey Wortman, Sally DeNardo, Gerald DeNardo, Show-Mei Huang, Kenneth Krohn, Chung Song. University of California, Davis, CA

Coagulation disorders are frequently found in cancer patients and *I-fibrinogen and *I-fibrin antibodies localize in experimental and spontaneous tumors in animals and man. We are investigating the coagulation properties of neoplastic tissues in order to enhance the tumor specificity of radiolabeled coagulation proteins. This paper reports the tissue TA and FA of three histologically and biologically

different transplantable mammary tumors (MMI, MMII, KHJJ) in Balb C mice, 5 spontaneous neoplasms in dogs, and normal tissues from these animals.

TA was quantitated by measuring the clotting time of recalcified plasma in the presence of tissue homogenate relative to a saline control. In mice significant TA was found in brain and lung and in all three tumor tissues. MMII had greater TA than MMI or KHJJ.

FA was quantitated by the time dependent release of radioactivity from an *I-fibrinogen/euglobulin clot formed in the presence of fresh tissue homogenate. MMII tumor also had distinctly greater FA than the other tumors.

The dog data also demonstrated significant TA and moderate FA in most tumors analyzed; however a relative absence of FA was characteristic of at least two tumors. Furthermore necrotic tissue from both a primary mammary adenocarcinoma and a pulmonary metastasis had no FA and much less TA than the corresponding viable tumor tissues.

Correlation of *I-fibrinogen distribution with the coagulation properties of normal and tumor tissues has provided information on the specificity of *I-fibrinogen localization in cancer. (Supported by American Cancer Society grants DT-45 and IN-95D; and by PHS-05245).

MECHANISMS OF LOCALIZATION OF *I-FIBRINOGEN IN CANCER. Gerald DeNardo, Sally DeNardo, Kenneth Krohn, Jeanne Meyers, Show-Mei Huang, Jeffrey Wortman. University of California, Davis, CA.

*I-fibrinogen and *I-fibrin antibodies have been demonstrated to localize in cancer, but the mechanism of localization is disputed. Quantitation of the significance of active mechanisms, e.g., those associated with coagulation activity, and passive mechanisms, e.g., those associated with blood flow, intravascular and interstitial spaces, and capillary permeability are necessary for the appraisal of the tumor-specificity of labeled coagulation proteins. In experimental and spontaneous tumors in animals, the time dependent tissue distribution of *I-fibrinogen has been compared with that of radiolabeled albumin and Rb-86 chloride, and with the amounts of fibrinolytic and thromboplastic activities in the same tissues. Rb-86 reflected nutrient blood flow and radiolabeled albumin reflected intravascular and interstitial spaces of the tissues depending upon the time of measurement.

The amount of *I-fibrinogen localization was not primarily determined by blood flow or intravascular space of the tumor, but was related to capillary permeability and interstitial space. Although there was some correlation between *I-fibrinogen localization and thromboplastic activity, particularly early after injection, later localization correlated better with fibrinolytic activity.

These results document the significance of active mechanisms for localization of *I-fibrinogen, provide insight into potential mechanisms for enhancing localization of *I-fibrinogen, and encourage clinical trials of its usefulness as a general tumor radiodiagnostic agent. Its utility and further applicability in understanding and controlling cancer is clearly documented by these results. (Supported by American Cancer Society Grant #DT-45.)

LABELED CELL-SPECIFIC ANTIBODIES IN THE DETECTION OF METASTASES. Roberto L. Ceriani, Shelby W. Miller, Karen E. Thompson, Jerry A. Peterson, and S. Abraham. Bruce Lyon Mem. Res. Lab., Children's Hospital Med. Ctr. and Highland General Hospital, Oakland, Ca.

Sensitivity and specificity are ideal characteristics for a tumor labeling agent. These characteristics are attributes of labeled antibodies to cell differentiation antigens. This study evaluates the sensitivity and specificity of a labeled mouse mammary epithelial cell antibody (anti-MMEC) as an imaging agent for mammary carcinoma. Anti-MMEC produced in rabbits, after appropriate absorptions, bound to normal mouse mammary epithelium but not to a variety of other mouse tissues, as judged by immunofluorescence techniques. Anti-MMEC also bound to mouse mammary tumor cells. I-125 labeled anti-MMEC was injected into BALB/c mice carrying simulated tumor metastases. The latter were grafts of a transplantable mammary tumor obtained from a BALB/c fostered C3H mouse. Tumor to tissue ratios appeared favorable for imaging. Pictures obtained with a scintillation camera of mice carrying simulated mammary tumor metastases after injection of I-131 labeled anti-MMEC show similarly favorable results. At present, efforts are being made to prepare a more purified anti-MMEC to lower non-specific background.

A highly specific anti-human mammary epithelial cell antibody has been prepared for which human use is anticipated after successful conclusion of the animal protocol. (Supported by NCI Contract No. NO1-CB-33906 and NCI Grant No. CA 11736.

COMPARATIVE STUDIES OF RADIOLABELED BLEOMYCIN AND THE IONIC RADIOLABELED SPECIES IN A BLEOMYCIN-SENSITIVE TUMOR MODEL. Jack N. Hall, Joseph D. Chen, James M. Woolfenden, Dennis D. Patton, Rosa L. Liu, and Sydney E. Salmon. University of Arizona Medical Center, Tucson, Az.

Previous investigations have demonstrated localization of various radiolabeled bleomycins in many experimental tumors in animals and known primary tumors in man. To our knowledge a comparative study of radiolabeled bleomycin and the ionic radioactive label in a proven bleomycin-sensitive animal tumor model has not been reported.

The tumor model used in this study was a Ridgeway osteogenic sarcoma transferred by subcutaneous passages in AKD2-F1 mice. The tumor has a high thymidine index and is sensitive to the most widely used DNA binders and intercalators (e.g. bleomycin). At the present time three radionuclide complexes and the ionic species have been evaluated in this tumor model both in vitro (isolated viable tumor cells) and in vivo at varying time intervals. Biological distribution studies were performed at 1, 4, 24 and 48 hours. The following table shows the maximum tumor to muscle and tumor to blood ratios obtained at 24 hours.

	T/M	T/B
Co-57 bleomycin	29.48	43.35
Co-57 chloride	4.51	0.80
Cu-67 bleomycin	7.41	2.47
Cu-67 chloride	3.92	1.40
In-111 bleomycin	4.15	2.10
In-111 chloride	3.23	1.75

On the basis of the in vitro and in vivo results, Co-57 bleomycin appears to have tumor localizing properties superior to In-111 or Cu-67 bleomycin or the ionic species of any of the three radionuclides. Bleomycin labeled with a shorter half-life radionuclide of cobalt (i.e. Co-55) should be evaluated for tumor localization.

INTERACTION OF ARTIFICIAL LIPID VESICLES WITH IMMUNOGLOBULIN, PEPTIDE HORMONE, AND MAMMALIAN CELLS. June K. Dunnick, and Joseph P. Kriss. Depts. of Medicine and Radiology, Stanford University School of Medicine, Stanford California.

Artificial lipid vesicles have potential use as carriers of drugs or tracers. The interaction of vesicles with proteins and mammalian cells was studied to determine factors affecting surface binding of proteins, vesicle-cell fusion or membrane exchange, and in vivo distribution. Vesicles are prepared by sonicating aqueous dispersions of phosphatidyl choline, cholesterol, and gangliosides to form bilayer spheres 500 Angstroms in diameter, enclosing whatever ingredients are in the sonicating medium. On incubation of vesicles (log 15.0) with 0.3μg I-125 antithyroglobulin, 16% of I-125 bound irreversibly to vesicles; binding was dependent on ganglioside content. I-125 human thyrotropin was similarly bound by vesicles. On incubation of vesicles with mammalian erythrocytes, spleen cells or tumor cells up to a million vesicles could interact with each cell; 20% of intravesicular Tc-99m marker was transferrable to cells; interchange of membrane between cells and vesicles was also observed. Pre-incubation of EMT6 cells with vesicles made of sterylamine or sphingomyelin inhibited subsequent cell growth by as much as 50%. Following injection of vesicles into rats, highest concentrations were found in liver and spleen, but some vesicles survived in blood up to 24 hr. Pre-incubation of vesicles with cells or with proteins reduced hepatic localization of vesicles from about 35% to 20%. The magnitude and type of cell-vesicle interaction may be selectively modified by chemical or physiologic means. Alteration of tumor cell membrane by fusion with vesicles alters biologic behavior of the cells.

TISSUE DISTRIBUTION STUDIES IN MICE WITH A CU-64 LABELED THIOSEMICARBAZONE. L.M. Lieberman and David Young, University of Wisconsin Hospitals, Madison, Wisconsin and D.H. Petering and Daniel Minkel, University of Wisconsin-Milwaukee, Wisconsin.

We have studied the tissue distribution of a Cu-64 complex; 3-ethoxy-2-oxobutryaldehyde bis(thiosemicarbazone), Cu-64-KTS, in mice transplanted with an adenocarcinoma and in mice transplanted with fibrosarcoma. A control group of mice transplanted with fibrosarcoma was studied with Cu-64-Cl as controls. CuKTS is a recognized anti-tumor agent and it has been shown that the presence of copper is necessary for the anti-tumor effect.

Following the intravenous administration by tail vein of Cu-64-KTS in dimethylsulfoxide, groups of three animals were killed by cervical dislocation at 15 minutes, 1 hour, 4 hours, and 24 hours. Control animals were given Cu-64-Cl and killed at the same intervals in a similar manner. Blood, tumor, and 10 additional tissues were obtained, weighed and counted in an automatic gamma well counter. Decay corrections were made when necessary. Animals were given from 2-20 uCi of Cu-64-KTS containing 0.10-0.15 umol CuKTS. A percent dose/gm was estimated for each tissue.

Both the transplanted adenocarcinoma and fibrosarcoma remained low in concentrations of Cu-64 radioactivity throughout the study although the fibrosarcoma demonstrated a small steady increase in concentration up to 24 hours. An unexpected observation was a 20:1 ratio of lung to blood radioactivity up to one hour following administration of the Cu-64-KTS, and approximately 10:1 lung:liver ratio at the 15 minute interval. Control animals with Cu-64-Cl showed very low values for the same organ ratios.

It does not appear that Cu-64-KTS will be a promising agent for tumor scanning. The unexpectedly high lung concentrations suggest that further investigations should be performed to determine the mechanism of this action.

TECHNOLOGISTS' SCIENTIFIC PROGRAM

The following papers have been accepted for the Technologists' Scientific Program. Complete abstracts may be found in the June issue of the *Journal of Nuclear Medicine Technology*.

TUESDAY, 10:30-12:06 ROOM N215/217

SUBMITTED PAPERS I

A RADIOPHARMACEUTICAL QUALITY CONTROL PROGRAM IN HALF THE TIME. D.J. Battaglia, C. DeFries, and M.L. Cianci. Oscar B. Hunter Memorial Laboratory, Washington, D.C.

ARTIFACTS FOUND IN TESTING PERCENTAGE OF LABELING IN Tc-99m PYROPHOSPHATE - A SOLUTION TO THE PROBLEM. Ghanshyam C. Patel, Lelio G. Colombetti, and Steven Pinsky. Michael Reese Medical Center, Chicago, Ill.

99mTc-HUMAN SERUM ALBUMIN : EFFICIENT LABELING TECHNIQUE AND ITS IN VIVO STABILITY. Jong Il Lee, Ghanshyam C. Patel. Michael Reese Hospital, Chicago, Ill.

RADIOASSAY: NORMAL RANGE DETERMINATION. D.J. Battaglia, C. Burkhead, J. Welton, and M.L. Cianci. Oscar B. Hunter Memorial Laboratory, Washington, D.C.

FACTORS AFFECTING RELIABILITY OF THE GASTRIN RADIOIMMUNOASSAY. Pamela Trusten and Tim Shea. Department of Radiology, Harvard Medical School and Peter Bent Brigham Hospital, Boston, Mass.

FACTORS AFFECTING BINDING OF FOLIC ACID TO BETA-LACTOGLOBULIN. Tim Shea and Pamela Trusten. Department of Radiology, Harvard Medical School and Peter Bent Brigham Hospital, Boston, Mass.

IN VITRO ANALYSIS OF THE PLASMA CLOTTING PROCESS USING Tc-99m LABELED AGGREGATES. Sheldon J. Ashley. Flushing Hospital and Medical Center, Flushing, N.Y.

A PROCEDURE FOR EVALUATING PATIENTS WITH THYROID CANCER. Lucille Bunz and Malcolm R. Powell. 350 Parnassus Ave., Suite 908, San Francisco, Calif.

WEDNESDAY, 10:30-12:06 ROOM N215/217

SUBMITTED PAPERS II

THE TECHNOLOGIST'S ROLE IN COMPREHENSIVE RENAL FUNCTION STUDY. F.N. Kontzen, M. Barber, E.V. Dubovsky, W.N. Tauxe. Veterans Administration Hospital, Birmingham, Ala.

COLOR IMAGING AND SELECTIVE CURVE GENERATION WITH COMPUTERIZED RENOGRAM IN KIDNEY TRANSPLANT MONITORING. John Mullins and Sheldon Chelsy. Division of Nuclear Medicine, UCLA-Harbor General Hospital, Torrance, Calif.

A SIMPLE, EFFECTIVE METHOD FOR AEROSOL INHALATION SCANNING. Robert Salk and John Mullins. Division of Nuclear Medicine, Harbor General Hospital, Torrance, Calif.

CONTAMINATION OF NON-DISPOSABLE XENON VENTILATION SYSTEMS. George B. Case, Philip Matin, C.B. Martin. Roseville Community Hospital, Roseville, Calif.

PRECAUTIONS AND CONSIDERATIONS FOR RADIOIODINE-131 THERAPY PATIENTS. Marie A. Costanza and Barbara C. Fasiska. Presbyterian University Hospital and the Radiation Health Physics Department of the University of Pittsburgh, Pittsburgh, Pa.

THE PARTICIPATION OF NUCLEAR MEDICINE TECHNOLOGISTS IN RADIATION ACCIDENT MANAGEMENT. Harold D. Hodges and William D. Gibbs. Medical and Health Sciences Division, Oak Ridge Associated Universities, Oak Ridge, Tenn.

BONE IMAGING ARTIFACTS. Sue Weiss and James J. Conway. The Children's Memorial Hospital, Chicago, Ill.

RECOGNITION OF SCAN ARTIFACTS - TECHNOLOGISTS' ROLE. Janet M. Marks, Russell Cain, Diane Winston, James Wing, Anne Schleif, Ronald Burks, and William Burt. VA Hospital, San Diego, Calif.

THURSDAY, 10:30-12:06 ROOM N215/217

SUBMITTED PAPERS III

A QUALITY CONTROL PROCEDURE FOR INSTITUTING USE OF A NEW RADIONUCLIDE. Theodore Sorandes. University of Maryland Hospital, Baltimore, Md.

DOSE CALIBRATOR FOIBLES. Walter L. Robinson. Bionucleonics, Inc., Fanwood, N.J.

A MULTI-DETECTOR SCANNER FOR WHOLE BODY IMAGING. David J. Phegley, Donald R. Bernier, and R. Edward Coleman. Washington University School of Medicine, St. Louis, Mo.

THE USE OF TANTALUM-TUBE COLLIMATORS FOR SCINTILLATION CAMERAS. S.J. Swann, D.W. Palmer, L. Kaufman, C.B. Lim, and P.B. Hoffer. University of California, San Francisco, Calif.

QUALITY ASSURANCE OF WHOLE BODY TABLES. Elbert L. Lands, Bhailal Patel. The University of Chicago, Chicago, Ill.